OAK RIDGE NATIONAL LABORATORY
operated by
UNION CARBIDE CORPORATION
for the
U.S. ATOMIC ENERGY COMMISSION

ORNL-TM-456

COPY NO. - 62

DATE - April 1, 1963

# PRESSURE EQUALIZATION BY FLUID EXCHANGE BETWEEN PARALLEL FLOW CHANNELS

T. G. Chapman P. N. Stevens

## ABSTRACT

Hydraulic and deflection analyses of the unequal flow passages in the HFIR control region revealed excessive pressure differentials. A proposal to drill connecting holes between the flow passages initiated an experimental program for investigating the effectiveness of crossflow on pressure equalization. Empirical constants for an analytical model and experimental design data on reduction of pressure differentials between channels were obtained. It was determined that crossflow between channels would satisfactorily reduce the pressure differentials.

**NOTICE**

This document contains information of a preliminary nature and was prepared primarily for internal use at the Oak Ridge National Laboratory. It is subject to revision or correction and therefore does not represent a final report. The information is not to be abstracted, reprinted or otherwise given public dissemination without the approval of the ORNL patent branch, Legal and Information Control Department.

LEGAL NOTICE

This report was prepared as an account of Government sponsored work. Neither the United States, nor the Commission, nor any person acting on behalf of the Commission:

A. Makes any warranty or representation, expressed or implied, with respect to the accuracy, completeness, or usefulness of the information contained in this report, or that the use of any information, apparatus, method, or process disclosed in this report may not infringe privately owned rights; or

B. Assumes any liabilities with respect to the use of, or for damages resulting from the use of any information, apparatus, method, or process disclosed in this report.

As used in the above, "person acting on behalf of the Commission" includes any employee or contractor of the Commission, or employee of such contractor, to the extent that such employee or contractor of the Commission, or employee of such contractor prepares, disseminates, or provides access to, any information pursuant to his employment or contract with the Commission, or his employment with such contractor.

## Contents


| | Page |
|---|---|
| Introduction | 5 |
| Phase I – Determination of Empirical Relationships | 6 |
| Results | 7 |
| Conclusions | 14 |
| Phase II – Study of Multiple Interconnections | 14 |
| Coupled Parallel Flow with Noncoupled Inlet and Exit | 14 |
| Coupled Parallel Flow with Nominally Equal Channels and Coupled Inlet and Exit | 17 |
| Coupled Parallel Flow with Unequal Channels and Coupled Inlet and Exit | 17 |
| Conclusions | 24 |
| Phase III – Investigation of Crossflow Pressure Equilization | 24 |
| Results | 27 |
| Conclusions | 32 |
| Acknowledgments | 32 |
| References | 32 |
| Appendix A. Potential and Orifice Coefficient Data | 33 |
| Appendix B. Pressure Distributions | 33 |

## Introduction

The control region of the HFIR consists of two concentric control cylinders (rods) that operate in the annulus between the reflector and the fuel element. The outer cylinder is segmented into four quadrants. A hydraulic analysis of the three coolant flow passages adjoining the two cylinders revealed that the geometry of the region produced pressure differentials across the control cylinders, the magnitudes of which were strongly influenced by fabrication tolerances, assembly tolerances, and the relative positions of the control rods. The combination of the fabrication and assembly tolerances resulted in unequal channel thicknesses and tapered channels, while the relative positions of the rods created unequal coolant flow channel lengths.

A deflection analysis of the outer control plate quadrants indicated that the aforementioned pressure differentials exceeded allowable limits by several order of magnitudes. A proposal was therefore made to drill connecting holes between the flow passages as a means of reducing the pressure differences, and an experimental program was initiated to investigate the effectiveness of crossflow on pressure equalization.

The experimental investigations covered the hydraulic behavior of two parallel flow channels and were conducted in three phases. Phase one of the investigations consisted of studies of equal-length, constant-thickness channels coupled by a single row of holes across the channel width. These studies provided empirical relationships for use in the preliminary analyses of multiple rows of holes.

Phase two consisted of analyses of equal-length, constant-thickness channels coupled by multiple rows of holes across the channel width. These studies were performed to facilitate the planning of a more exact mockup of the control region.

Phase three was a test of a more exact mockup of the flow channels. Various hole sizes, hole patterns, flow rates, and direction of crossflow were studied in this test. The results were used to establish the hole size and pattern that would effect the necessary pressure equalization for a reliable mechanical design.

## Phase I – Determination of Empirical Relationships

The model used to determine the empirical constants for the equations to be used in the analytical study consisted of two rectangular and parallel channels with a single transverse row of connecting holes.[1,2] A one-dimensional momentum balance was used to describe the pressure change resulting from a flow change in each channel, and an energy balance was used to describe the flow through the holes. The one-dimensional momentum balance was written for each channel as:

$$P_2 - P_1 = \frac{\rho k}{g_c} (V_1^2 - V_2^2) ,$$

where

$P_2$ = pressure downstream of hole, psf,

$P_1$ = pressure upstream of hole, psf,

$V_2$ = velocity downstream of hole, ft/sec,

$V_1$ = velocity upstream of hole, ft/sec,

$k$ = potential coefficient (determined by experiment),

$\rho$ = fluid density, $lb/ft^3$.

The energy balance was written in the form of the orifice equation, that is,

$$\Delta = CA \, [2g_c(H_1 - H_2)]^{1/2} ,$$

where

$\Delta$ = orifice flow, $ft^3/sec$,

$C$ = orifice coefficient (determined by experiment),

$A$ = cross sectional area of holes, $ft^2$,

$H_1$ = arithmetic average of upstream and downstream pressure in channel giving up fluid, psf/lb,

$H_2$ = arithmetic average of upstream and downstream pressure in channel gaining fluid, psf/lb.

The constants k and C were determined with the experimental setup shown in Fig. 1. Each channel was 40 in. long, 2 in. wide, and of constant thickness. The thickness combinations were either 1/8 in. for both channels or 1/8 in. for one channel and 1/2 in. for the other channel. The channels were connected at a point 24 in. from the inlet by either three 1/4-in.-diam holes, equally spaced across the width, or a longitudinal slot with a length-to-width ratio of 10:1 and an area equivalent to three 1/4-in.-diam holes. A hole length-to-diameter ratio of 1.0 was used without breaking the edges (i.e., square edges). Each channel had a control valve on the inlet and exit for adjusting the flow rates and pressures before and after the holes. The inlet flow to each channel and the exit flow from one channel were obtained from rotameters. Each channel had 13 pressure taps on 2-in. centers along the channel length. The taps began 13 in. upstream of the holes and extended 11 in. downstream from the holes. The pressure drop along each channel and the static pressure differentials between channels were obtained with a manometer and an associated manifold system.

An experimental run consisted of setting the inlet flows and pressures by adjusting the four control valves to give the desired crossflow, which was varied from 1 to 10 gpm. The flows, pressure drops, and pressure differentials were recorded. The data were then plotted, as shown in Fig. 2. The pressure-drop information was extrapolated to the hole centerlines from the upstream and downstream directions for use in evaluating the experimental constants.

The one-dimensional momentum constant, k, that is, the potential coefficient, was evaluated for each channel for each pressure change, in conjunction with the velocities before and after the holes. The orifice coefficient was then evaluated from the orifice flow and the difference between the arithmetic average pressures for the two channels. Tables of experimental data for the coefficient determinations are given in Appendix A.

## Results

The potential coefficient for the channel giving up mass is shown for all runs in Fig. 3. The data were correlated, using a least squares

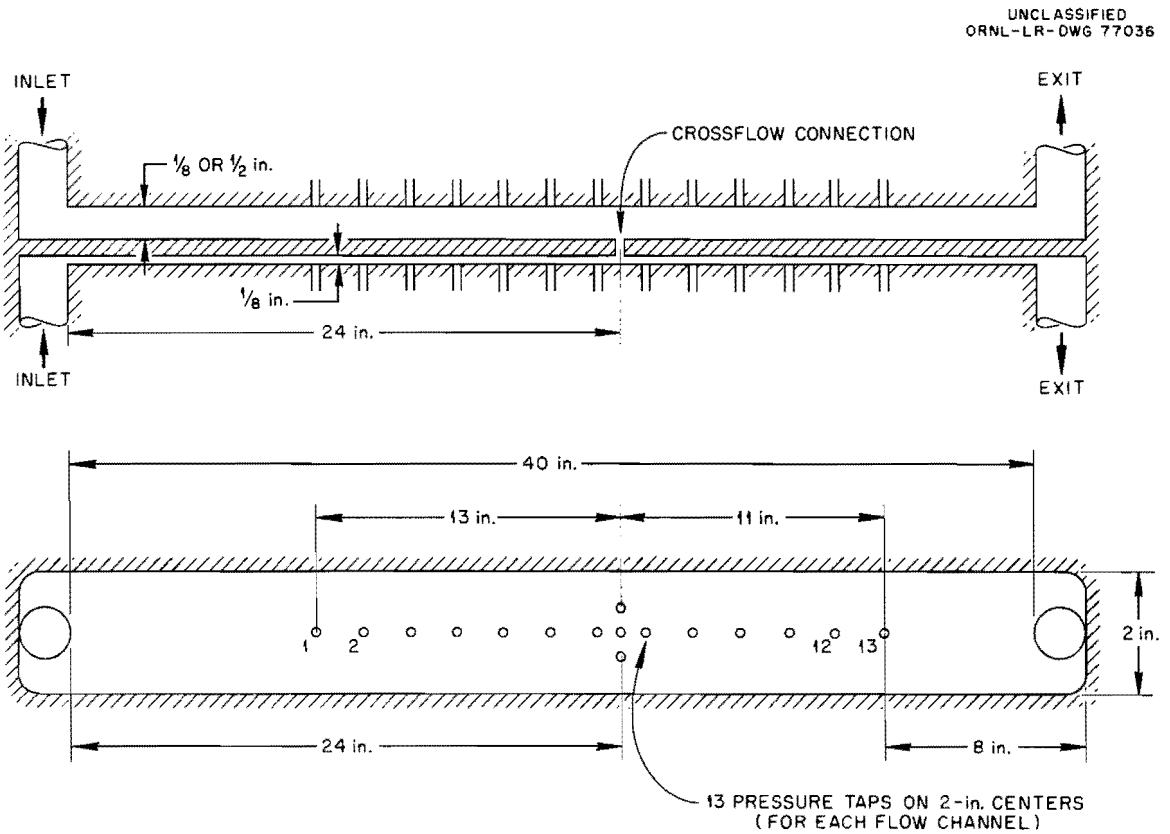


Fig. 1. Schematic Flow Diagram for Coefficient Measurement.

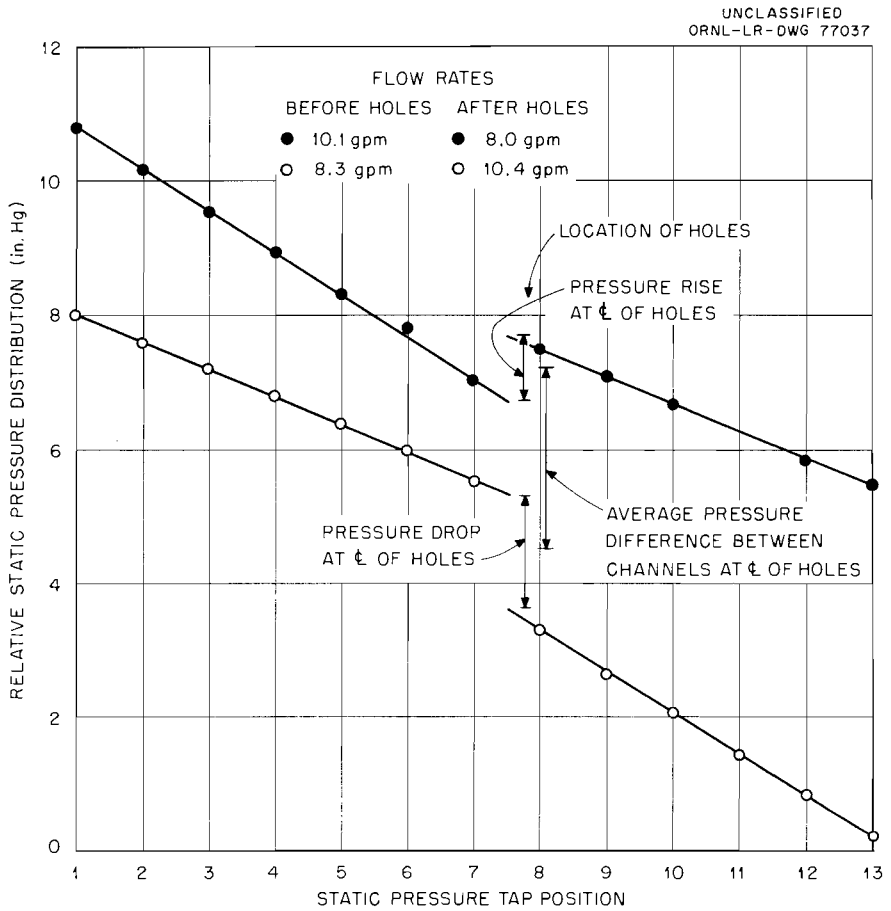


Fig. 2. Typical Experimental Data Obtained in Phase I.

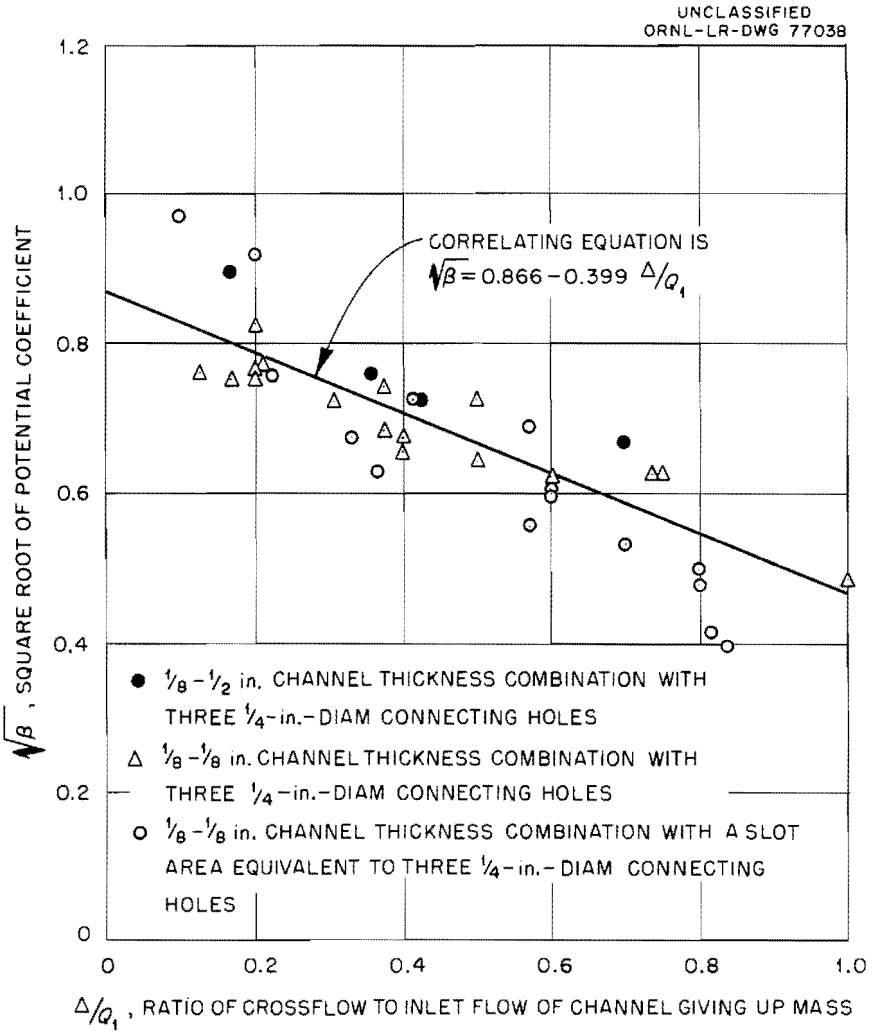


Fig. 3. Potential Coefficient for Channel Giving Up Mass.

fit, with the expression

$$\sqrt{\beta} = 0.866 - 0.399 \frac{\Delta}{Q_1} ,$$

where

$\beta$ = one-dimensional momentum constant for channel giving up mass,

$\Delta$ = orifice flow, $ft^3/sec$,

$Q_1$ = channel flow before holes in channel giving up mass, $ft^3/sec$.

The correlation predicts the experimental values with a maximum error of 20%.

The potential coefficient for the channel gaining mass, $\gamma$, is given in Fig. 4. The data were correlated with the expression

$$\sqrt{\gamma} = \frac{0.891 - 0.471 \frac{\Delta}{Q_1}}{0.866 - 0.399 \frac{\Delta}{Q_1}} ,$$

which is a least-squares fit that gives a maximum error of 20%.

The orifice coefficient data are compared in Fig. 5 with the correlating expression

$$C = 0.646 \left(\frac{\Delta}{Q_2}\right)^{0.4} ,$$

where

$C$ = orifice coefficient,

$\Delta$ = orifice flow, $ft^3/sec$,

$Q_2$ = channel flow after the holes in channel gaining mass, $ft^3/sec$.

This correlating expression, found by a least-squares fit, gives a maximum error of 20%.

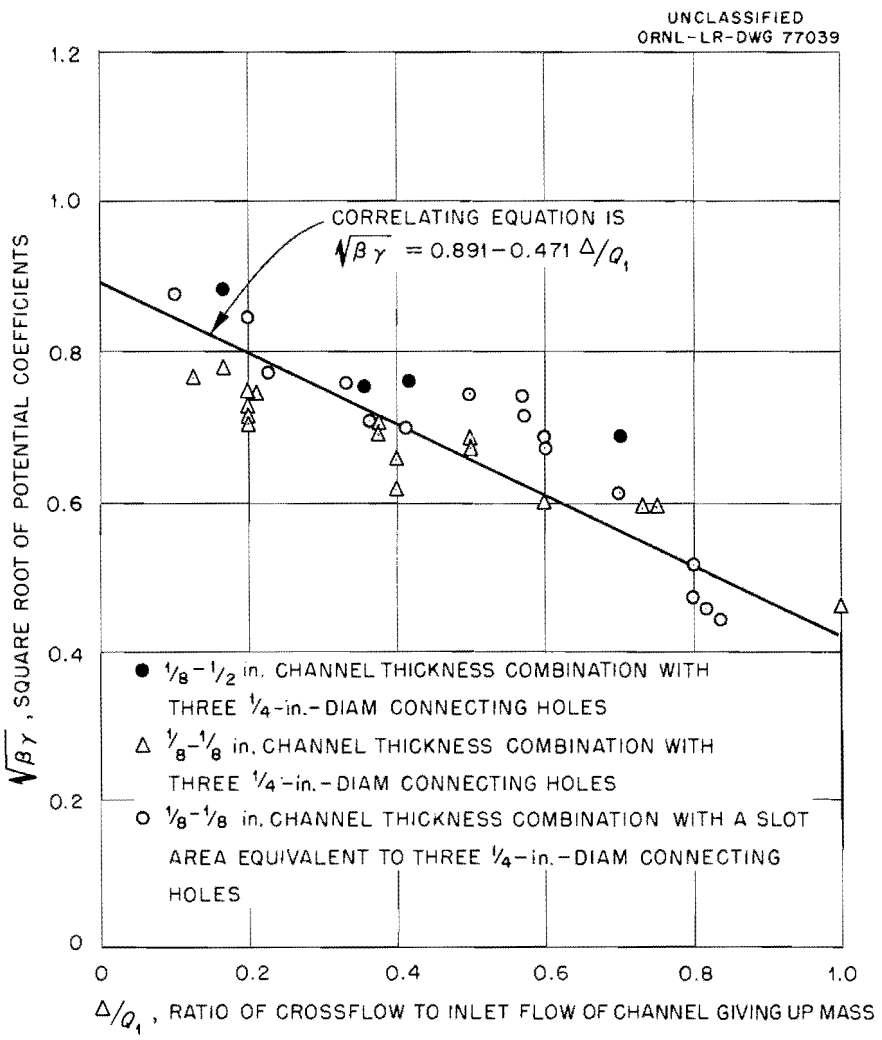


Fig. 4. Potential Coefficient for Channel Gaining Mass.

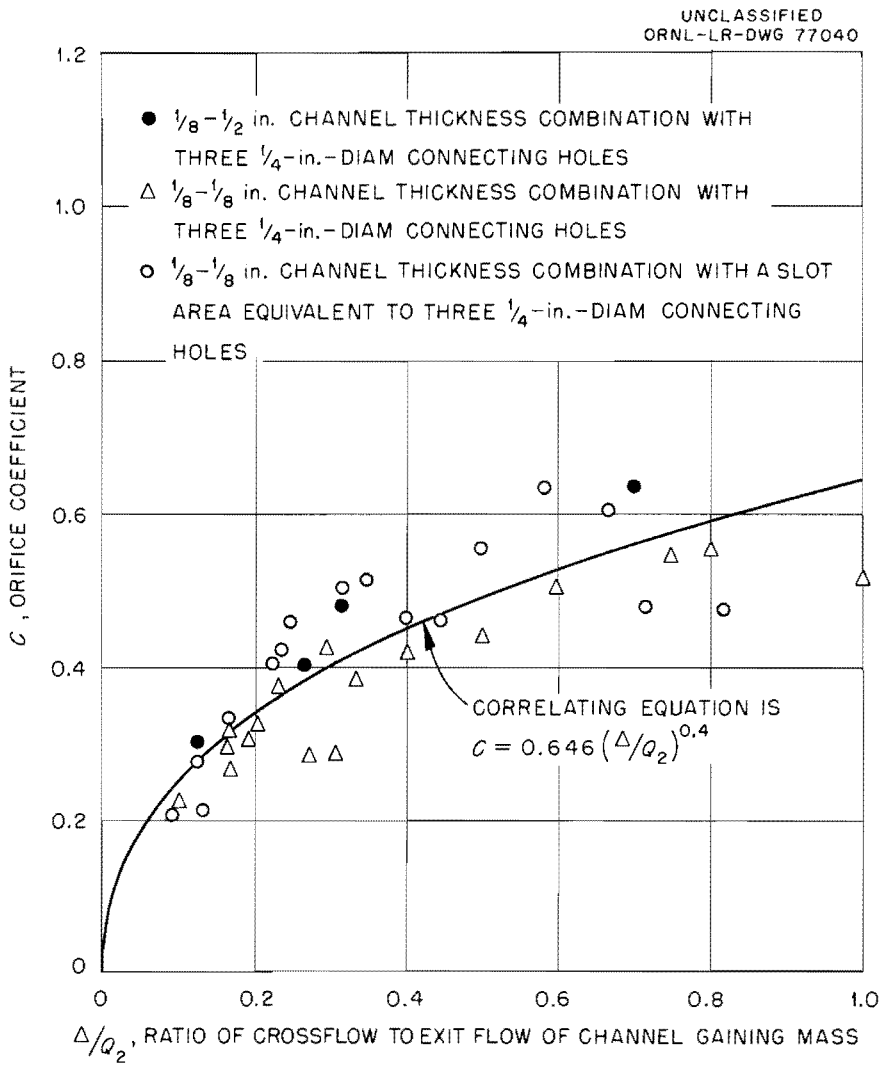


Fig. 5. Cross-Flow Orifice Coefficient.

## Conclusions

The data plotted in Figs. 3, 4, and 5 include the two channel thickness combinations of either 1/8 in. for both channels or 1/8 in. for one channel and 1/2 in. for the other channel. Also the data include both types of crossflow connections. The data correlations found could be used in an analytical model to extrapolate to the case of multiple rows of crossflow connections between adjacent channels. Additional experimental information on the interaction of multiple rows of holes was required, however, before an accurate determination of optimum number, size, and pattern of holes could be made by analytical methods.

## Phase II – Study of Multiple Interconnections

The existing "coefficient-measurement" experimental setup was utilized with minor modifications to study the basic aspects of parallel-channel hydraulics with multiple interconnections. This investigation was performed for three types of flow: (1) coupled parallel flow with noncoupled inlet and exit, (2) coupled parallel flow with nominally equal channels and coupled inlet and exit, and (3) coupled parallel flow with unequal channels and coupled inlet and exit.

### Coupled Parallel Flow with Noncoupled Inlet and Exit

Comparison of the flow scheme studied first and the actual flow system (Figs. 6 and 7, respectively) shows that the two systems bear little hydraulic resemblance. Nevertheless, this first study was deemed desirable because it could be accomplished immediately and with little modification to the existing experimental setup. Briefly, the flow scheme consisted of two parallel flow channels (1/2 and 1/8 in. thick, respectively) partly coupled by various patterns of 1/4-in.-diam holes. Each channel had its own piping system. Desired inlet and exit pressure differentials were established by controlling the inlet and exit flows for both channels. Static pressure differentials were obtained between any of the pressure-tap positions by means of a mercury manometer coupled to a manifold system.

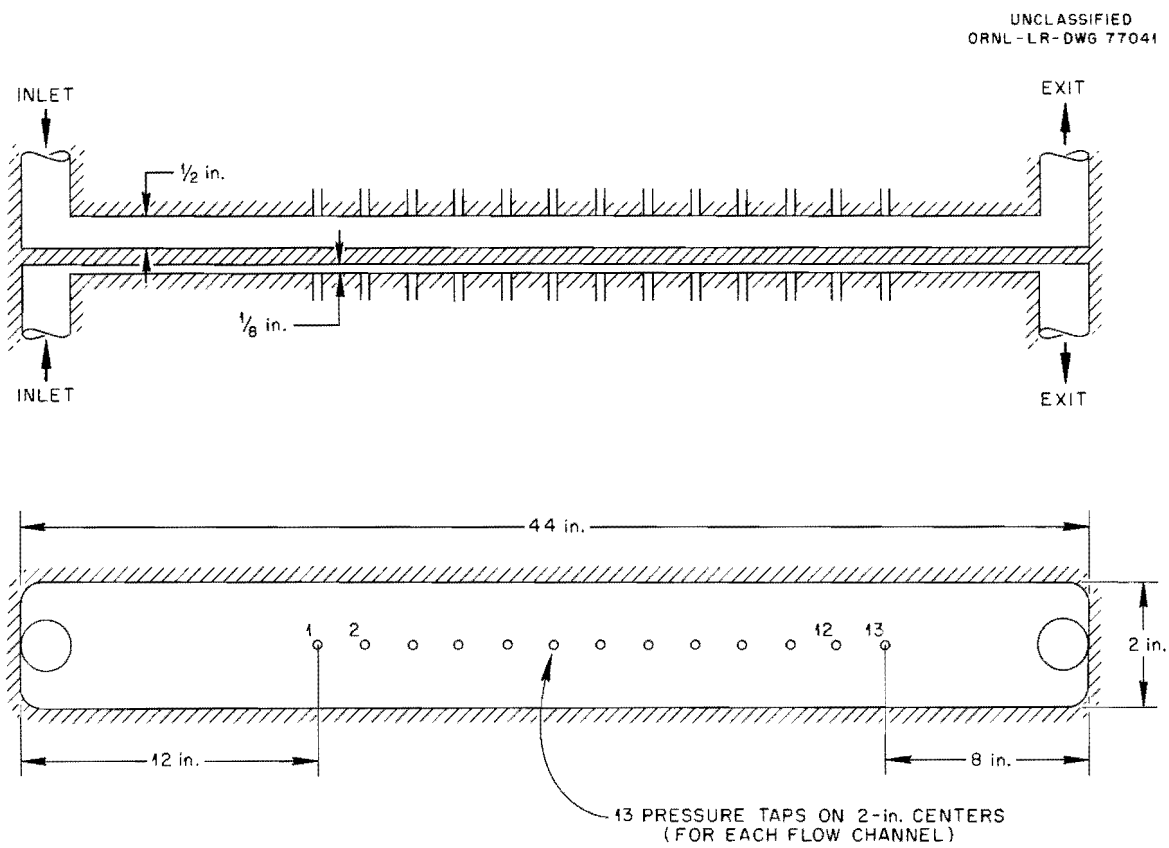


Fig. 6. Schematic Noncoupled Inlet and Exit Flow Diagram.

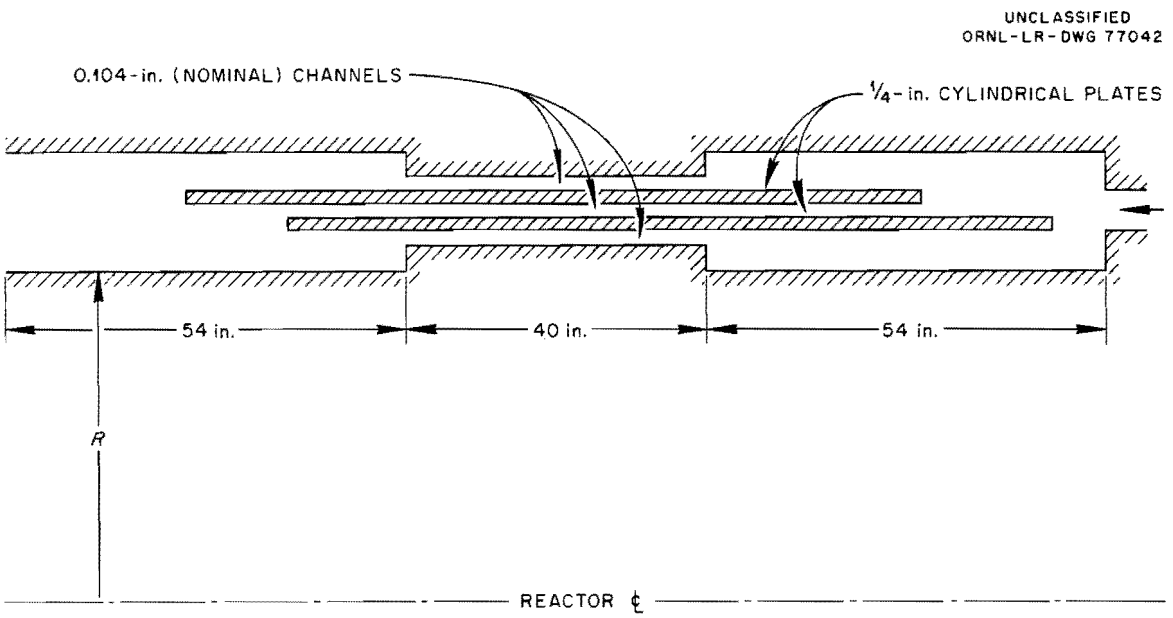


Fig. 7. HFIR Control-Rod Flow Scheme.

The results for two different flow combinations are illustrated in Figs. 8 and 9. The pressure differentials were apparently reduced in all cases, with the largest reductions occurring at mid-positions. The manner of obtaining a given set of flow conditions prevented the establishment of a meaningful reference point.

Coupled Parallel Flow with Nominally Equal Channels and Coupled Inlet and Exit

The flow scheme used consisted of two equal (1/8-in) channels coupled by inlet and exit plenums, as shown in Fig. 10. This configuration more closely approximates, but does not duplicate, the actual flow scheme (Fig. 7). Runs with total flow rates of 25 and 50 gpm were made, and static pressures were measured throughout both channels. A "no-hole" reference point was established for both flow rates.

It was found for both "reference point" runs that the manufacturing tolerances and other slight differences in the two channels did not generate appreciable pressure differentials. The channels were then further coupled by a pattern of 1/4-in. holes (two per row on 6-in. row centers) and the runs were repeated. Little change in the distribution and magnitude of the pressure differential was observed. The results for the 50-gpm runs are shown in Fig. 11. Apparently the holes had little influence on the flow.

Coupled Parallel Flow with Unequal Channels and Coupled Inlet and Exit

The flow scheme was evolved by increasing one channel thickness from 1/8 to 1/2 in. Other features of the flow scheme remained unchanged (Fig. 12). Much larger pressure differentials were observed; however, the hydraulic characteristics remained vastly different from those of the actual flow scheme (Fig. 7). Runs with total flow rates of 50 and 75 gpm were made, and static pressures were measured throughout both channels. A "no-hole" reference point was again established for the two flow rates.

The plate separating the two channels was then perforated with various patterns of 1/4-in. holes (two per row position on 6-, 4-, 2-, and 1-in. row centers, as shown in Fig. 13), and the runs were repeated for each

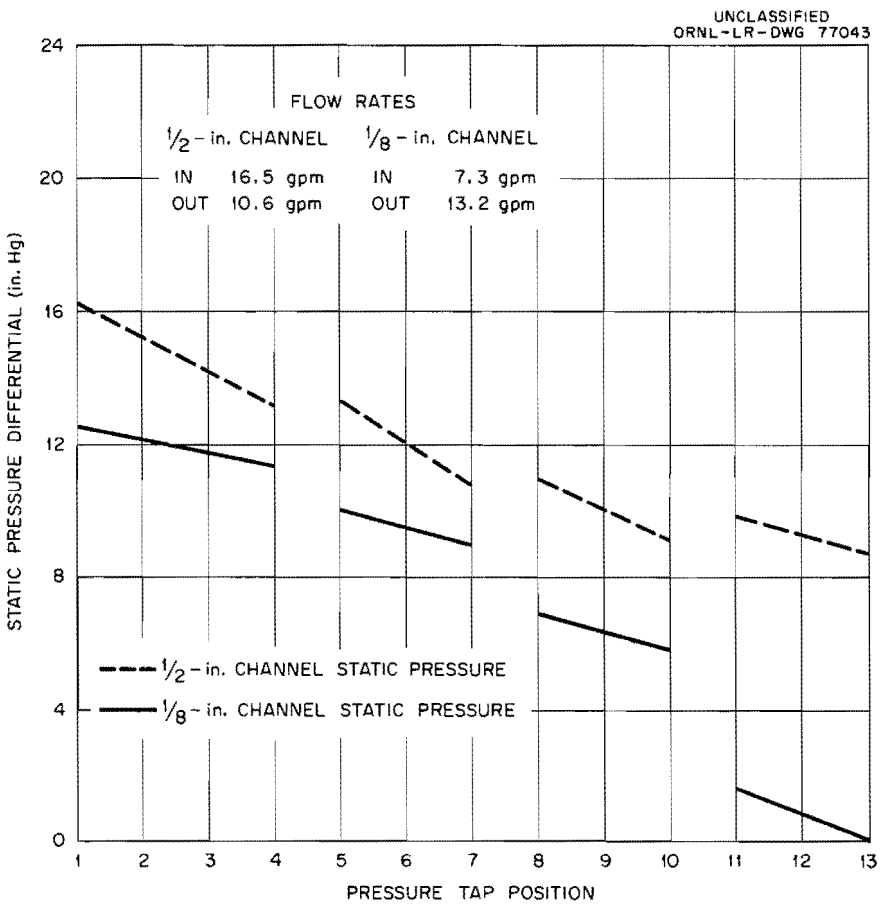


Fig. 8. Experimental Data for Noncoupled Inlet and Exit Configuration with Crossflow.

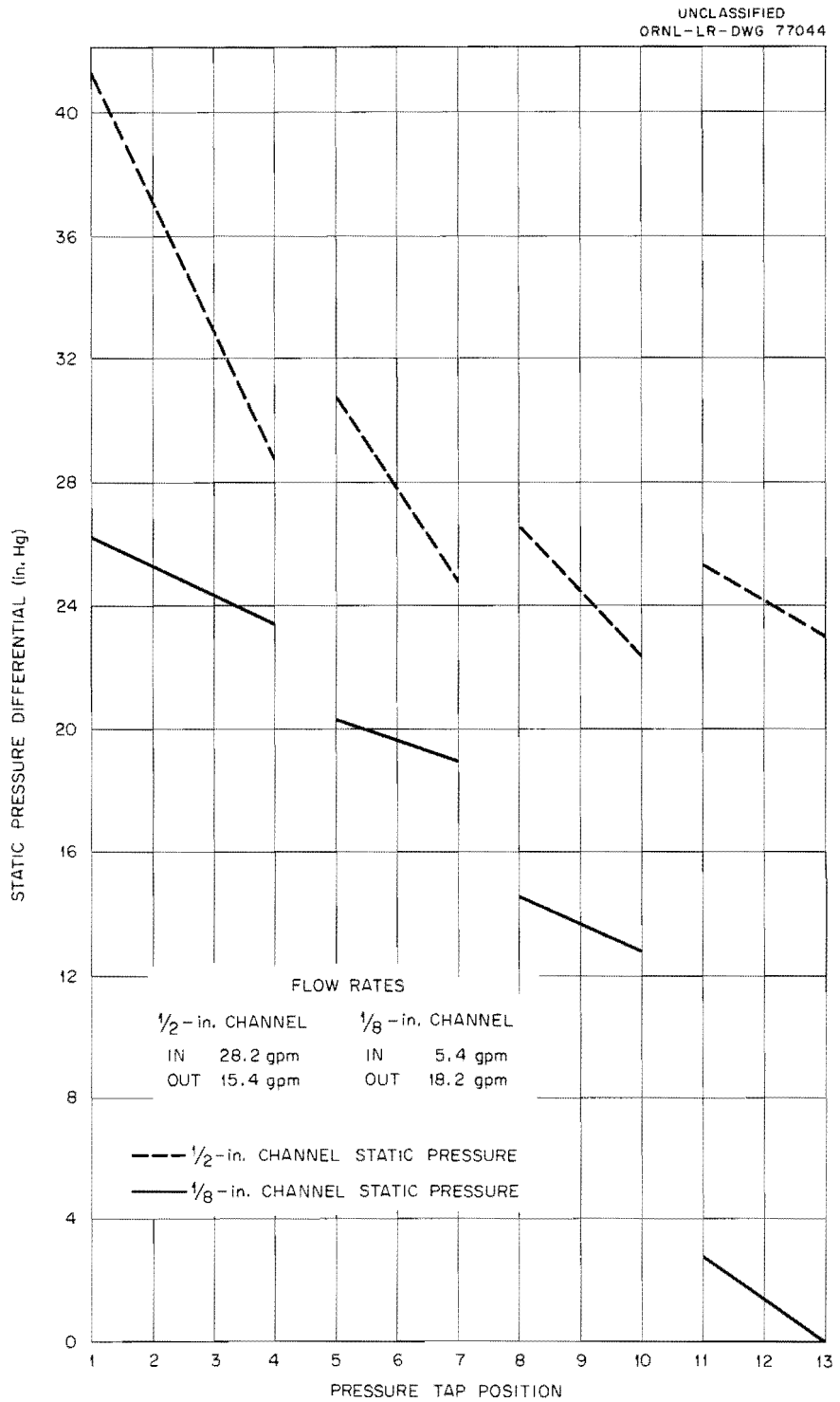


Fig. 9. Experimental Data for Noncoupled Inlet and Exit Configuration with Crossflow.

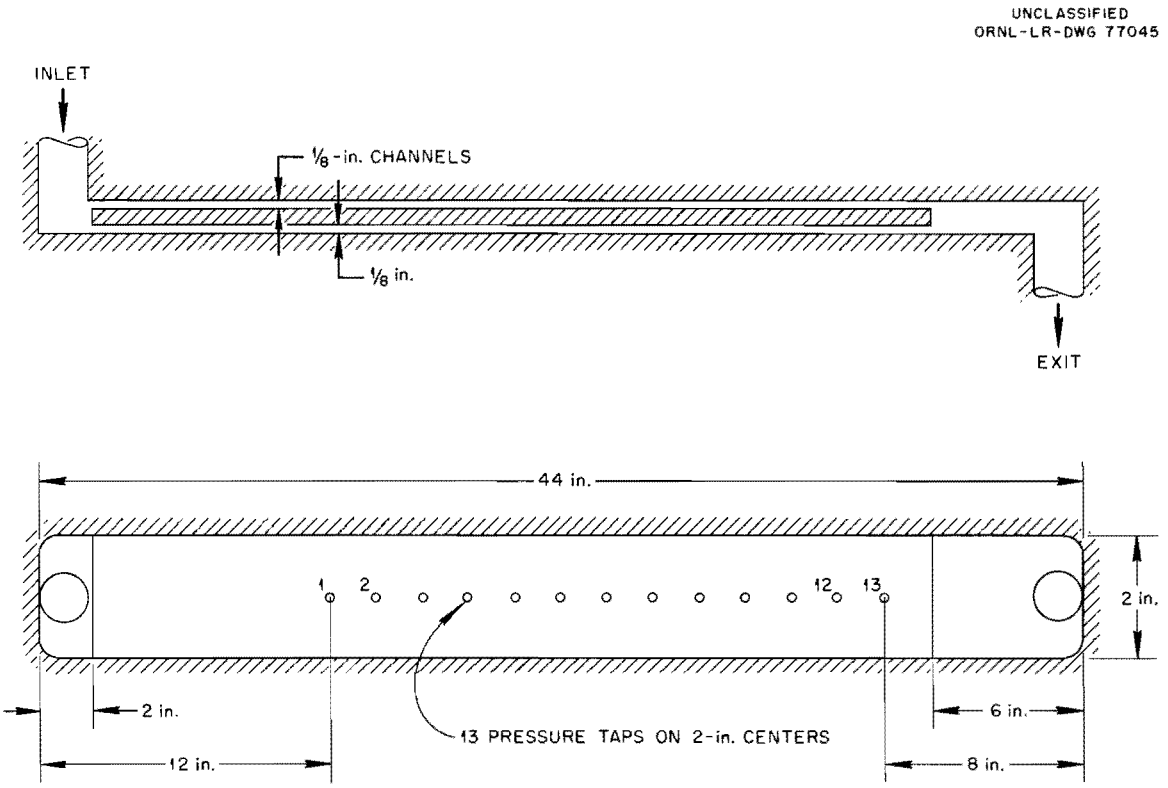


Fig. 10. Schematic Flow Diagram for Coupled Inlet and Exit and Equal Channel Thicknesses.

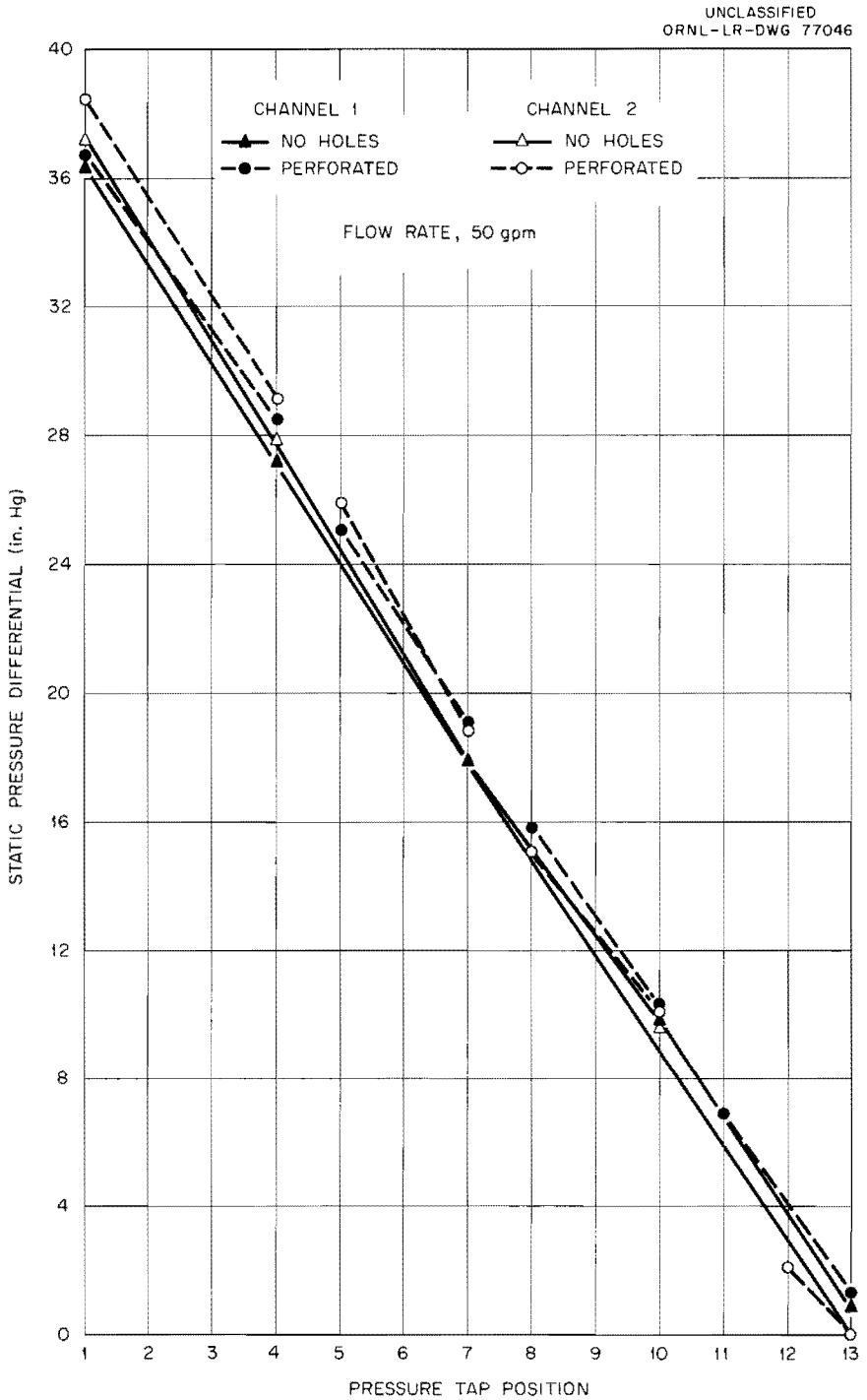


Fig. 11. Static Pressures for Equal Channel Thickness.

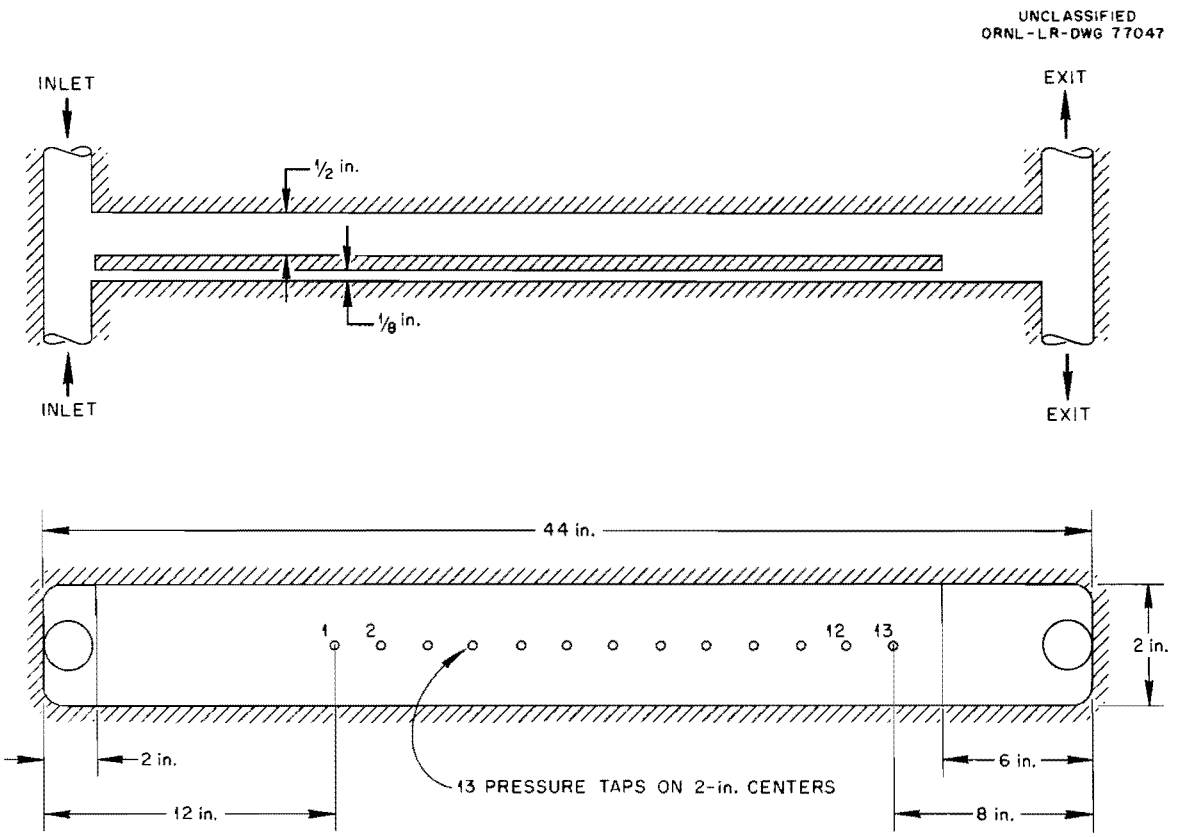


Fig. 12. Schematic Flow Diagram for Coupled Inlet and Exit and Unequal Channel Thicknesses.

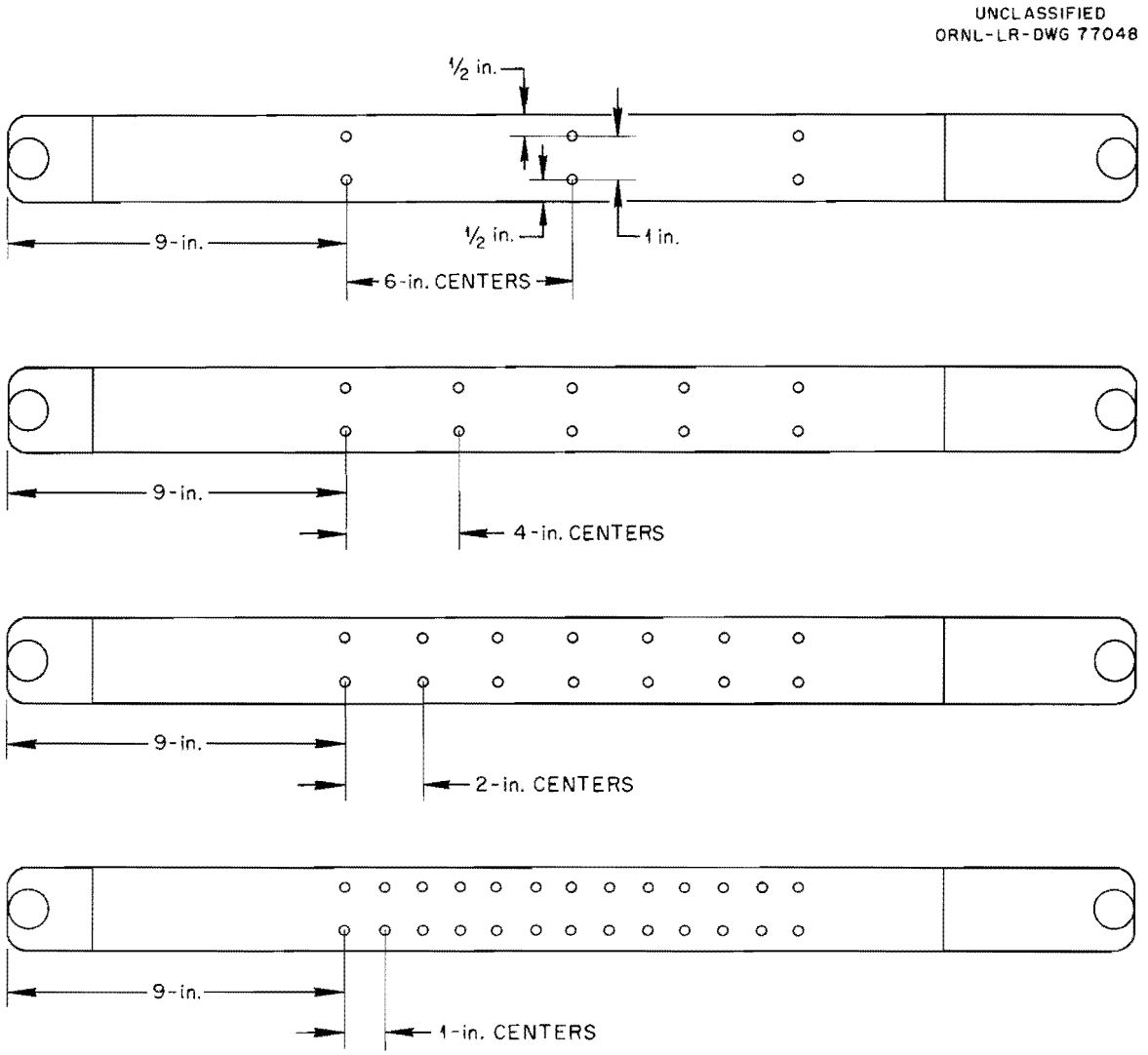


Fig. 13. Crossflow Hole Patterns.

pattern. The results for the 75-gpm runs are shown in Figs. 14 and 15. It is apparent that the pressure differentials were reduced in a consistent fashion as the number of holes increased. Figure 15 clearly indicates that an asymptotic behavior was being approached at about 24 holes (5% void); however, the point at which this asymptotic behavior occurs may well differ for different flow geometries. The pressure differentials near the entrance (region without holes) were little affected by the addition of holes elsewhere, indicating a need for holes throughout regions of high pressure differentials. These results show that the pressure differentials tend to equalize, as well as decrease, over the entire perforated region, with increased numbers of holes.

## Conclusions

It is concluded on the basis of these tests that a few holes, regardless of how carefully located, will not achieve an effective reduction of hydraulically induced pressure differentials, but many holes distributed in a uniform pattern throughout the plate can provide the desired effect. Unfortunately, usable design data were not obtained from these tests; however, it is estimated that a 1% hole pattern will reduce the pressure differentials by at least 50%, and a 5% hole pattern will reduce the pressure differentials by at least 80%. It is felt that these estimates are conservative and that the actual system hydraulic characteristics will be more receptive to pressure reduction. Also, other combinations of hole size or pattern or both (for a given void percentage) could be more effective.

The equipment used could not be modified to effect a significant improvement in the estimate of pressure reduction. Also, the poor hydraulic similarity with the actual flow system would make extrapolation doubtful. It was therefore deemed desirable to construct a more exact mockup of the actual system with respect to channel length and width.

## Phase III – Investigation of Crossflow Pressure Equalization

The more exact hydraulic mockup of two extreme control plate positions was utilized in accumulating flow-rate, hole-size, and hole-pattern

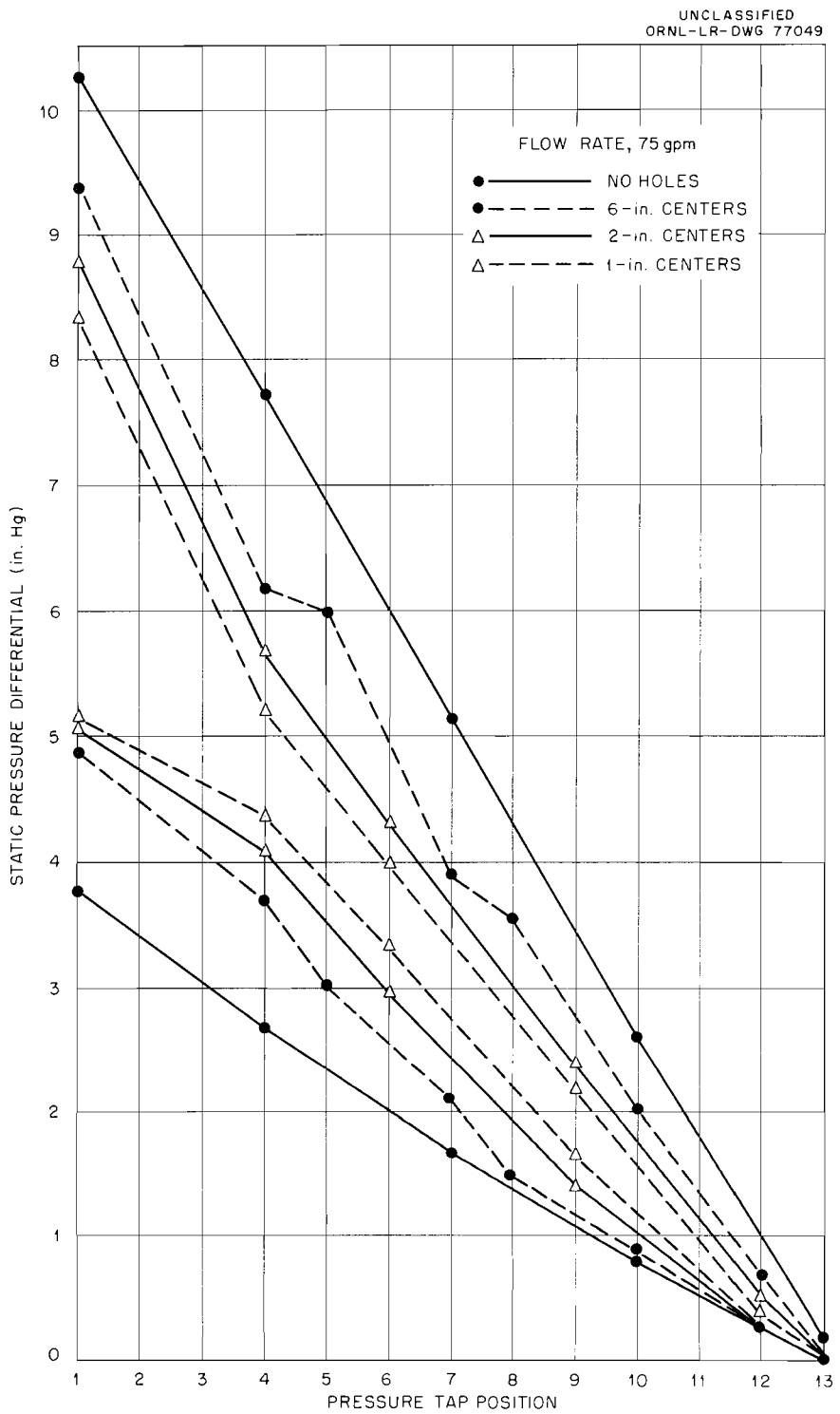


Fig. 14. Effect of Hole Patterns on Pressure Reductions.

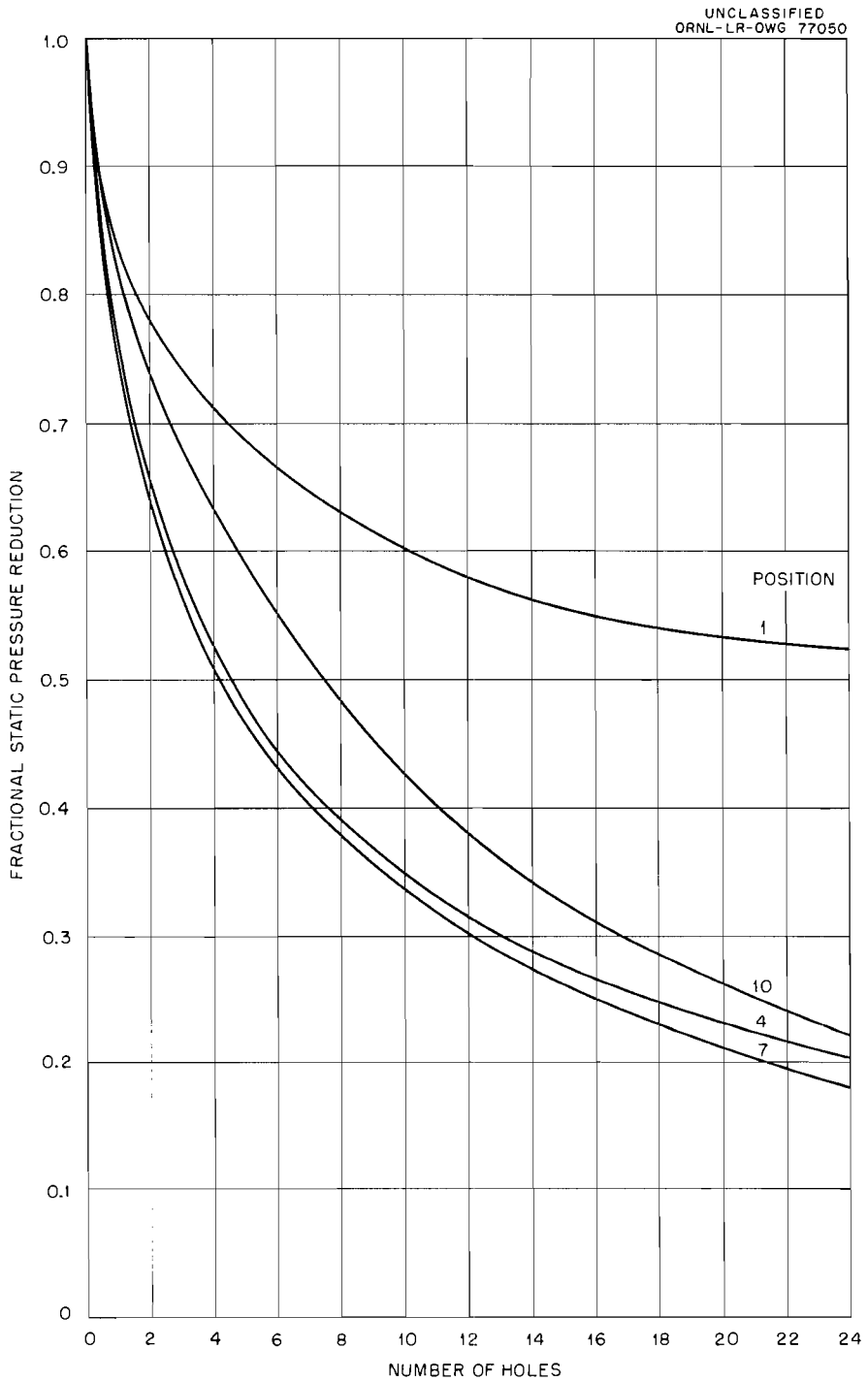


Fig. 15. Effect of Number of Holes on Static Pressure Reduction.

data to clearly establish the effect of crossflow on pressure equalization. The experimental setup was a mockup of the two channels adjacent to the outer control rod for two extreme geometries (Figs. 16 and 17). The 82-in.-long, 8-in.-wide rectangular channels were connected to common plenums at each end. One channel had a constant thickness of 1/8 in. for its entire length, and the other channel had a constant thickness of 1 5/8 in. for 40 in. and a step change to 1/8 in. for the remaining channel length.

The piping system was arranged to discharge flow from either plenum and thus simulate the two extreme flow geometries. A valve and rotameter on the inlet plenum controlled and measured the combined channel flow rates. Flow rate values of 75, 90, and 105 gpm were selected as representative of the expected operating range.

Pressure taps were included in each channel on 4-in. nominal longitudinal centers, with additional taps installed near cross-sectional area changes. The taps were connected to two manifold systems containing manometers for obtaining pressure distributions.

Tests were conducted on square-edge holes 1/8, 3/16, and 1/4 in. in diameter. Each hole size was arranged in a rectangular pattern in the 1/4-in. plate separating the two channels. The total area removed varied from 0.15 to 4.92% for the combined hole size and pattern variables.

A test series consisted of selecting a combination of geometry, hole size, and hole pattern and then measuring the longitudinal pressure distributions in both flow channels over the entire test section for each flow rate. A graph was then made of the measured pressure distributions in order to ascertain the effectiveness of crossflow on equalization relative to the corresponding "no-hole" reference point. The pressure distribution graphs for the reference points and range of variables considered are given in Appendix B.

## Results

The effectiveness of crossflow on pressure equalization is easily seen by a comparison of the pressure distributions with and without holes. The comparison is made on the integrated load outlined by the longitudinal pressure distribution in each channel. These loads were determined and

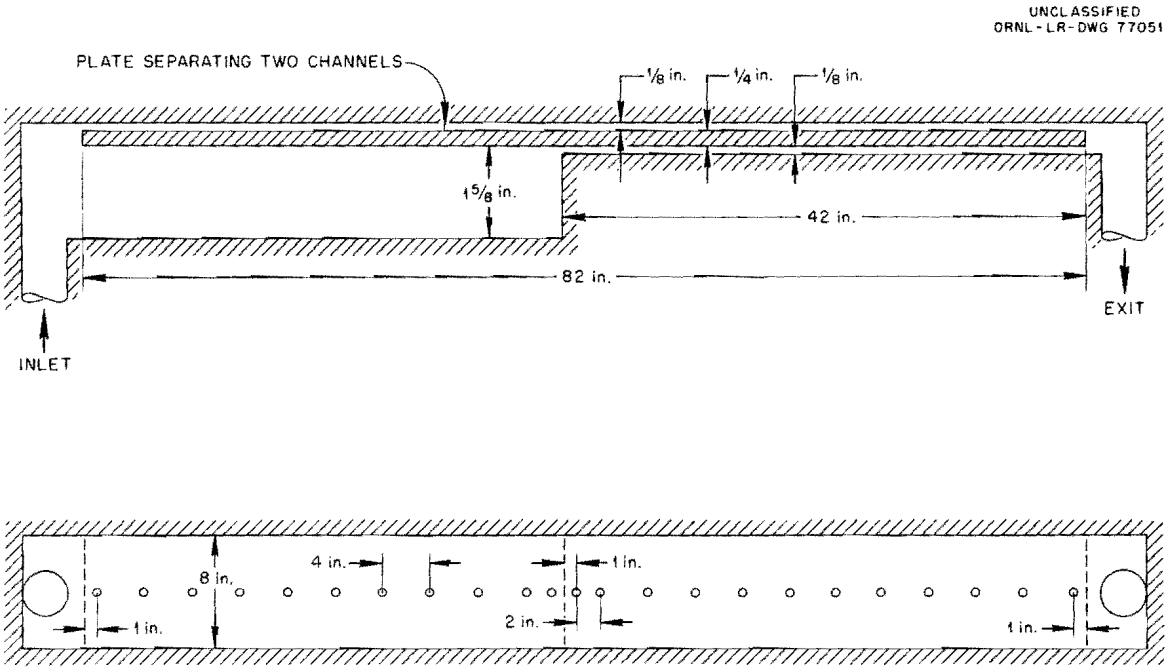


Fig. 16. Schematic Flow Diagram of Mockup No. 1.

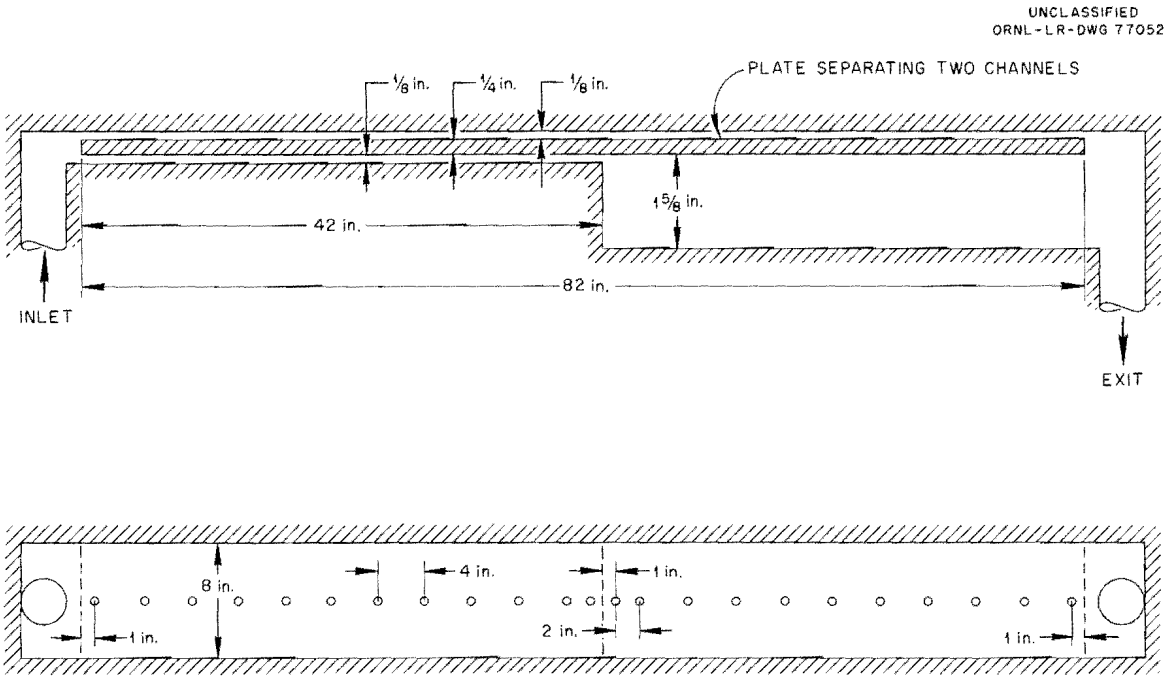


Fig. 17. Schematic Flow Diagram of Mockup No. 2.

used to calculate pressure reductions. Pressure reduction is defined as the ratio of the integrated load with holes to the integrated load without holes at corresponding geometries and flow rates. The pressure-reduction factors are given in Table 1 for all the cases examined experimentally, and Fig. 18 gives a comparison of pressure reductions as a function of void percentage (percentage of plate area occupied by holes; see Table 2) for the three flow rates and two flow configurations examined.

Table 1. Pressure Reductions Effected by Holes

| Geometry | Combined Flow Rate (gpm) | Hole Diameter (in.) | Pressure Reduction for Various Hole Spacings (%) | | | | |
|---|---|---|---|---|---|---|---|
| | | | 2 × 8[a] | 2 × 4 | 2 × 2 | 2 × 1 | 1 × 1 |
| Fig. 16 | 105 | 1/4 | 31.7 | 15.5 | 7.3 | 4.3 | 3.57 |
| | 105 | 3/16 | | 22.5 | 12.8 | | |
| | 105 | 1/8 | | 38.2 | 19.7 | 11.9 | |
| | 90 | 1/4 | 28.6 | 13.7 | 7.6 | 4.59 | 3.73 |
| | 90 | 3/16 | | 24.0 | 12.2 | | |
| | 90 | 1/8 | | 38.0 | 23.4 | 14.0 | |
| | 75 | 1/4 | 26.6 | 13.2 | 7.7 | 5.32 | 3.27 |
| | 75 | 3/16 | | 23.7 | 14.1 | | |
| | 75 | 1/8 | | 38.8 | 21.7 | 14.5 | |
| Fig. 17 | 105 | 1/4 | | | 9.2 | | |
| | 90 | 1/4 | | | 10.7 | | |
| | 75 | 1/4 | | | 9.4 | | |

[a]Hole centers given as center-to-center hole spacing (in.) perpendicular to flow direction followed by center-to-center hole spacing (in.) parallel to flow direction.

Dependence on hole size and void percentage was observed. The hole size and commensurate pattern had some effect on pressure reduction up to about 0.7% void. The smaller hole size with its more uniform distribution of area removed (for a given void percentage) gave a greater overall pressure reduction. There was no observable dependence on hole size for area removals greater than 0.7%. The greatest pressure reduction effects were realized at a small void percentage for all three hole sizes (i.e., for void percentages up to ~1%). Increased numbers of holes brought additional pressure reductions; not, however, in proportion to the area

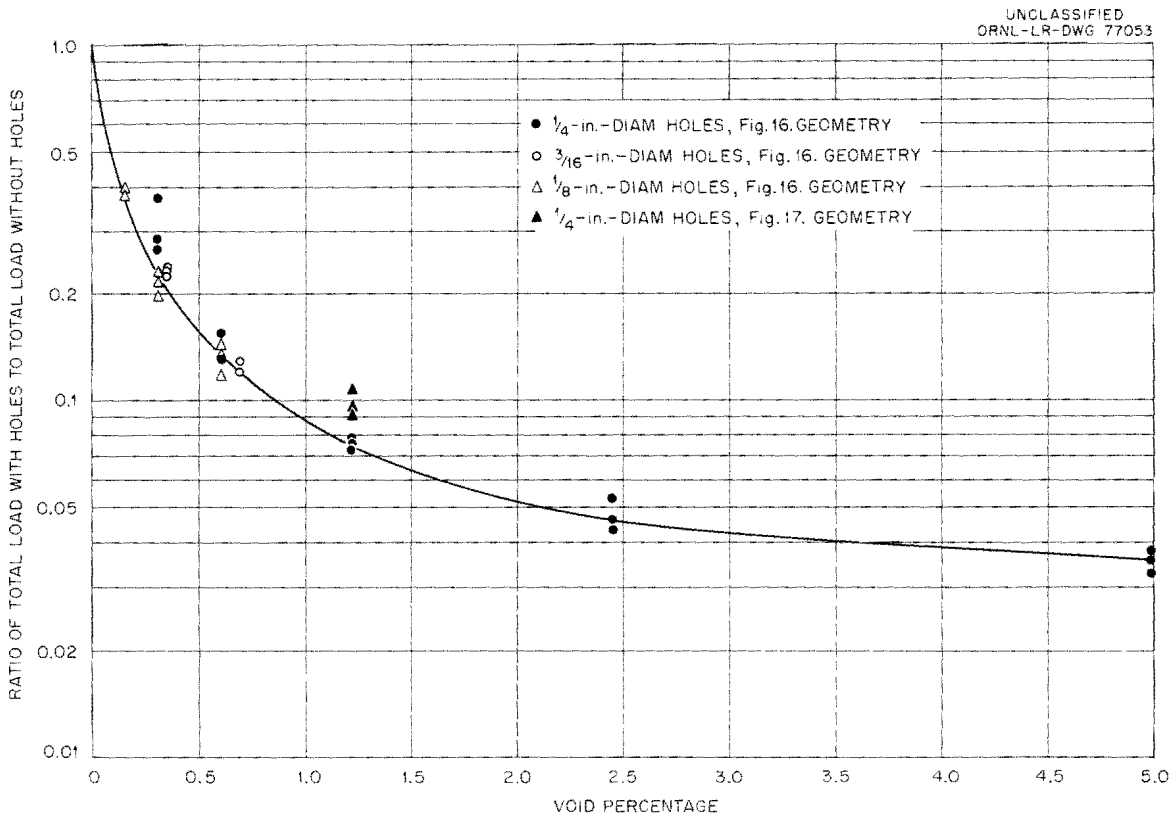


Fig. 18. Pressure Reduction Effect with Crossflow Holes.

Table 2. Plate Area Removed by Holes

| Hole Diameter (in.) | Void Obtained with Various Hole Spacings (%) | | | | |
|---|---|---|---|---|---|
| | 2 × 8[a] | 2 × 4 | 2 × 2 | 2 × 1 | 1 × 1 |
| 1/4 | 0.307 | 0.614 | 1.227 | 2.454 | 4.908 |
| 3/16 | | 0.345 | 0.690 | | |
| 1/8 | | 0.154 | 0.307 | 0.614 | |

[a]Hole centers given as center-to-center hole spacing (in.) perpendicular to flow direction followed by center-to-center hole spacing (in.) parallel to flow direction.

removed. A maximum pressure-reduction factor of about 30 was achieved in this experimental investigation at a void percentage of 5%.

## Conclusions

The ability of crossflow between two rectangular-parallel channels to reduce the pressure differentials was satisfactorily demonstrated, and design information was obtained for two extreme flow geometries. The pressure differentials were shown to be drastically effected by small percentages of plate-area removed from the plate separating the two channels. An order of magnitude in pressure reduction was easily effected by a 1% plate-area removal, and a factor of about 30 was achieved with a 5% area removal.

## Acknowledgments

The authors wish to express their appreciation for the competent assistance of W. H. Kelley, Jr., and G. M. Winn in the accumulation of the experimental data. Also, the authors extend their thanks to H. A. McLain and F. N. Peebles for reviewing the experimental results and for their many helpful suggestions.

## References

1. A. Acrivos, B. D. Babcock, and R. L. Pigford, "Flow Distributions in Manifolds," Chem. Eng. Sci., 10, 112–124 (1959).

2. B. R. Bronfin, D. J. Burkhart, and E. E. Wright, Jr., "Experimental Investigation of the Flow Rate Distribution from a Manifold with Wall Orifices," USAEC Report KT-556, M.I.T. Engineering Practice School, Union Carbide Nuclear Co., Dec. 21, 1960.

## Appendix A

### POTENTIAL AND ORIFICE COEFFICIENT DATA

The experimental data obtained in phase I for the determination of empirical constants for use in the proposed analytical model are presented in Tables A.1 and A.2.

## Appendix B

### PRESSURE DISTRIBUTIONS

The experimental pressure distributions obtained in phase III of this investigation for determining the effectiveness of crossflow are presented in Figs. 19 through 63.

Table A.1. Potential Coefficient Measurements

| Channel Thickness Combinations (in.) | Channel Giving up Mass | | | | Channel Gaining Mass | | | |
|---|---|---|---|---|---|---|---|---|
| | Flow Rate Before Holes (gpm) | Flow Rate After Holes (gpm) | Pressure Rise at Centerline of Holes (in. Hg) | Potential Coefficient, $\beta$ | Flow Rate Before Holes (gpm) | Flow Rate After Holes (gpm) | Pressure Drop at Centerline of Holes (in. Hg) | Potential Coefficient, $\gamma$ |
| 1/8 - 1/8 | 10.0 | 8.0 | 0.84 | 0.494 | 10.0 | 12.0 | 2.39 | 1.168 |
| 1/8 - 1/8 | 10.0 | 6.25 | 1.40 | 0.492 | 10.0 | 13.75 | 4.65 | 1.131 |
| 1/8 - 1/8 | 10.0 | 8.0 | 0.95 | 0.559 | 10.0 | 12.0 | 2.18 | 1.061 |
| 1/8 - 1/8 | 10.1 | 8.0 | 0.95 | 0.547 | 8.3 | 10.4 | 1.81 | 0.988 |
| 1/8 - 1/8 | 12.0 | 10.0 | 1.13 | 0.599 | 8.3 | 10.3 | 1.64 | 0.950 |
| 1/8 - 1/8 | 10.0 | 8.0 | 0.88 | 0.512 | 0.0 | 2.0 | 0.28 | 1.336 |
| 1/8 - 1/8 | 13.0 | 9.0 | 2.20 | 0.534 | 9.0 | 13.0 | 4.06 | 0.983 |
| 1/8 - 1/8 | 2.0 | 0.0 | 0.04 | 0.212 | 10.0 | 12.0 | 2.33 | 1.120 |
| 1/8 - 1/8 | 15.0 | 9.0 | 2.55 | 0.380 | 6.0 | 12.0 | 5.75 | 1.140 |
| 1/8 - 1/8 | 12.0 | 3.0 | 2.21 | 0.349 | 3.0 | 12.0 | 7.00 | 1.127 |
| 1/8 - 1/8 | 12.0 | 3.2 | 2.19 | 0.351 | 2.2 | 11.0 | 6.05 | 1.122 |
| 1/8 - 1/8 | 10.0 | 4.0 | 1.42 | 0.360 | 4.0 | 10.0 | 4.22 | 1.077 |
| 1/8 - 1/8 | 10.0 | 6.0 | 1.30 | 0.432 | 6.0 | 10.0 | 3.26 | 1.098 |
| 1/8 - 1/8 | 8.0 | 5.0 | 0.88 | 0.489 | 10.0 | 13.0 | 3.08 | 0.957 |
| 1/8 - 1/8 | 10.0 | 5.0 | 1.58 | 0.466 | 12.0 | 17.0 | 6.00 | 0.426 |
| 1/8 - 1/8 | 8.0 | 4.0 | 0.99 | 0.451 | 8.0 | 12.0 | 4.34 | 1.165 |
| 1/8 - 1/8 | 16.0 | 14.0 | 1.65 | 0.591 | 18.1 | 20.1 | 3.50 | 0.995 |
| 1/8 - 1/8 | 7.8 | 4.6 | 0.88 | 0.486 | 21.8 | 25.0 | 7.35 | 1.067 |
| 1/8 - 1/8[a] | 7.9 | 3.4 | 1.30 | 0.548 | 13.6 | 18.1 | 5.80 | 0.871 |
| 1/8 - 1/8[a] | 10.0 | 8.0 | 1.24 | 0.738 | 13.0 | 15.0 | 3.00 | 1.147 |
| 1/8 - 1/8[a] | 11.0 | 7.0 | 1.69 | 0.501 | 13.0 | 17.0 | 4.43 | 0.793 |
| 1/8 - 1/8[a] | 12.0 | 6.0 | 2.55 | 0.466 | 13.0 | 19.0 | 6.95 | 0.781 |
| 1/8 - 1/8[a] | 10.0 | 9.0 | 0.70 | 0.769 | 10.0 | 11.0 | 1.22 | 1.229 |
| 1/8 - 1/8[a] | 9.0 | 7.0 | 0.70 | 0.602 | 10.0 | 12.0 | 1.98 | 0.959 |
| 1/8 - 1/8[a] | 10.0 | 2.0 | 1.22 | 0.268 | 10.0 | 18.0 | 8.95 | 0.857 |
| 1/8 - 1/8[a] | 10.0 | 2.0 | 1.00 | 0.223 | 12.0 | 20.0 | 10.15 | 1.110 |
| 1/8 - 1/8[a] | 12.0 | 2.2 | 1.30 | 0.208 | 2.2 | 12.0 | 5.35 | 0.832 |
| 1/8 - 1/8[a] | 12.0 | 2.0 | 1.30 | 0.194 | 4.0 | 14.0 | 6.75 | 0.818 |
| 1/8 - 1/8[a] | 14.0 | 14.0 | 0.0 | | 14.0 | 14.0 | 0.0 | |
| 1/8 - 1/8[a] | 12.0 | 8.0 | 2.20 | 0.578 | 14.0 | 18.0 | 4.65 | 0.788 |
| 1/8 - 1/8[a] | 10.0 | 4.0 | 1.80 | 0.459 | 14.0 | 20.0 | 7.85 | 0.820 |
| 1/8 - 1/8[a] | 10.0 | 3.0 | 1.68 | 0.400 | 5.0 | 12.0 | 3.95 | 0.711 |
| 1/8 - 1/8[a] | 12.0 | 6.0 | 2.80 | 0.557 | 6.0 | 12.0 | 3.32 | 0.659 |
| 1/8 - 1/8[a] | 14.0 | 6.0 | 2.02 | 0.507 | 4.0 | 12.0 | 3.65 | 0.611 |

Table A.1. (Continued)

| Channel Thickness Combinations (in.) | Channel Giving up Mass | | | | Channel Gaining Mass | | | |
|---|---|---|---|---|---|---|---|---|
| | Flow Rate Before Holes (gpm) | Flow Rate After Holes (gpm) | Pressure Rise at Centerline of Holes (in. Hg) | Potential Coefficient, $\beta$ | Flow Rate Before Holes (gpm) | Flow Rate After Holes (gpm) | Pressure Drop at Centerline of Holes (in. Hg) | Potential Coefficient, $\alpha$ |
| 1/8 - 1/2 | 9.8 | 5.7 | 0.07[b] | 0.580 | 9.1 | 13.2 | 3.91 | 0.918 |
| 1/8 - 1/2 | 14.5 | 5.8 | 0.22[b] | 0.614 | 6.8 | 15.5 | 7.82 | 1.083 |
| 1/8 - 1/2 | 10.0 | 3.0 | 0.11[b] | 0.473 | 3.0 | 10.0 | 4.01 | 0.944 |
| 1/8 - 1/2 | 12.0 | 7.7 | 0.10[b] | 0.571 | 11.7 | 16.0 | 5.64 | 1.016 |
| 1/8 - 1/2 | 12.0 | 10.0 | 0.09[b] | 0.780 | 14.0 | 16.0 | 2.89 | 1.032 |

[a]Longitudinal slot having a length-to-width ratio of 10:1 and an area equivalent to three 1/4-in.-diam holes.

[b]Pressure rise is given in inches of water.

Table A.2. Orifice Coefficient Measurements

| Channel Thickness Combinations (in.) | Flow Rate Through Holes (gpm) | Average Pressure Difference Between Channels at Center-line of Holes (in. Hg) | Orifice Coefficient, C |
|---|---|---|---|
| 1/8 - 1/8 | 2.0 | 3.70 | 0.265 |
| 1/8 - 1/8 | 3.75 | 11.43 | 0.283 |
| 1/8 - 1/8 | 2.0 | 2.95 | 0.297 |
| 1/8 - 1/8 | 2.1 | 2.77 | 0.322 |
| 1/8 - 1/8 | 2.0 | 2.79 | 0.303 |
| 1/8 - 1/8 | 2.0 | 0.97 | 0.518 |
| 1/8 - 1/8 | 4.0 | 7.13 | 0.287 |
| 1/8 - 1/8 | 2.0 | 2.51 | 0.322 |
| 1/8 - 1/8 | 6.0 | 12.24 | 0.437 |
| 1/8 - 1/8 | 9.0 | 17.54 | 0.546 |
| 1/8 - 1/8 | 8.8 | 16.65 | 0.551 |
| 1/8 - 1/8 | 6.0 | 9.04 | 0.501 |
| 1/8 - 1/8 | 4.0 | 5.92 | 0.420 |
| 1/8 - 1/8 | 3.0 | 4.18 | 0.375 |
| 1/8 - 1/8 | 5.0 | 9.01 | 0.426 |
| 1/8 - 1/8 | 4.0 | 7.00 | 0.386 |
| 1/8 - 1/8 | 2.0 | 5.18 | 0.225 |
| 1/8 - 1/8 | 3.2 | 8.87 | 0.274 |
| 1/8 - 1/8[a] | 4.5 | 6.20 | 0.460 |
| 1/8 - 1/8[a] | 2.0 | 5.77 | 0.212 |
| 1/8 - 1/8[a] | 4.0 | 5.79 | 0.423 |
| 1/8 - 1/8[a] | 6.0 | 9.08 | 0.507 |
| 1/8 - 1/8[a] | 1.0 | 1.48 | 0.210 |
| 1/8 - 1/8[a] | 2.0 | 2.40 | 0.334 |
| 1/8 - 1/8[a] | 8.0 | 19.47 | 0.463 |
| 1/8 - 1/8[a] | 8.0 | 19.28 | 0.465 |
| 1/8 - 1/8[a] | 9.8 | 26.88 | 0.478 |
| 1/8 - 1/8[a] | 10.0 | 28.28 | 0.480 |
| 1/8 - 1/8[a] | 0 | 0 | |
| 1/8 - 1/8[a] | 4.0 | 6.28 | 0.409 |
| 1/8 - 1/8[a] | 6.0 | 8.88 | 0.514 |
| 1/8 - 1/8[a] | 7.0 | 7.95 | 0.634 |
| 1/8 - 1/8[a] | 6.0 | 7.49 | 0.559 |
| 1/8 - 1/8[a] | 8.0 | 10.38 | 0.607 |
| 1/8 - 1/2 | 4.1 | 4.68 | 0.482 |
| 1/8 - 1/2 | 8.7 | 13.97 | 0.571 |
| 1/8 - 1/2 | 7.0 | 7.92 | 0.633 |
| 1/8 - 1/2 | 4.3 | 6.71 | 0.405 |
| 1/8 - 1/2 | 2.0 | 2.81 | 0.303 |

[a]Longitudinal slot having a length-to-width ratio of 10:1 and an area equivalent to three 1/4-in.-diam holes.

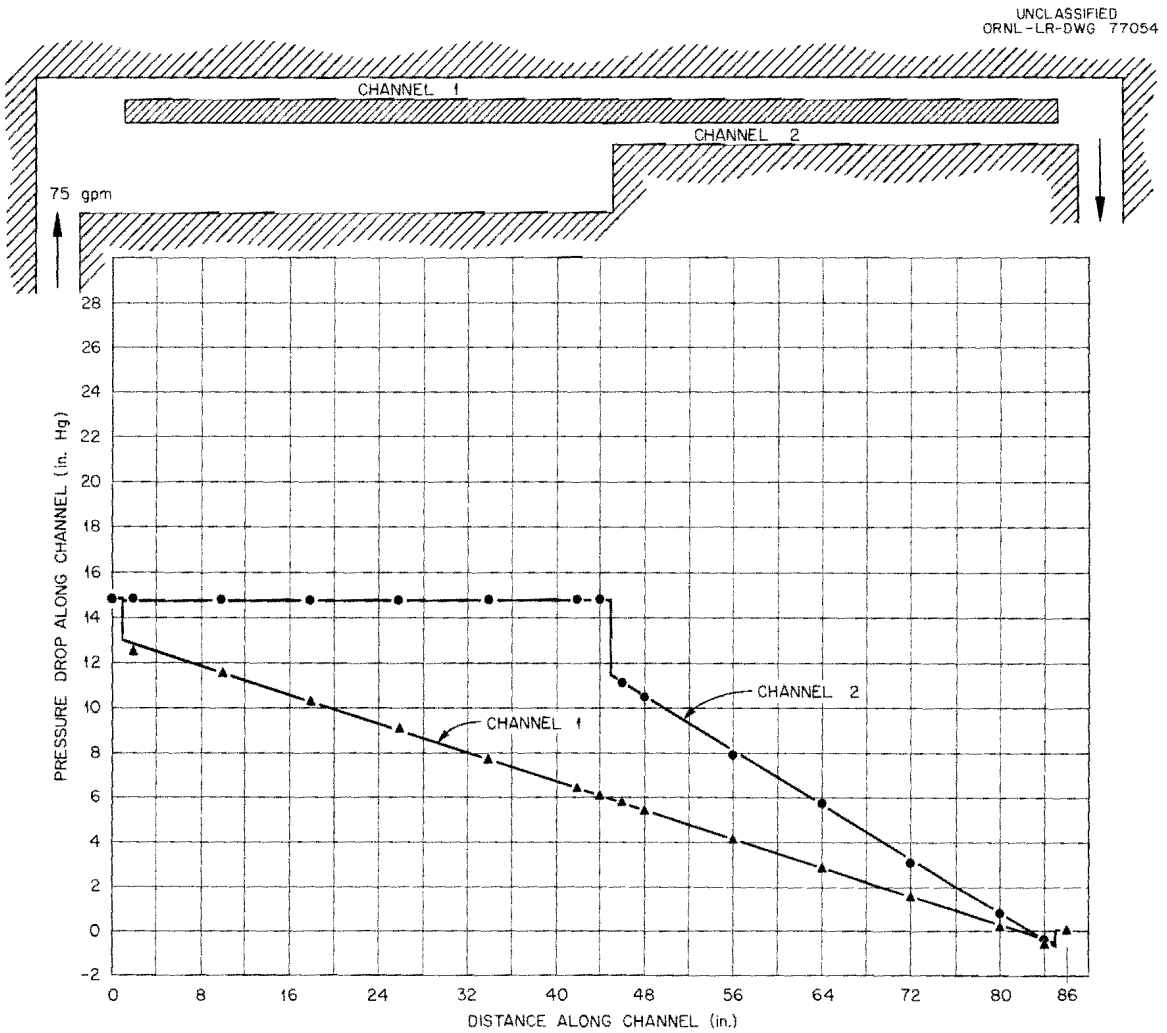


Fig. 19. Pressure Drop for Parallel Channels with No Holes.

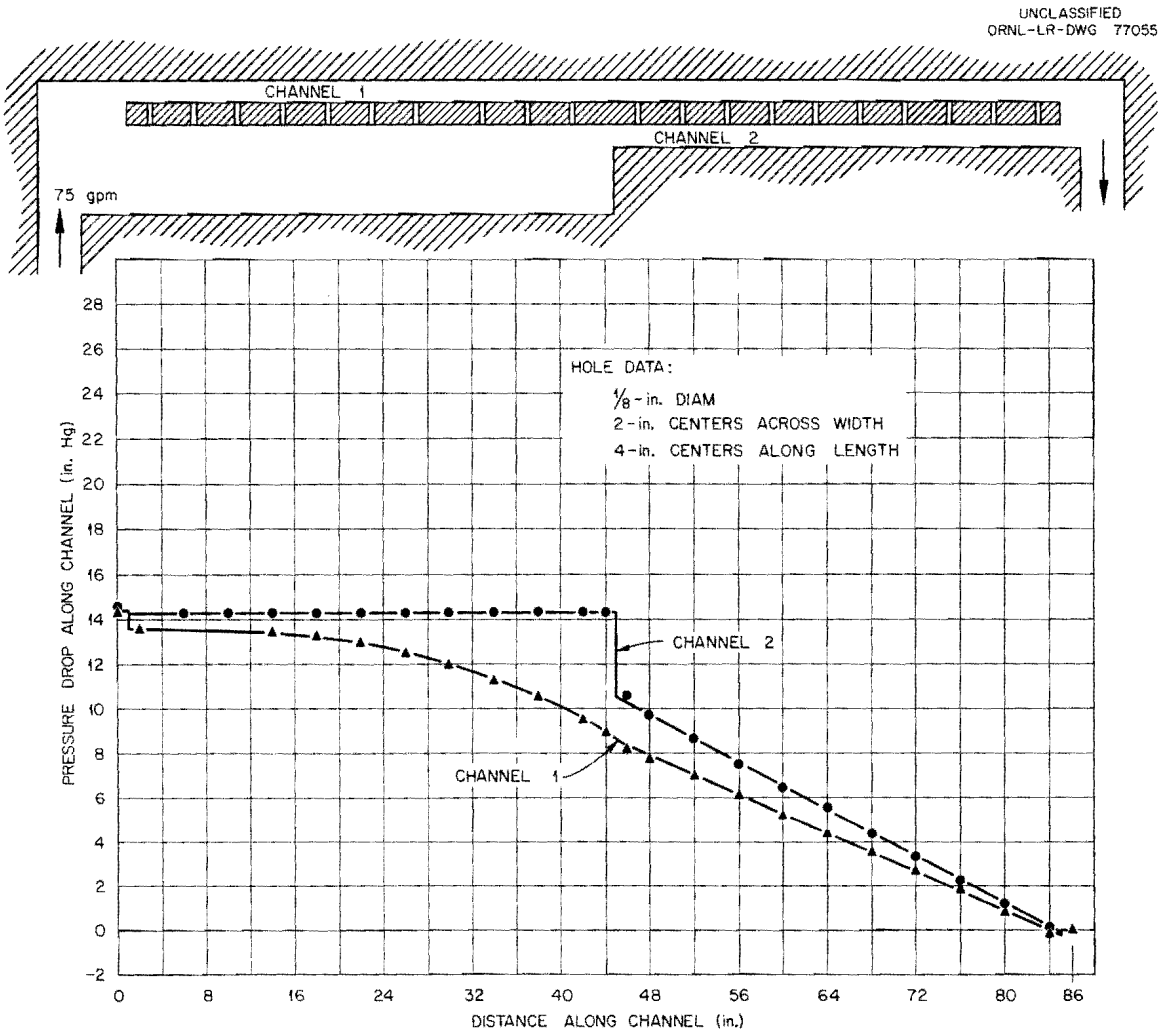


Fig. 20. Pressure Drop for Parallel Channels with 0.154% of Plate Area Occupied by Holes.

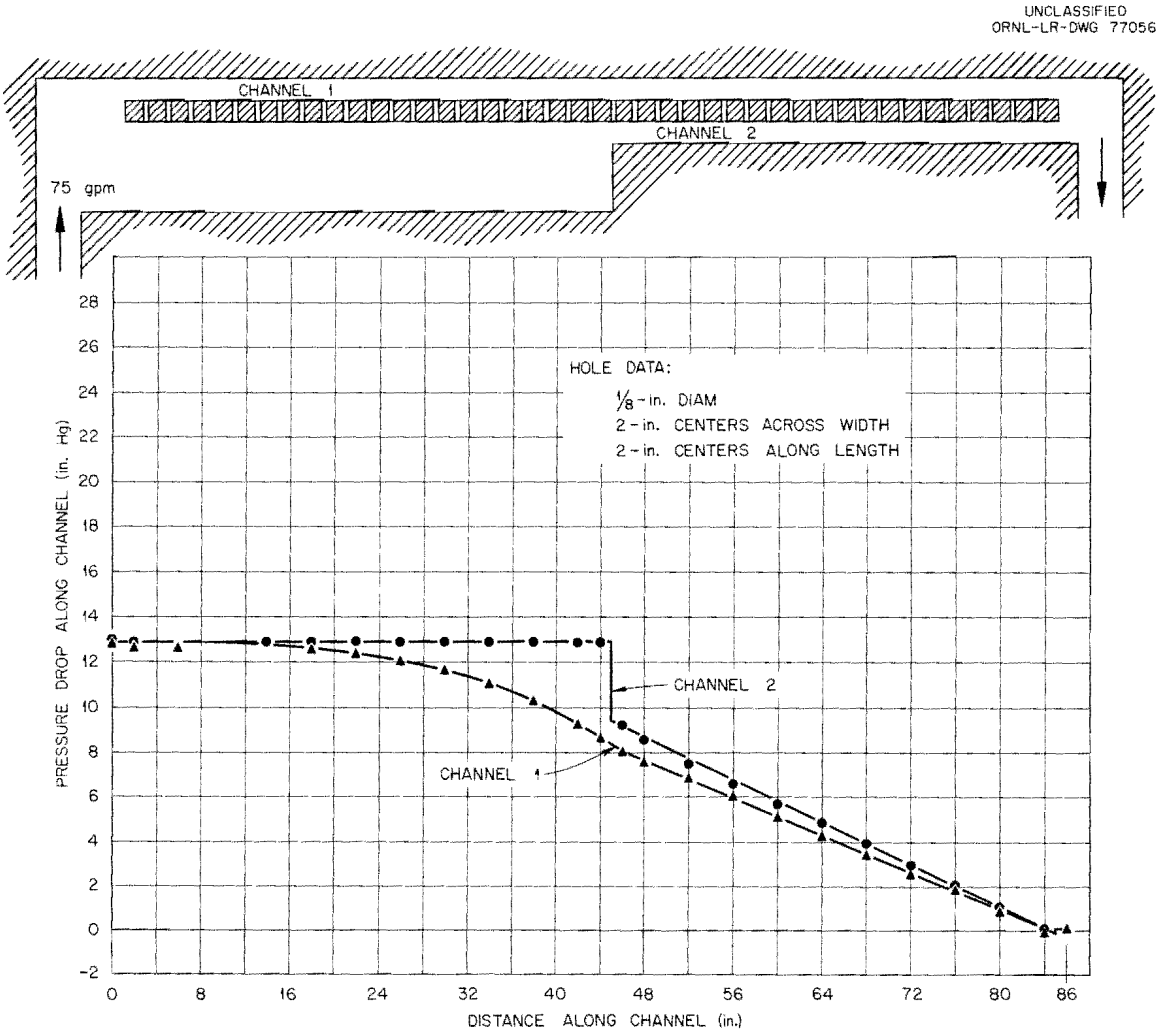


Fig. 21. Pressure Drop for Parallel Channels with 0.307% of Plate Area Occupied by Holes.

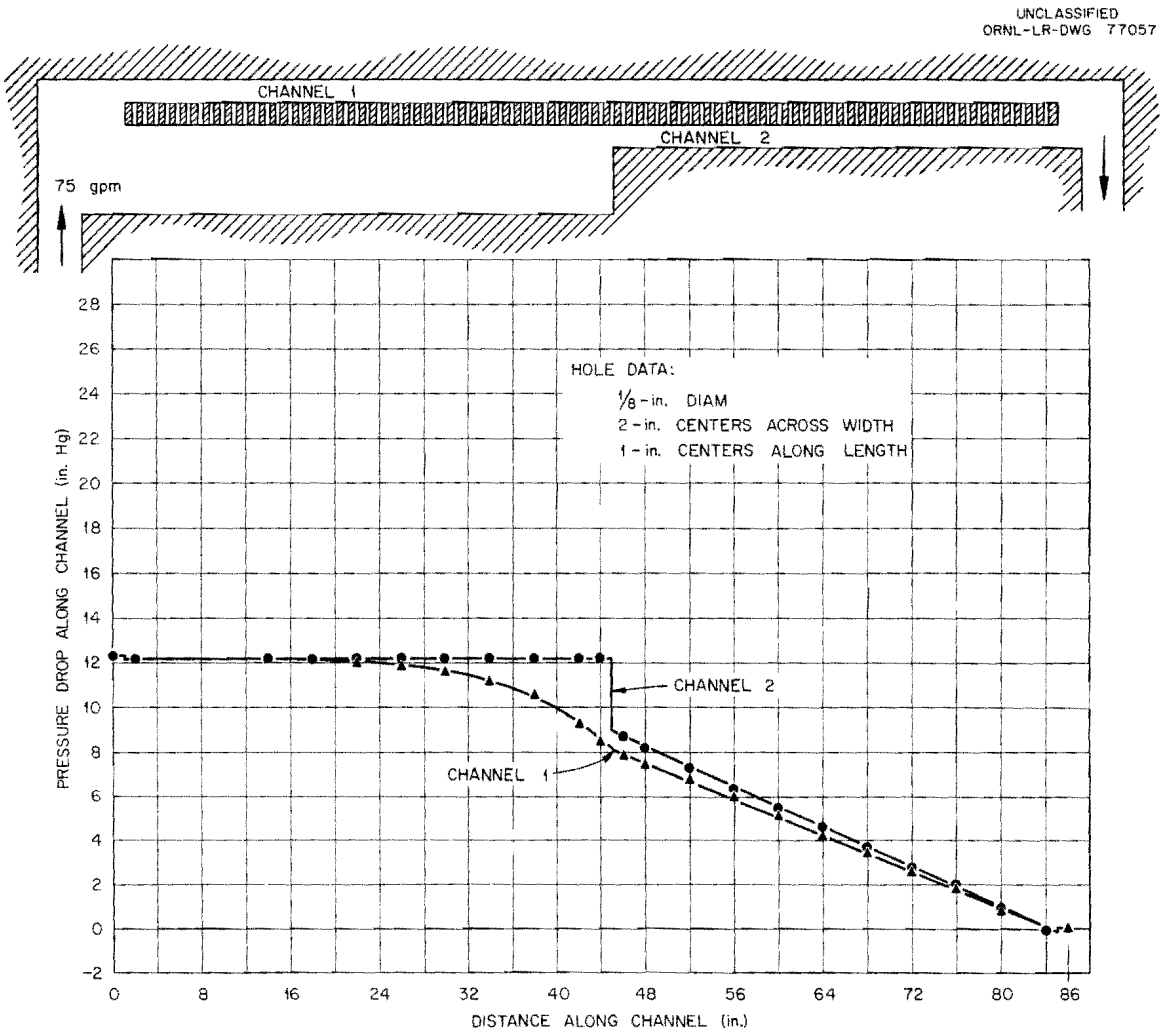


Fig. 22. Pressure Drop for Parallel Channels with 0.614% of Plate Area Occupied by Holes.

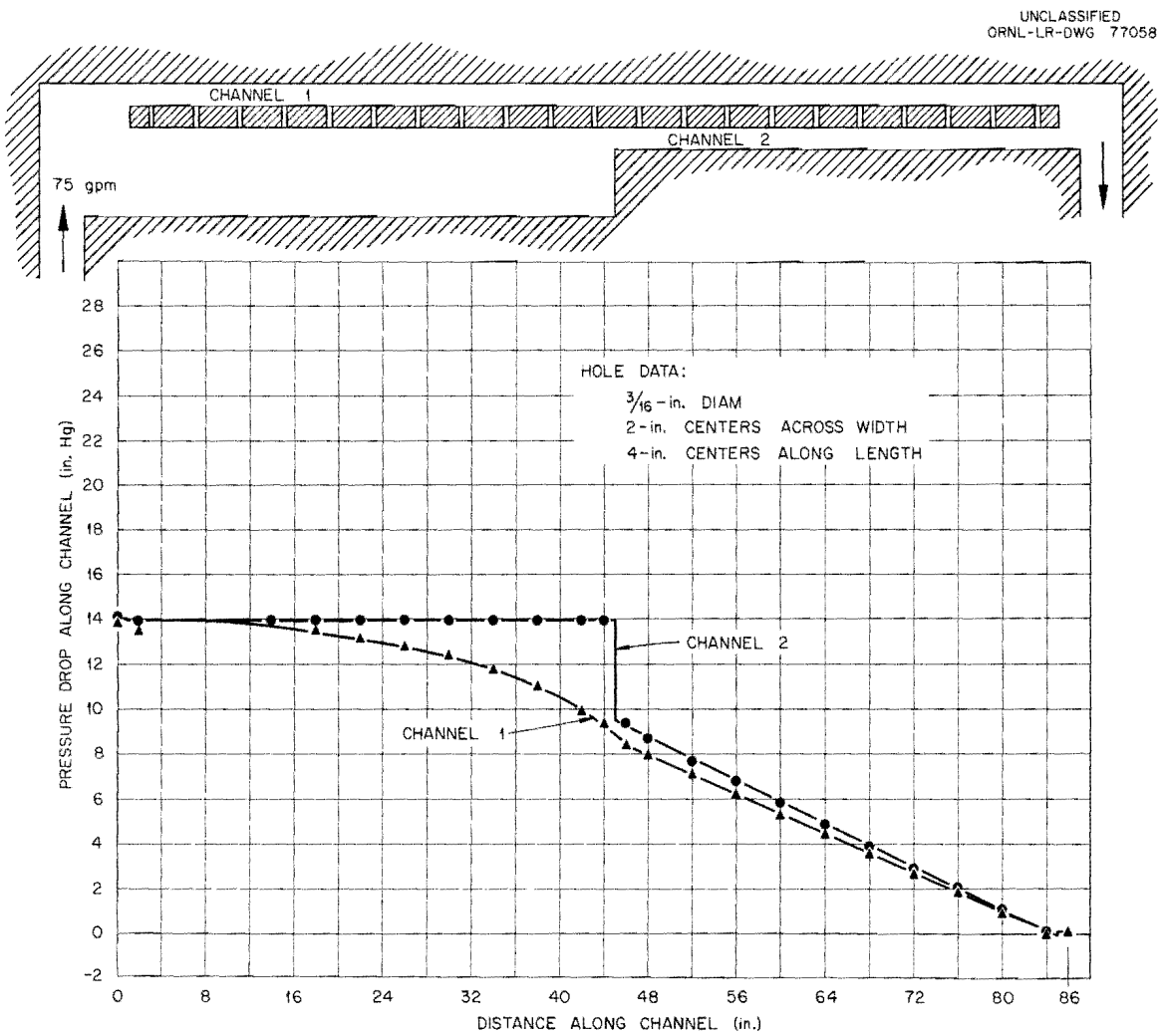


Fig. 23. Pressure Drop for Parallel Channels with 0.345% of Plate Area Occupied by Holes.

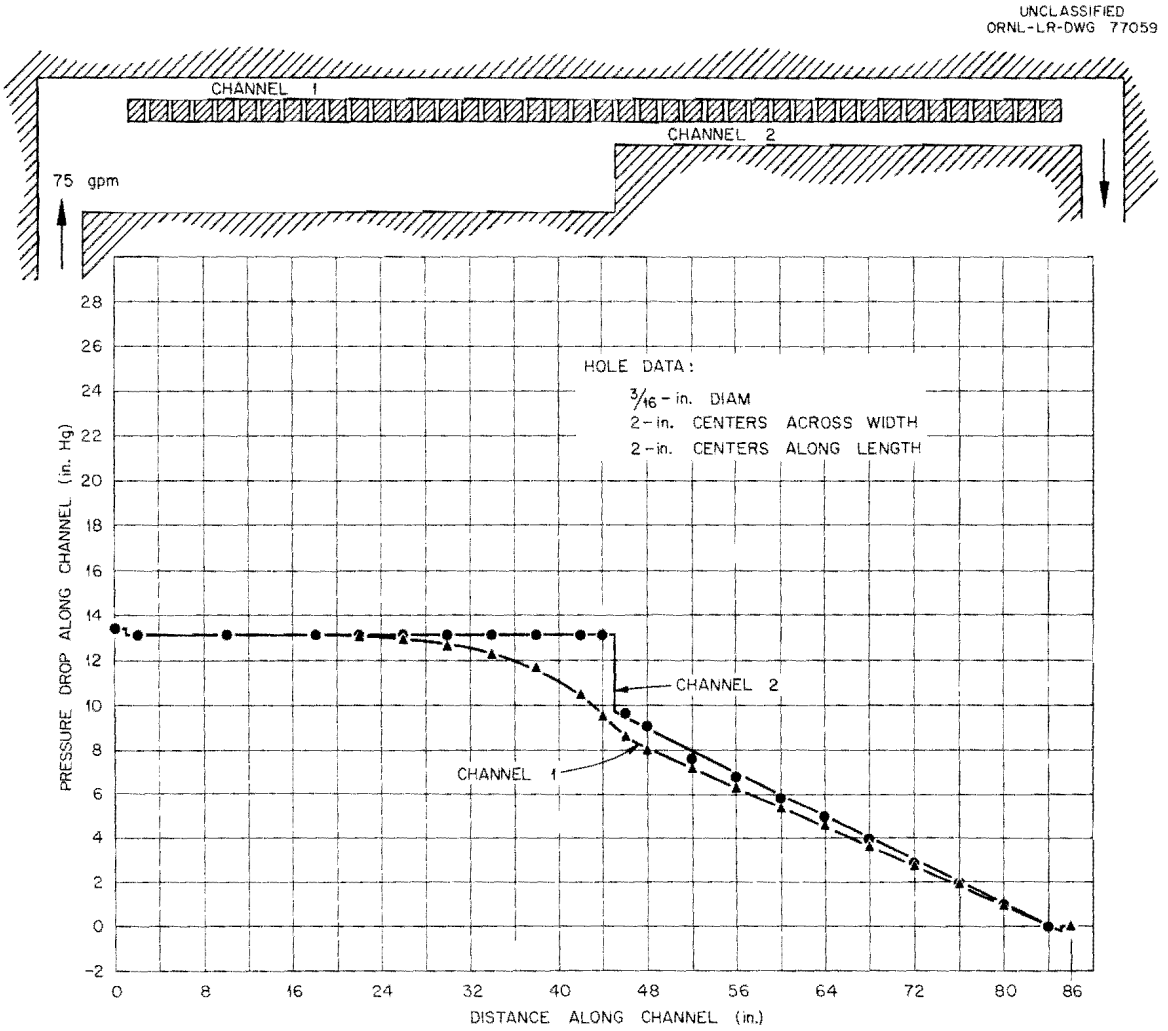


Fig. 24. Pressure Drop for Parallel Channels with 0.690% of Plate Area Occupied by Holes.

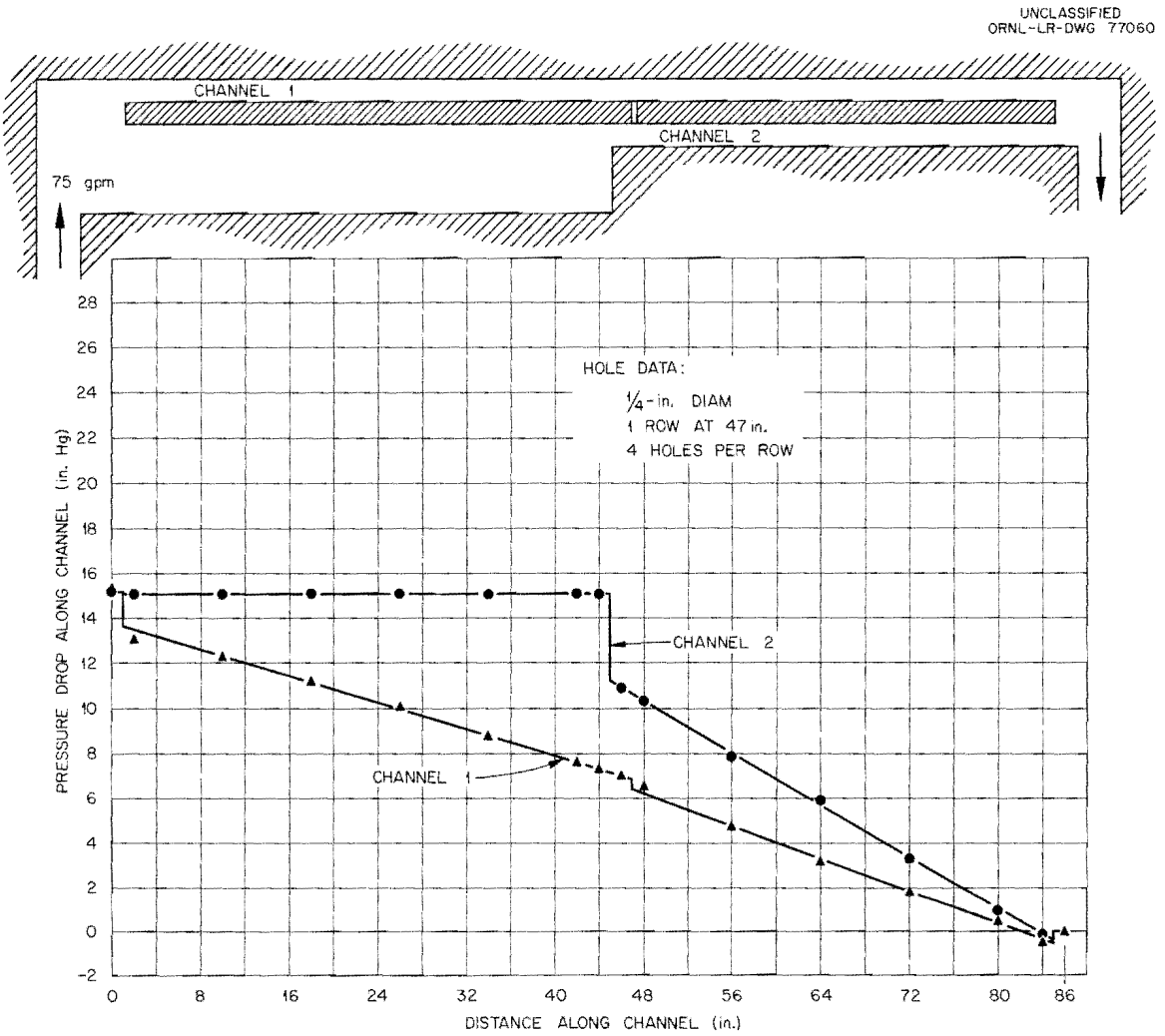


Fig. 25. Pressure Drop for Parallel Channels with Four Connecting Holes.

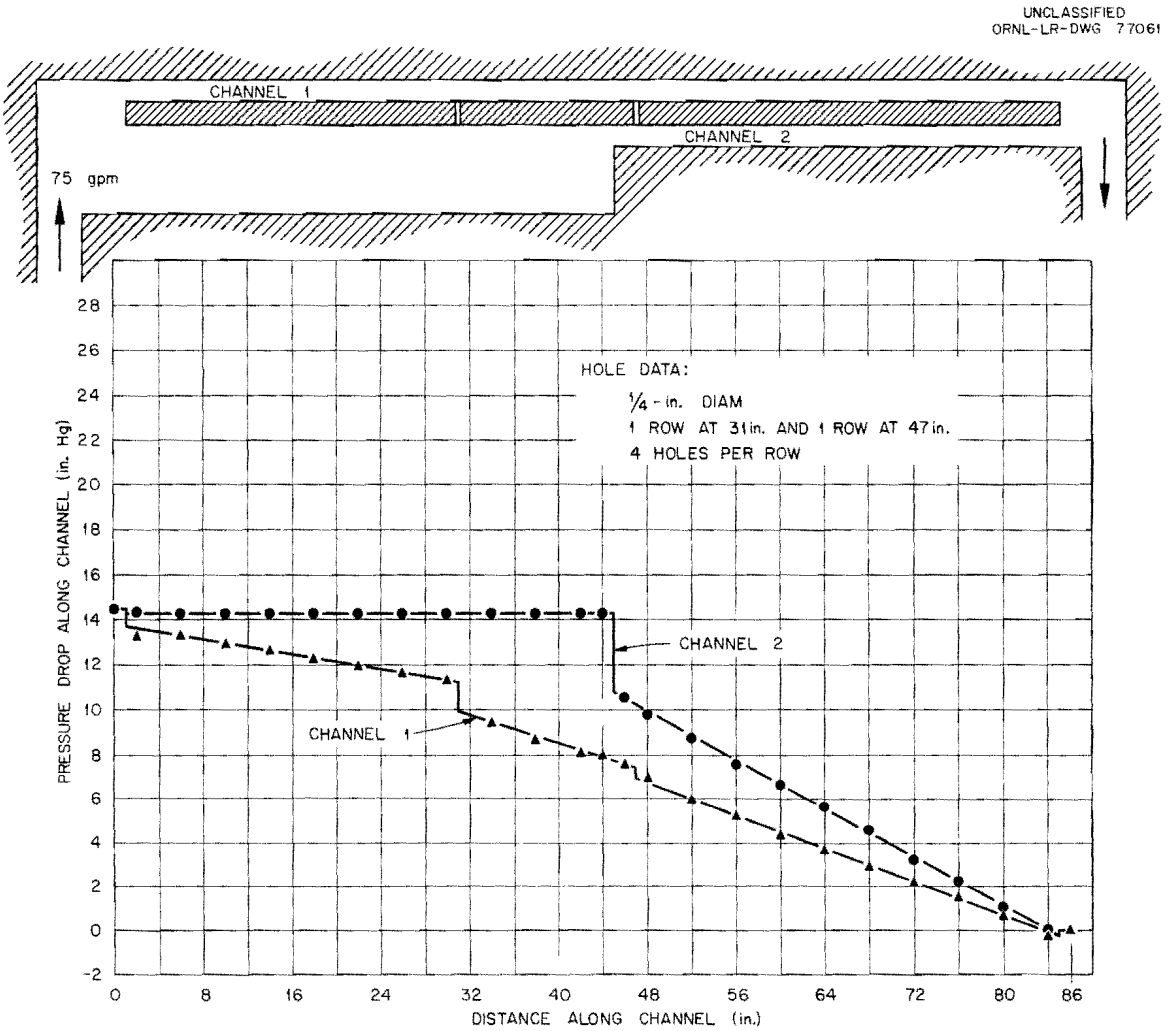


Fig. 26. Pressure Drop for Parallel Channels with Eight Connecting Holes.

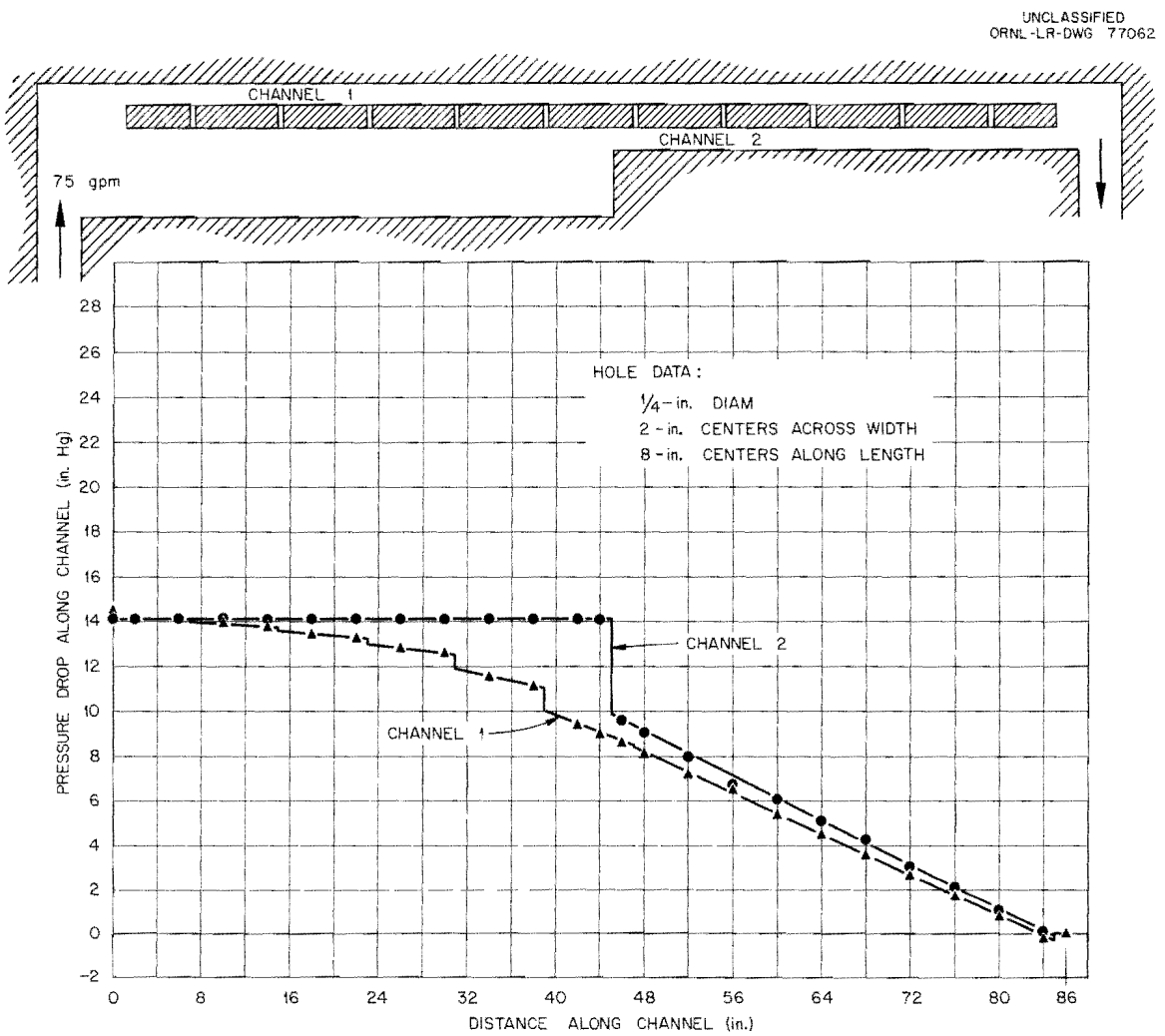


Fig. 27. Pressure Drop for Parallel Channels with 0.307% of Plate Area Occupied by Holes.

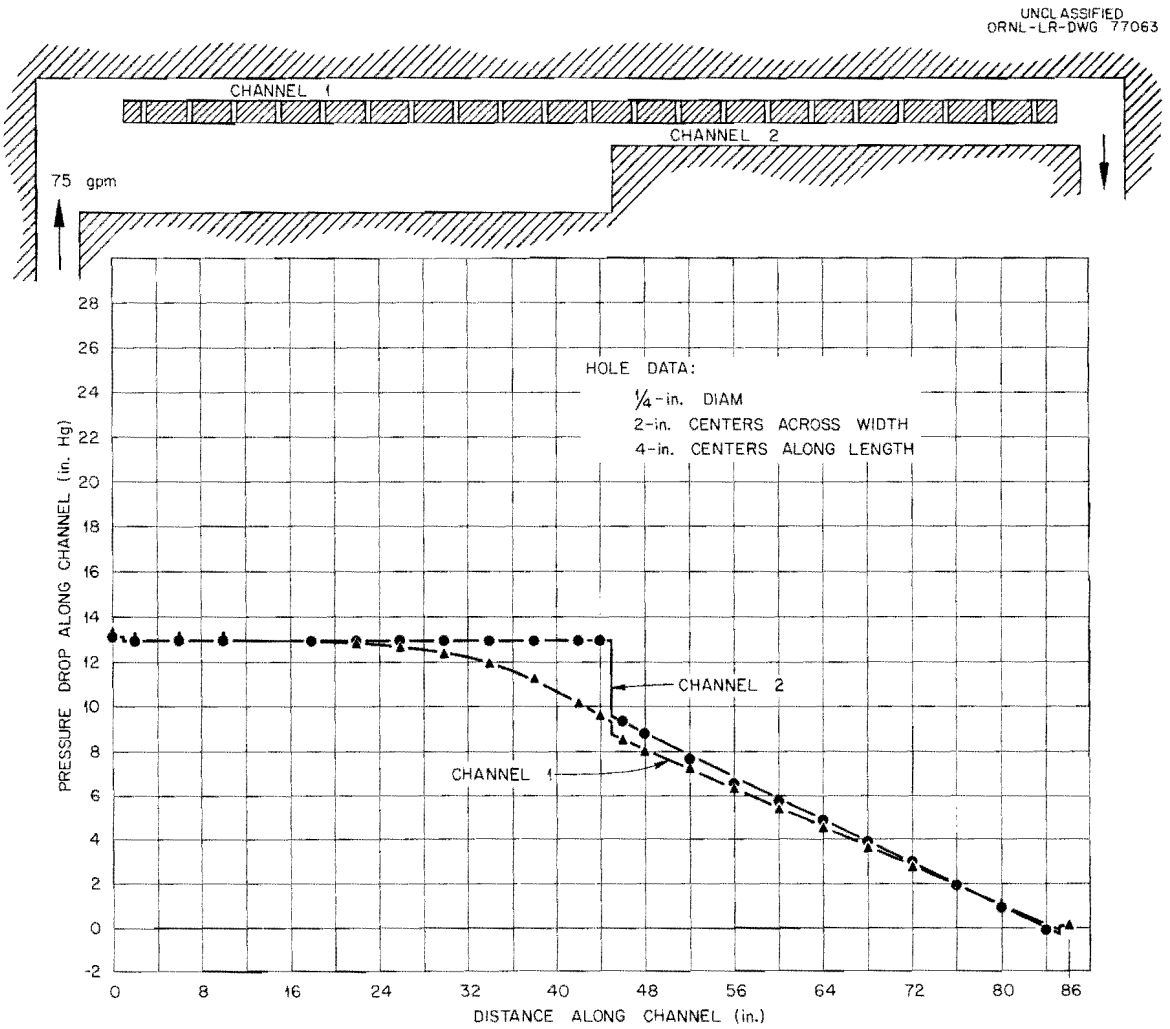


Fig. 28. Pressure Drop for Parallel Channels with 0.614% of Plate Area Occupied by Connecting Holes.

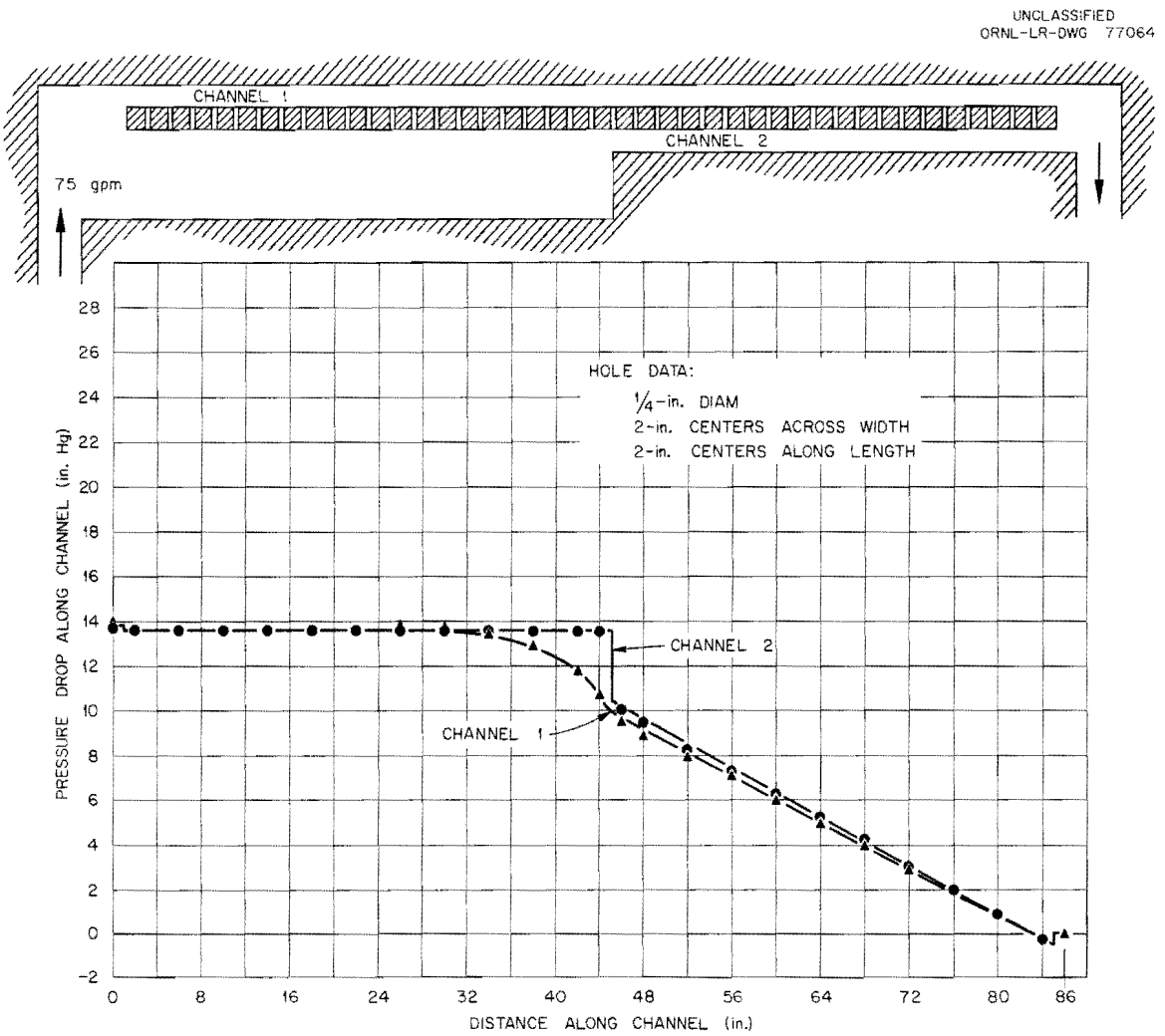


Fig. 29. Pressure Drop for Parallel Channels with 1.227% of Plate Area Occupied by Connecting Holes.

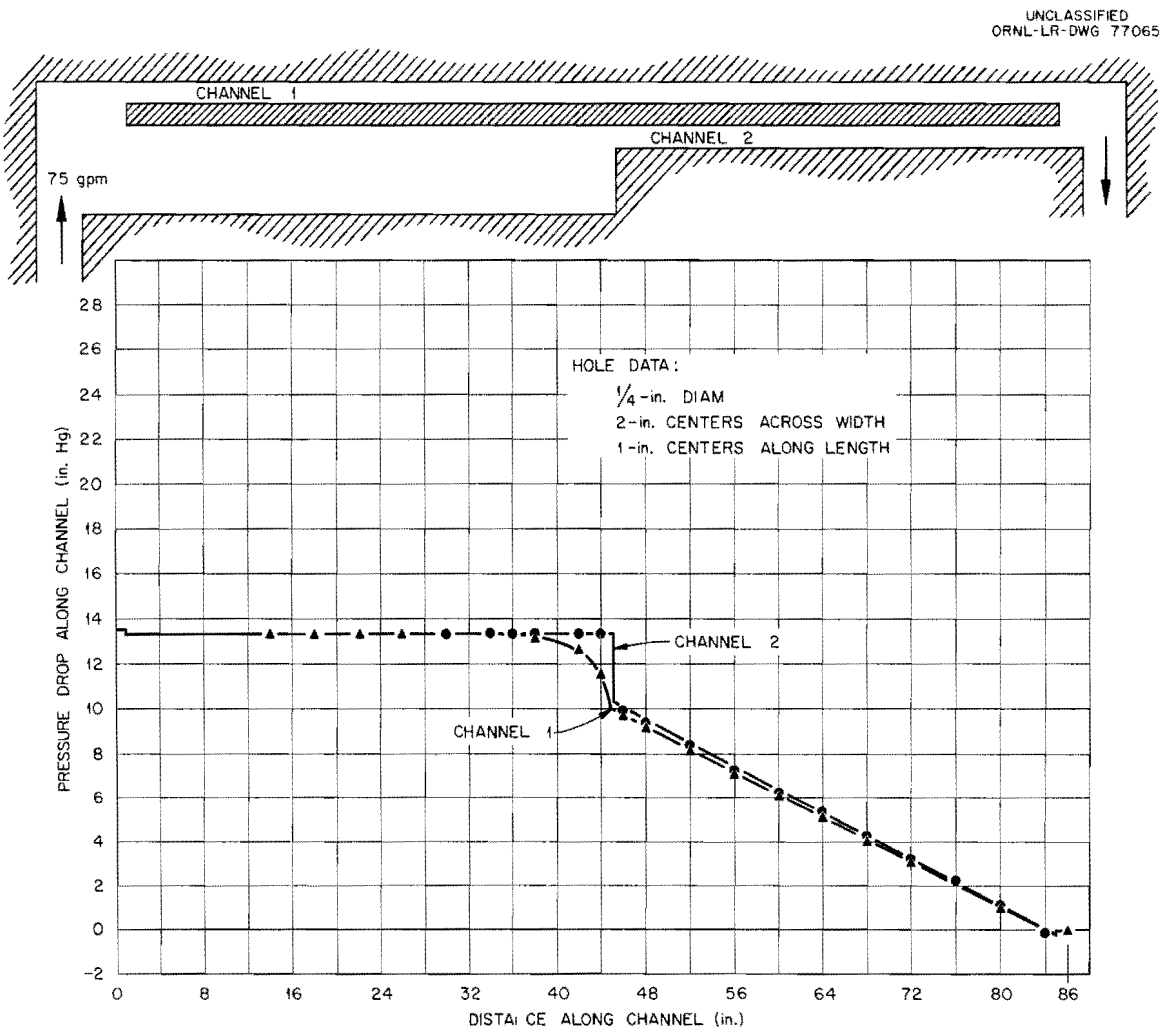


Fig. 30. Pressure Drop for Parallel Channels with 2.454% of Plate Area Occupied by Holes.

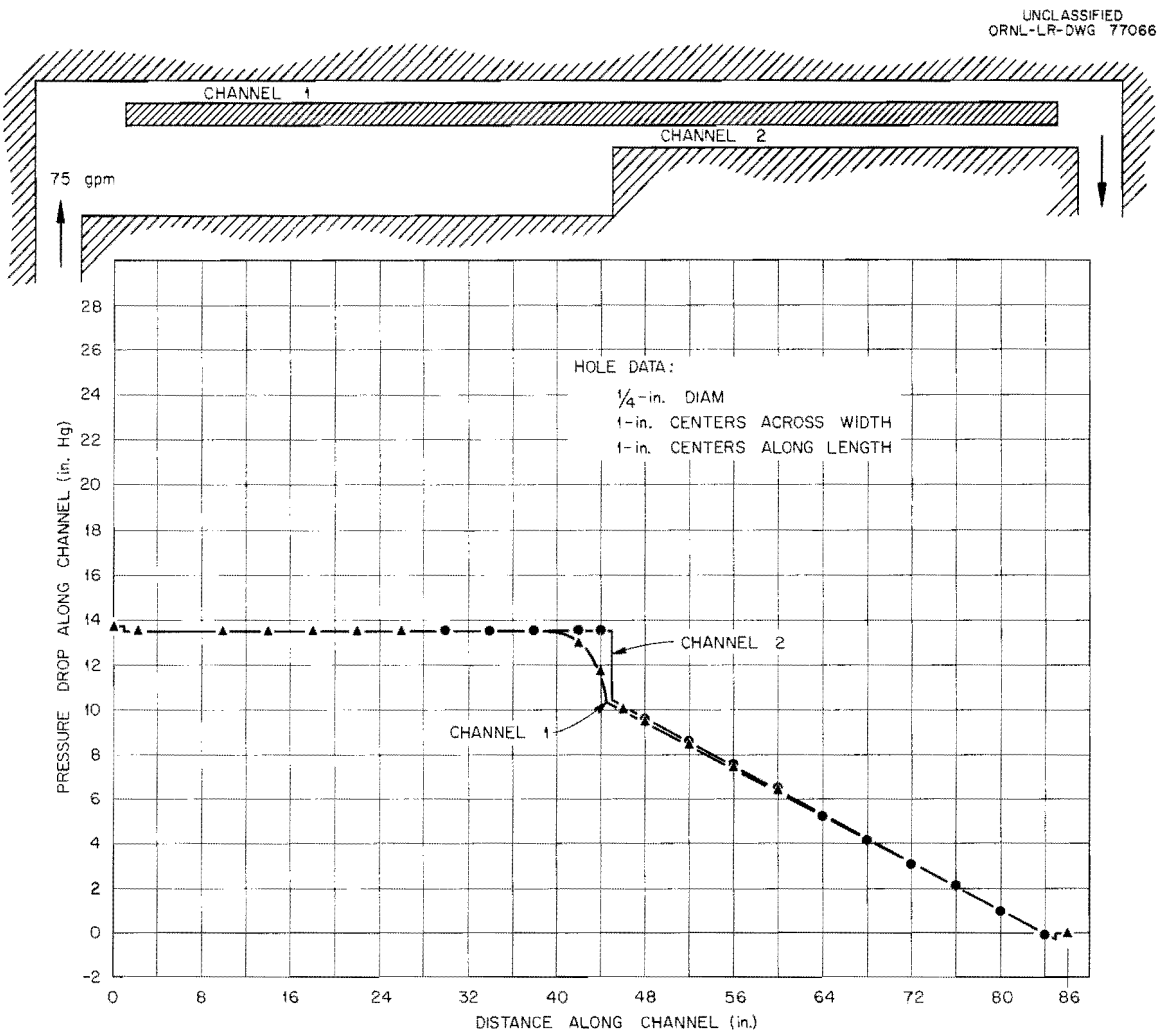


Fig. 31. Pressure Drop for Parallel Channels with 4.908% of Plate Area Occupied by Holes.

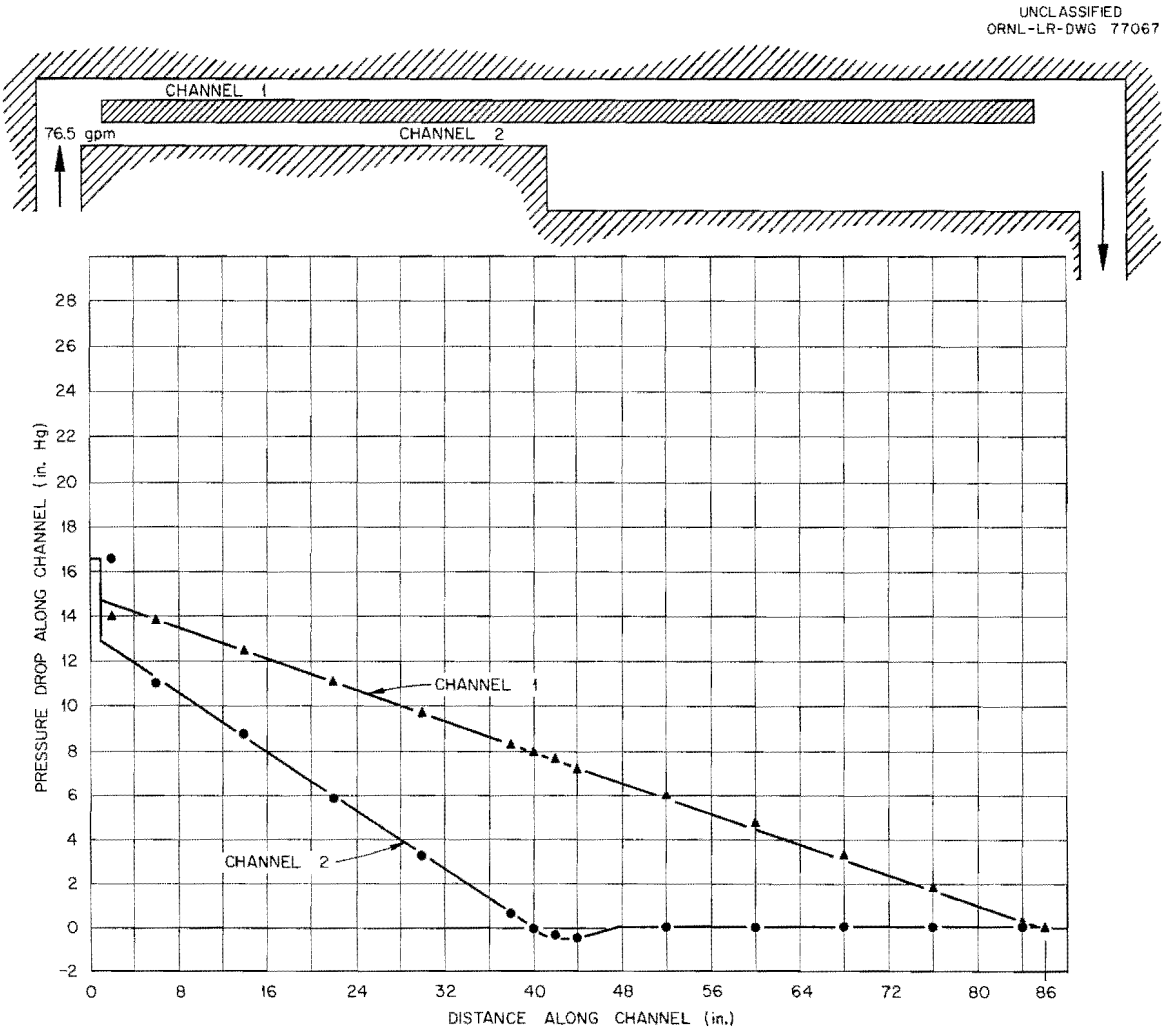


Fig. 32. Pressure Drop for Parallel Channels with No Holes.

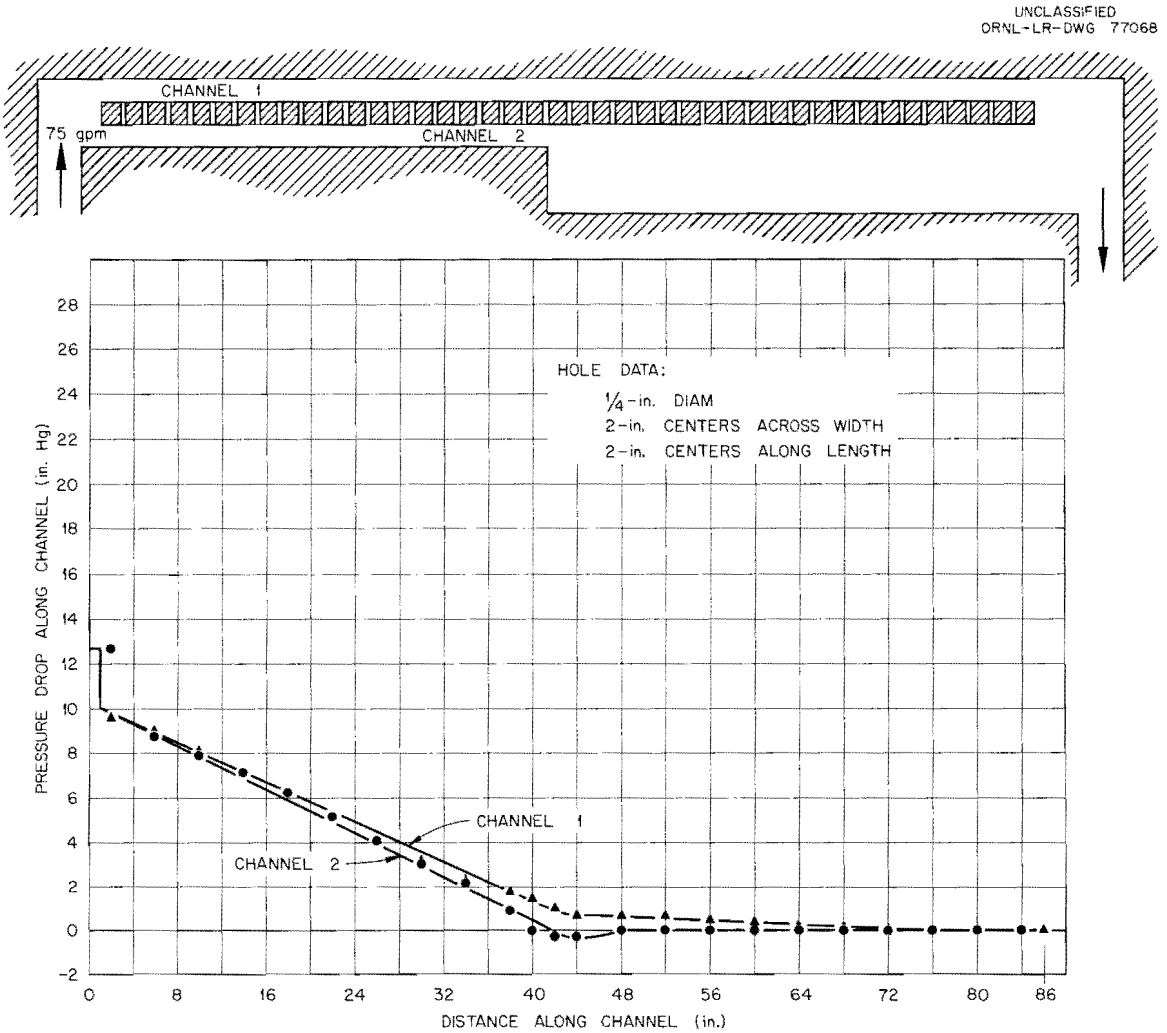


Fig. 33. Pressure Drop for Parallel Channels with 1.227% of Plate Area Occupied by Holes.

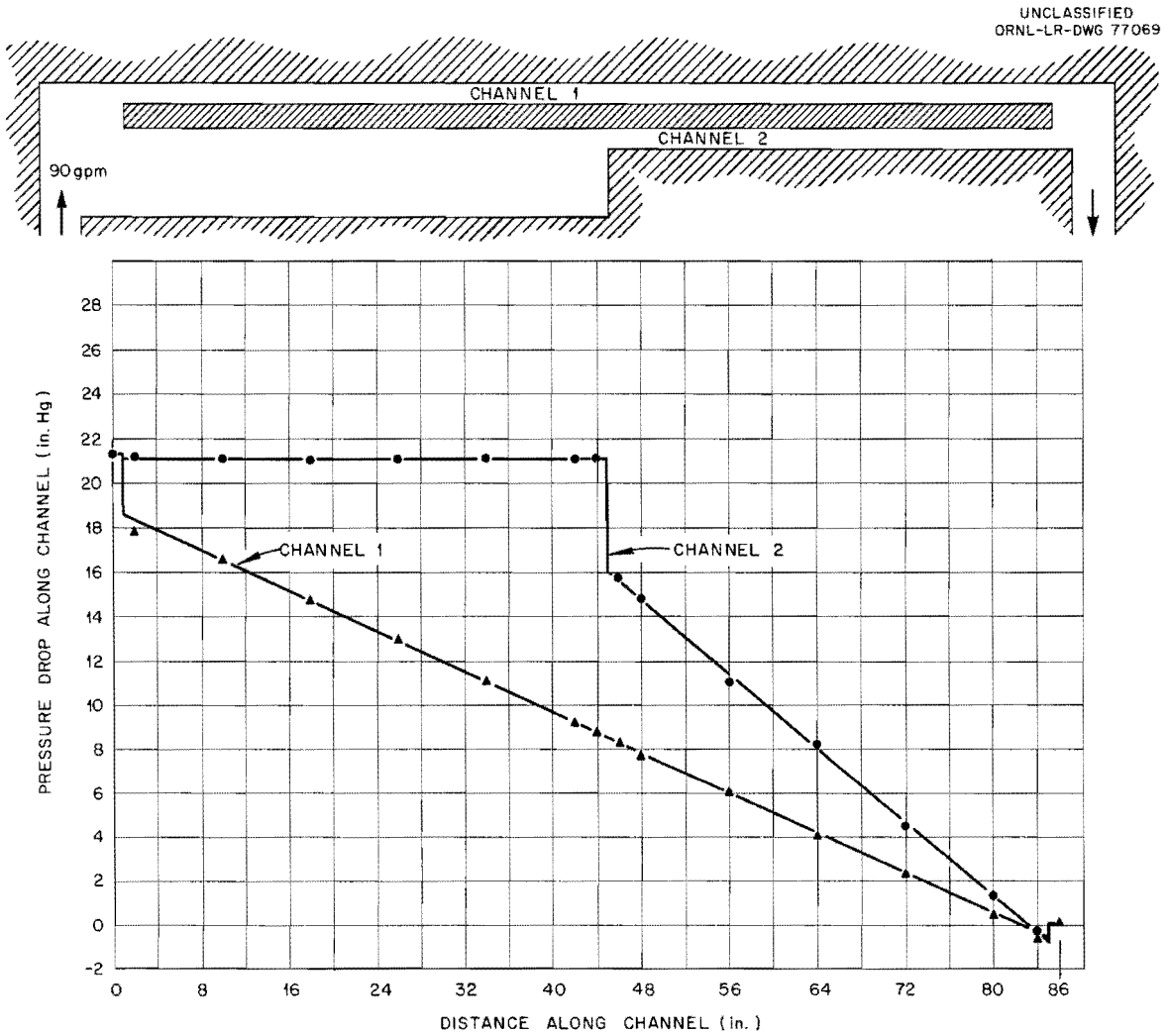


Fig. 34. Pressure Drop for Parallel Channels with No Holes.

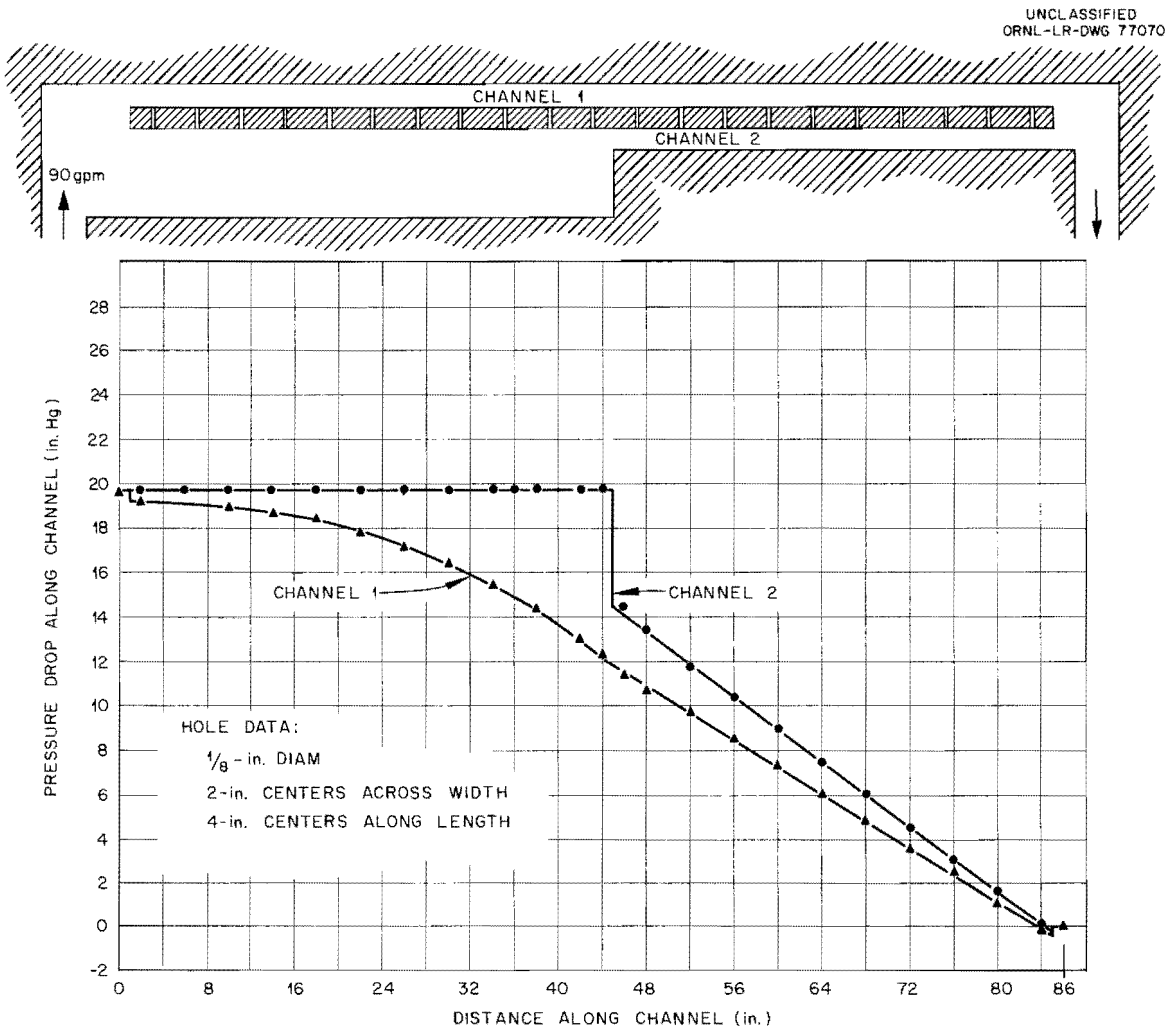


Fig. 35. Pressure Drop for Parallel Channels with 0.154% of Plate Area Occupied by Holes.

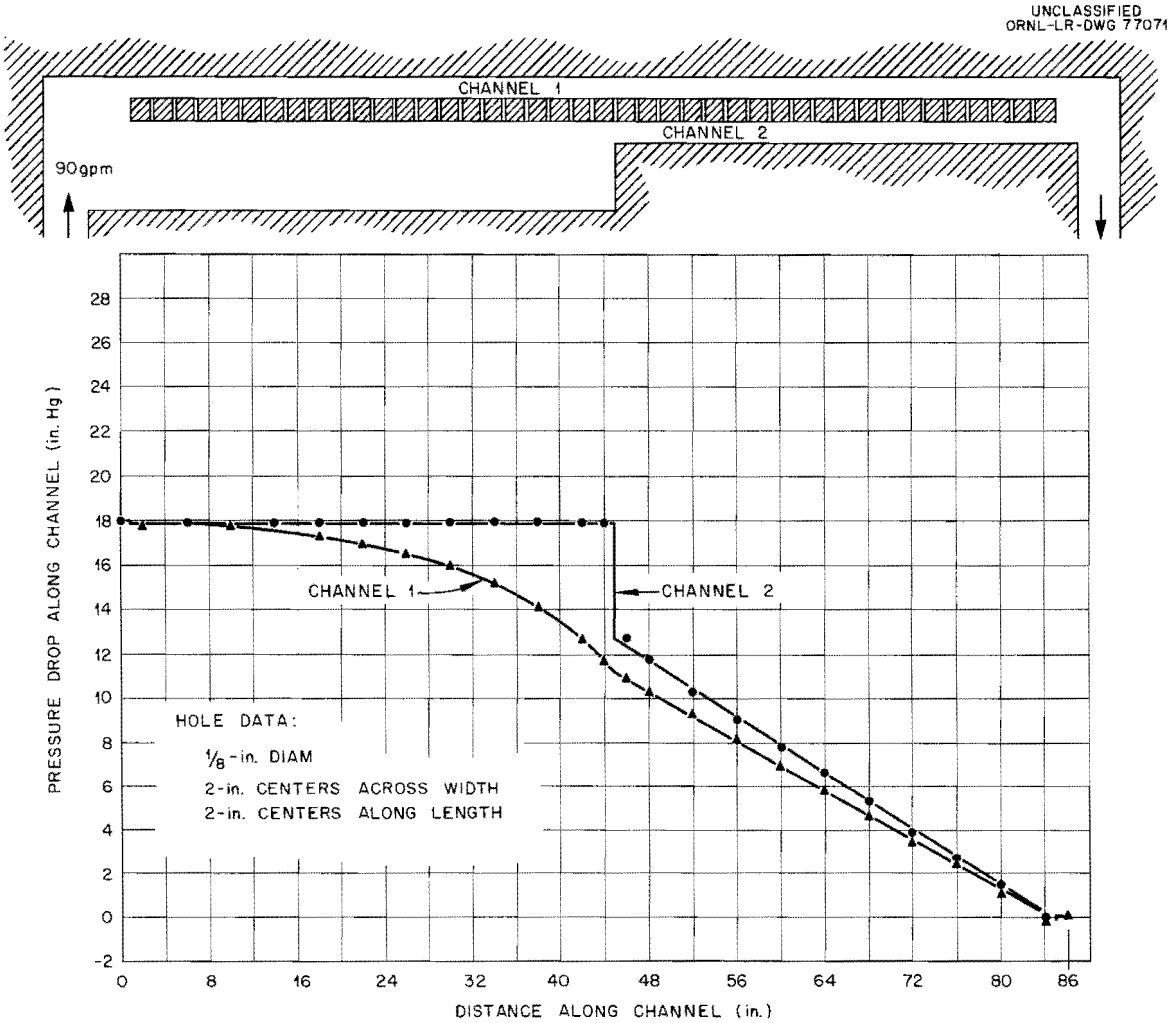


Fig. 36. Pressure Drop for Parallel Channels with 0.307% of Plate Area Occupied by Holes.

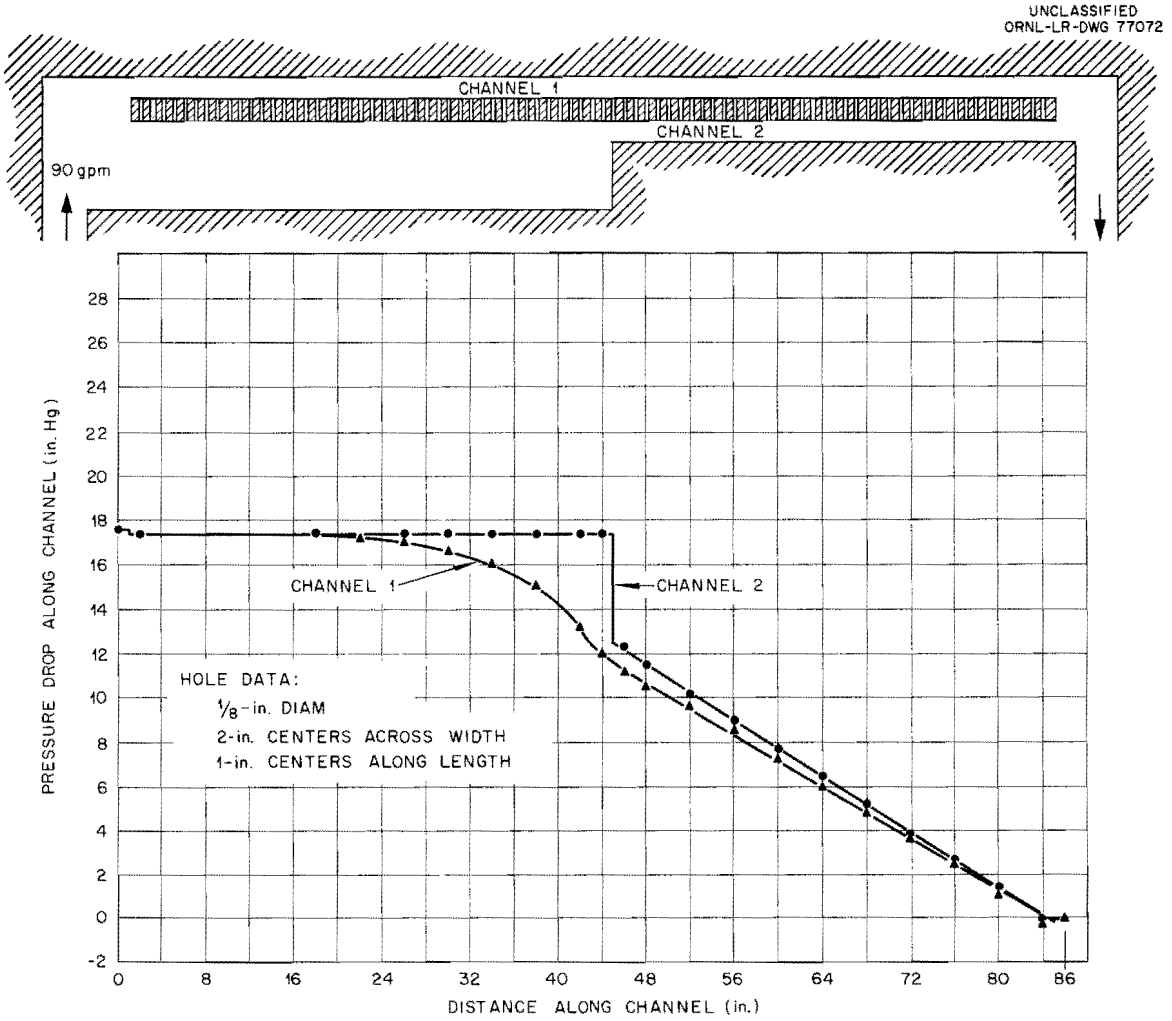


Fig. 37. Pressure Drop for Parallel Channels with 0.614% of Plate Area Occupied by Holes.

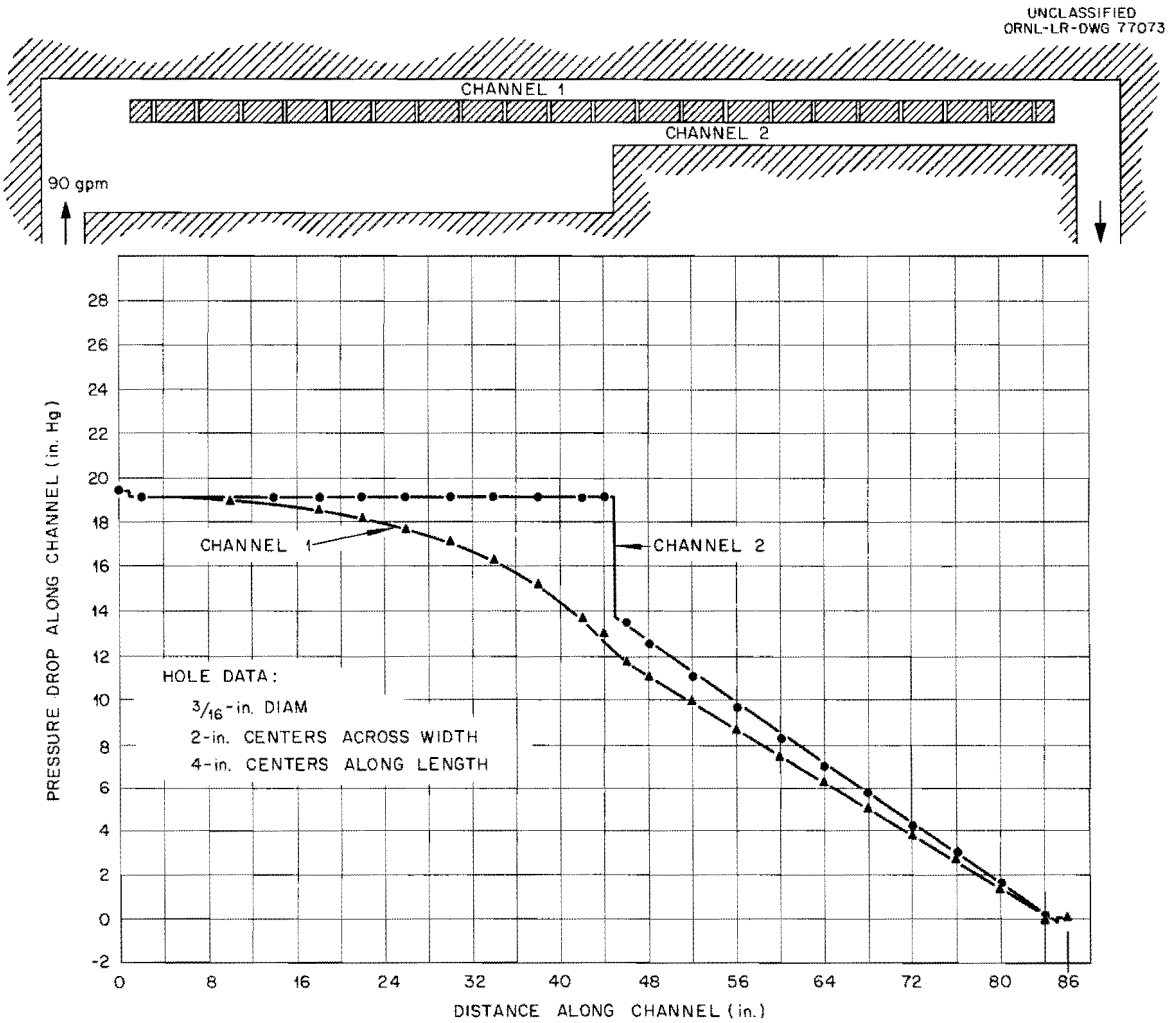


Fig. 38. Pressure Drop for Parallel Channels with 0.345% of Plate Area Occupied by Holes.

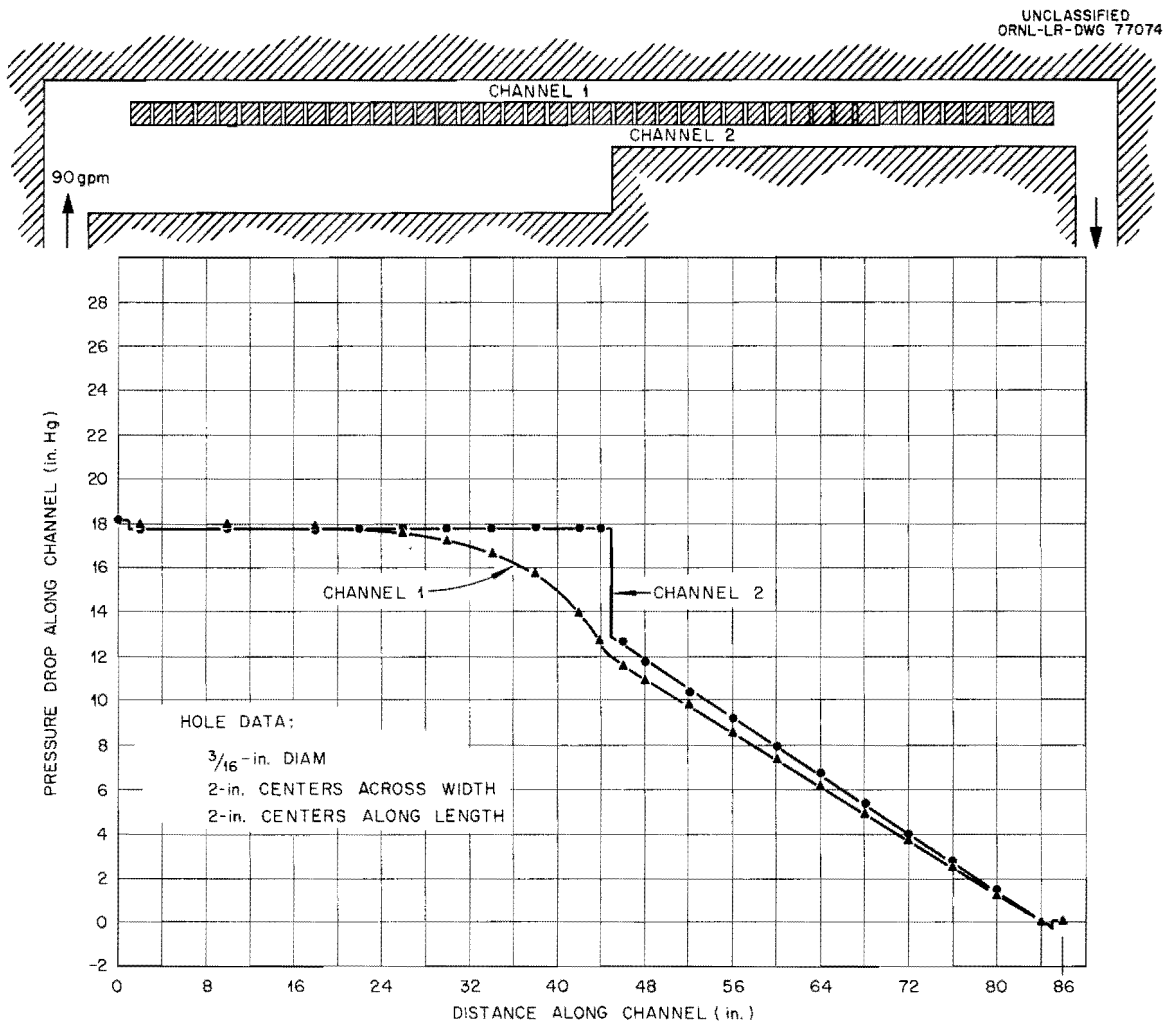


Fig. 39. Pressure Drop for Parallel Channels with 0.690% of Plate Area Occupied by Holes.

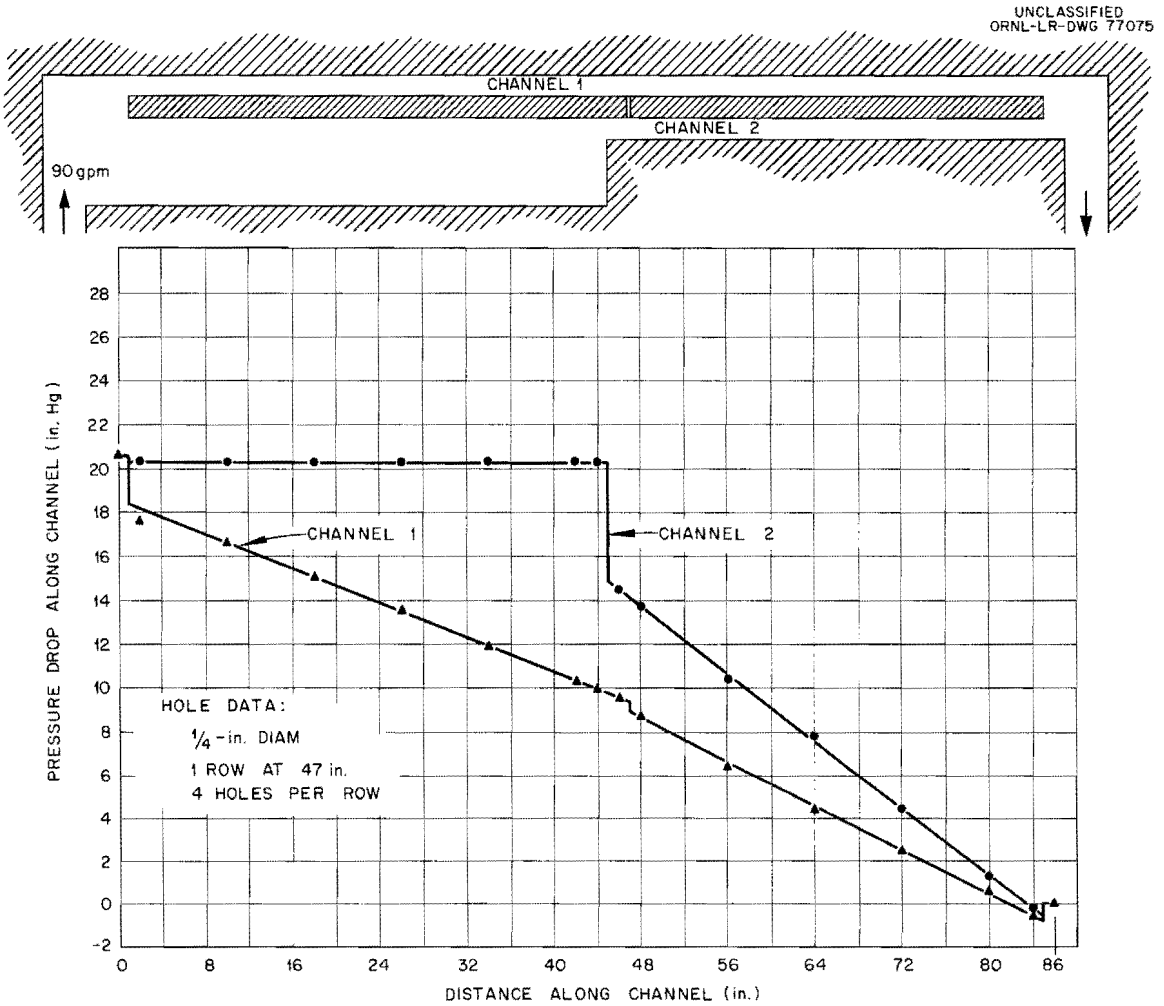


Fig. 40. Pressure Drop for Parallel Channels with Four Connecting Holes.

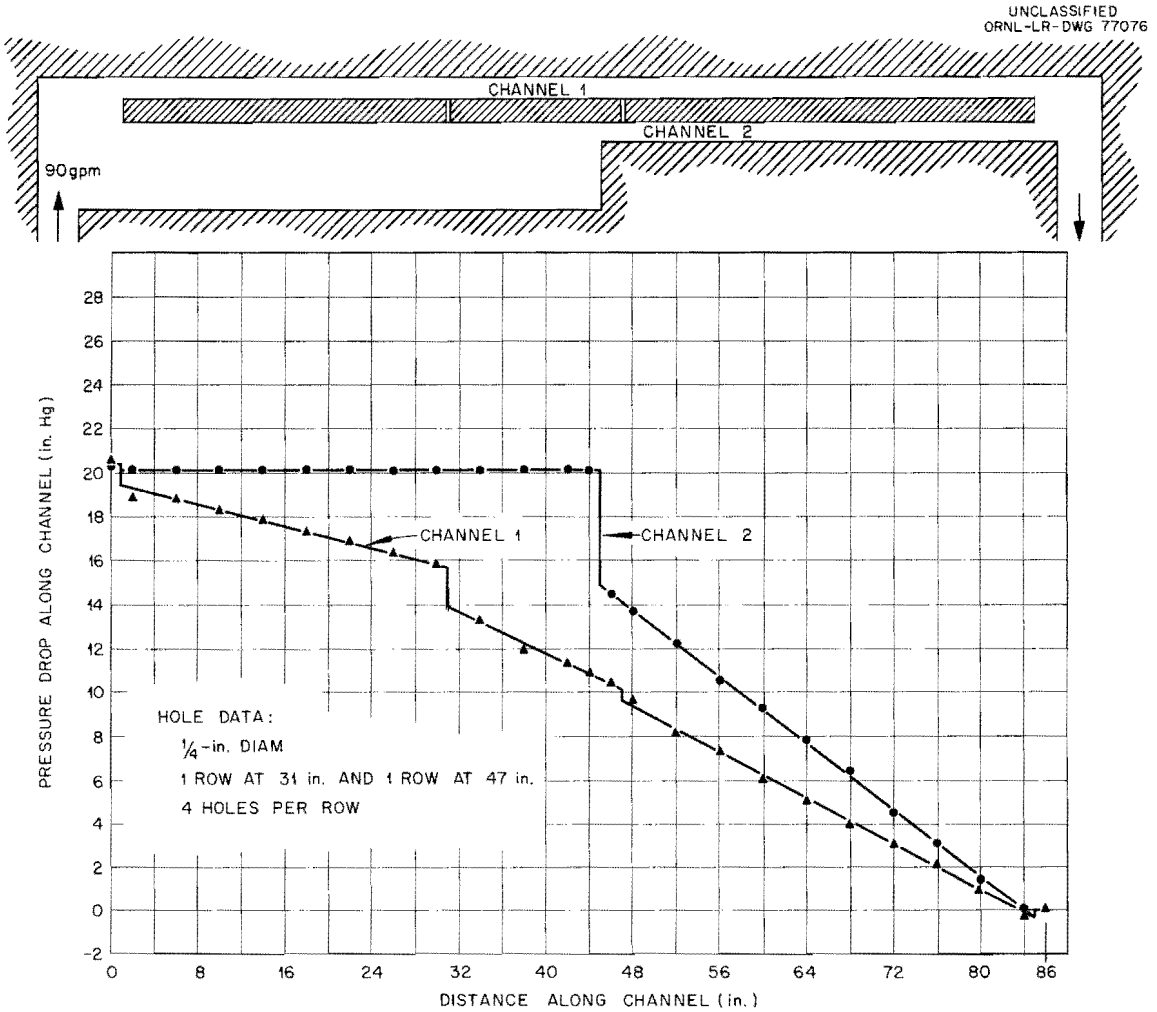


Fig. 41. Pressure Drop for Parallel Channels with Eight Connecting Holes.

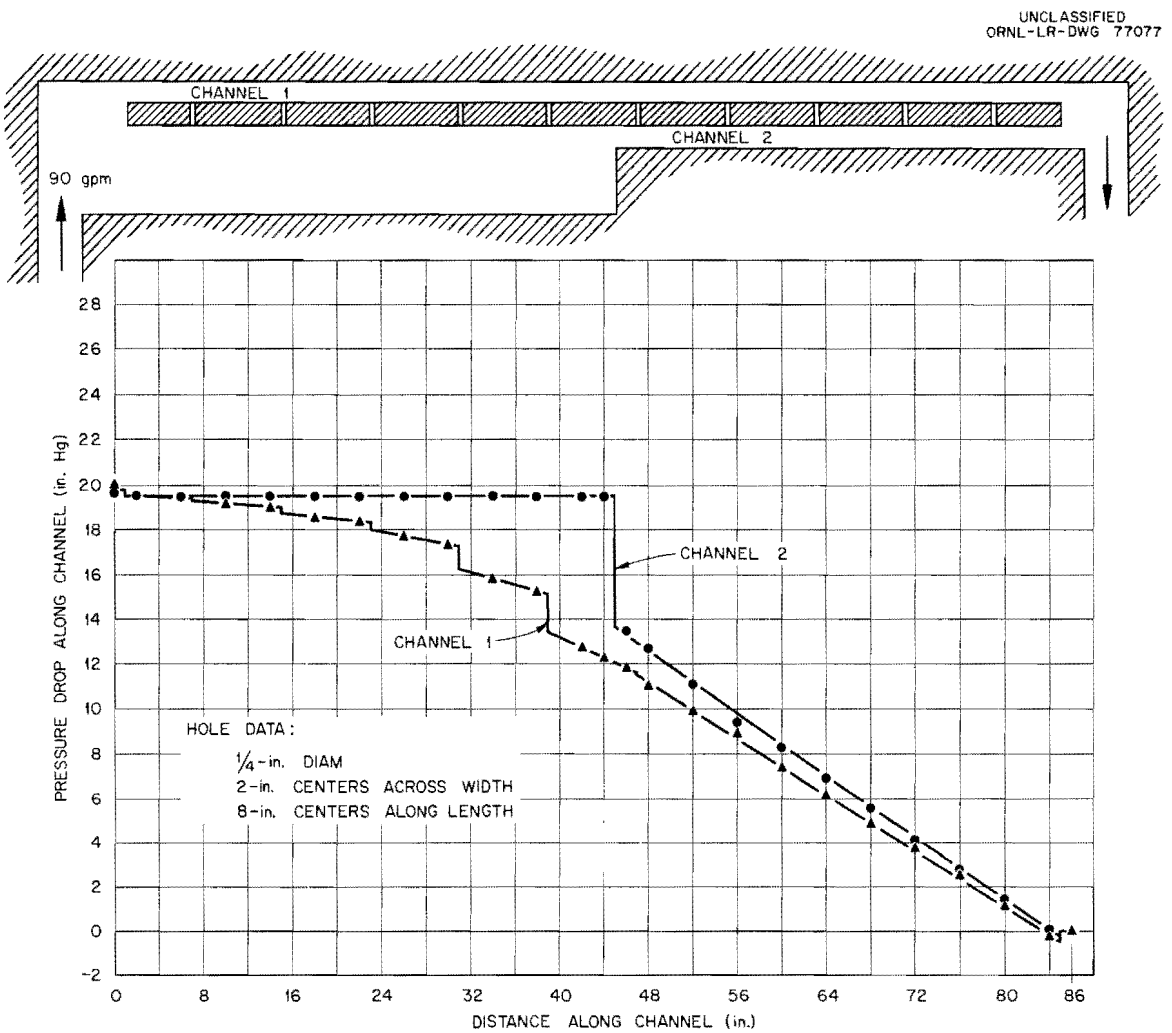


Fig. 42. Pressure Drop for Parallel Channels with 0.307% of Plate Area Occupied by Holes.

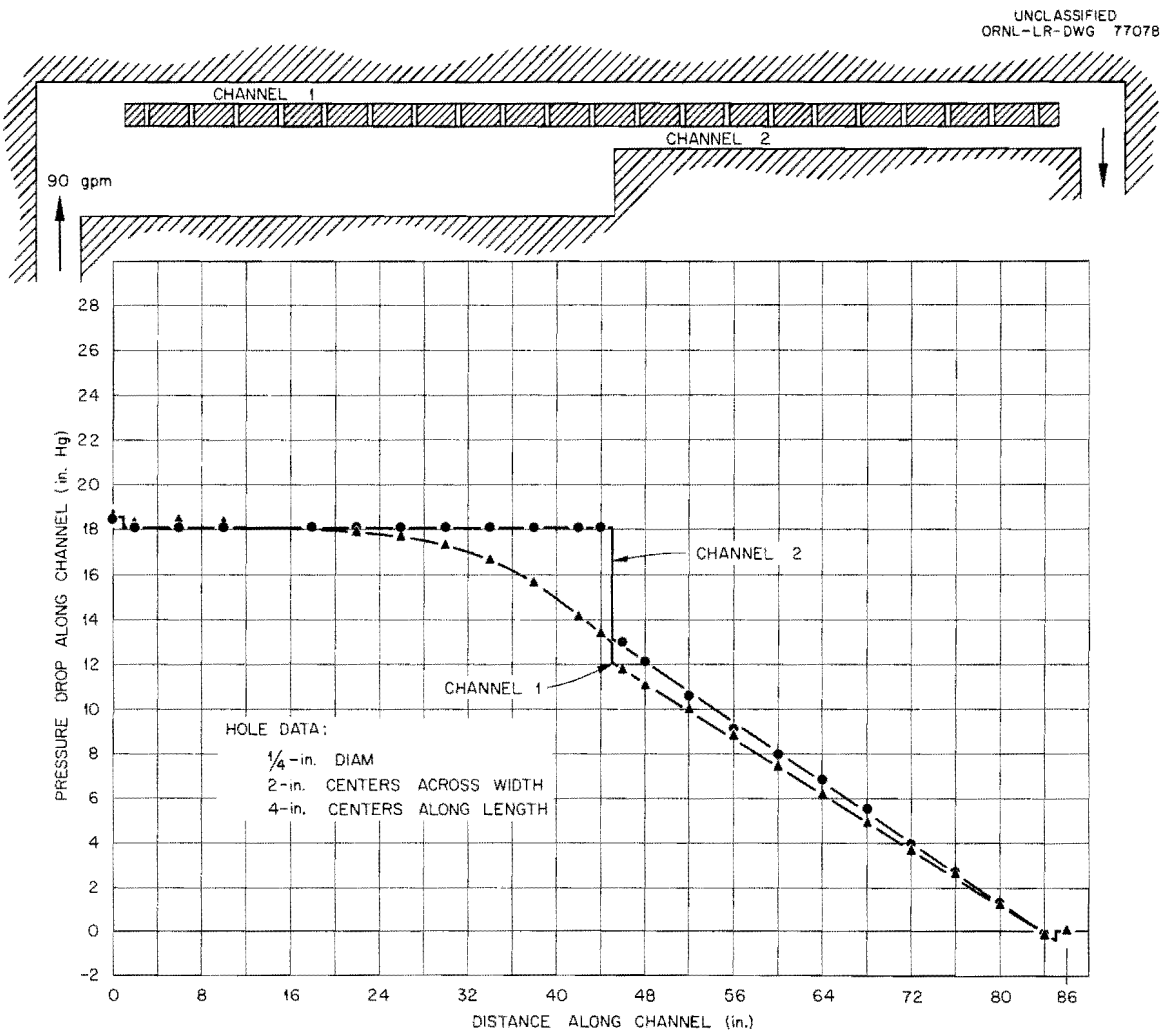


Fig. 43. Pressure Drop for Parallel Channels with 0.614% of Plate Area Occupied by Holes.

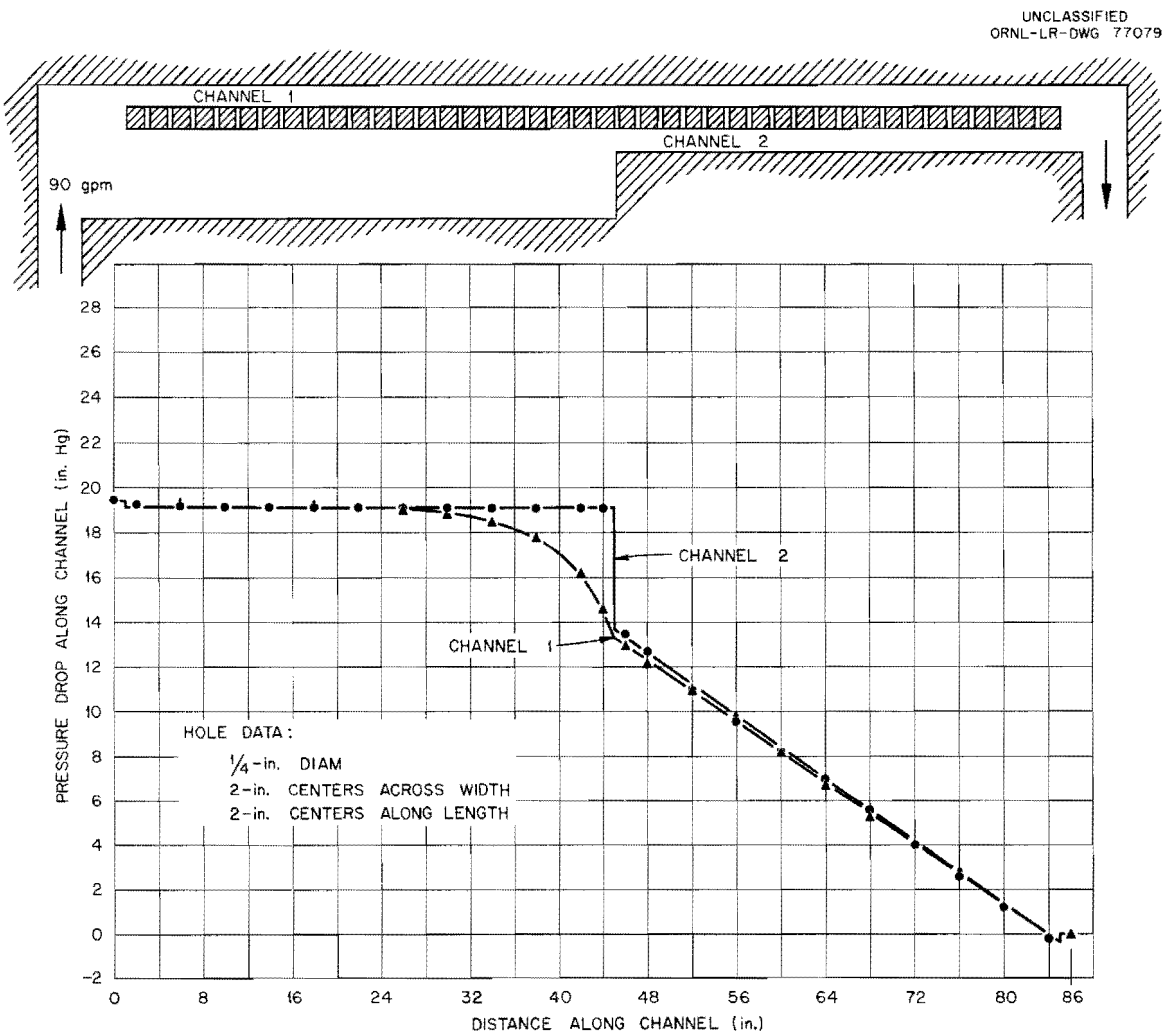


Fig. 44. Pressure Drop for Parallel Channels with Nominal 1.227% of Plate Area Occupied by Holes.

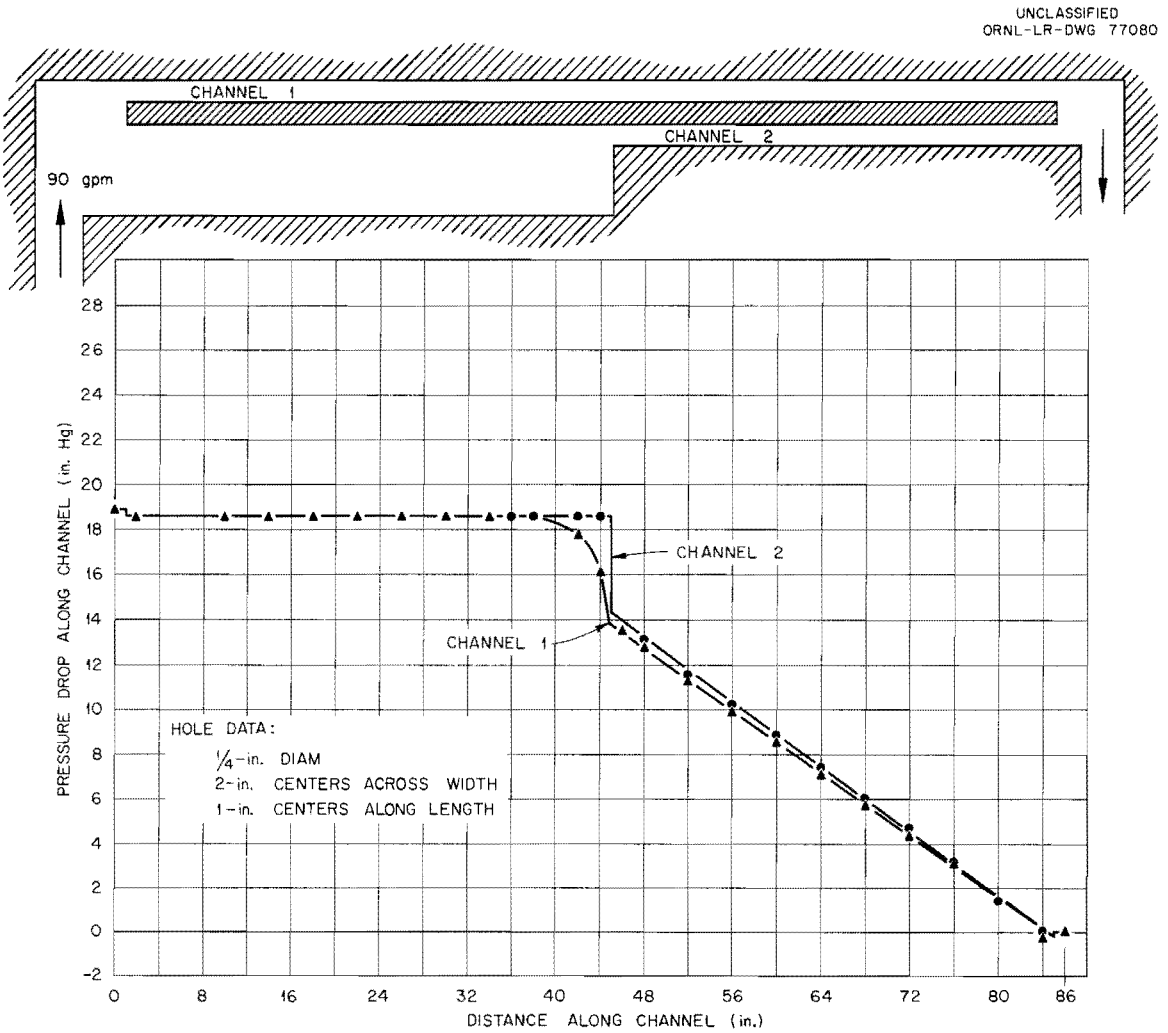


Fig. 45. Pressure Drop for Parallel Channels with 2.454% of Plate Area Occupied by Holes.

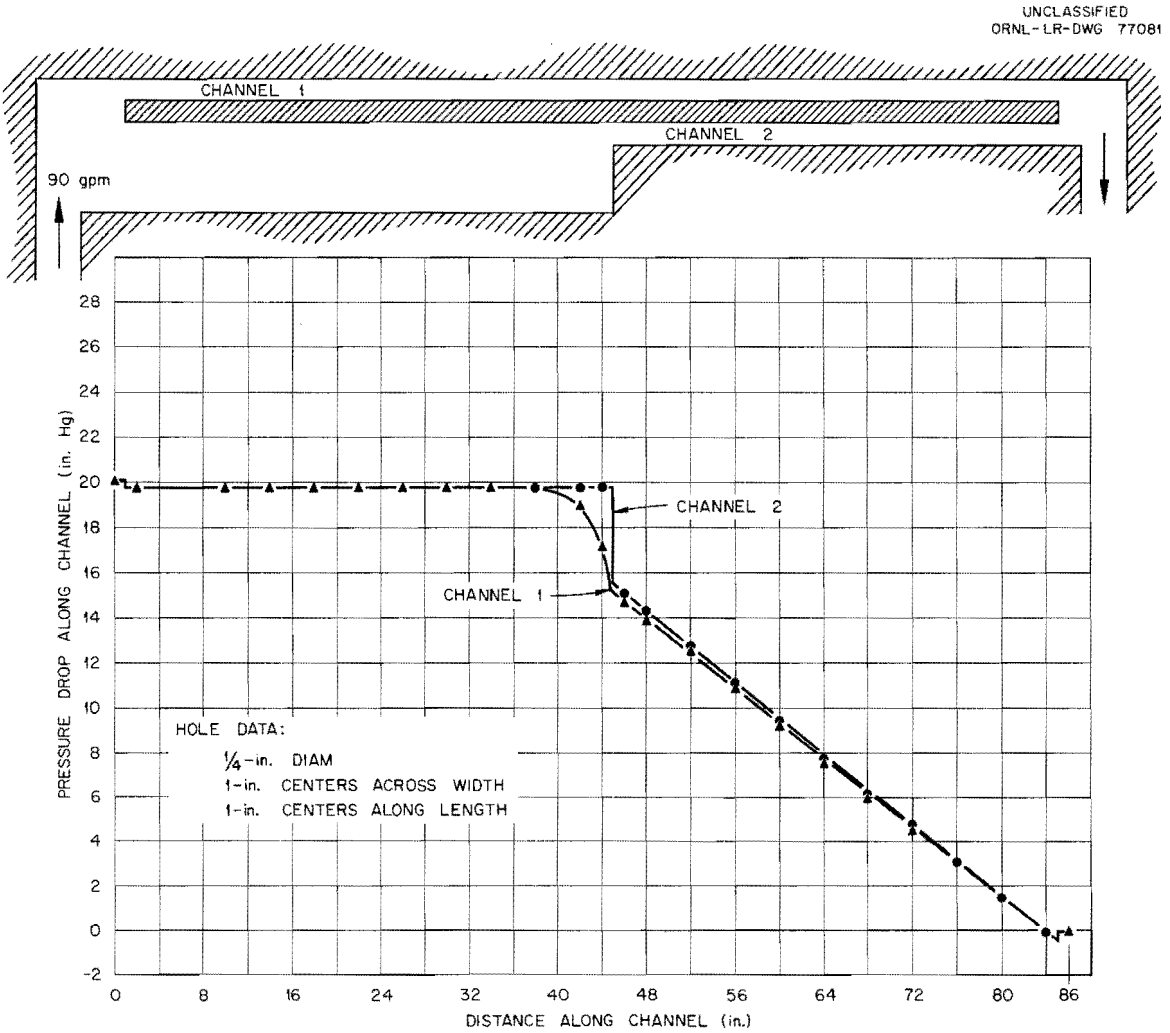


Fig. 46. Pressure Drop for Parallel Channels with 4.908% of Plate Area Occupied by Holes.

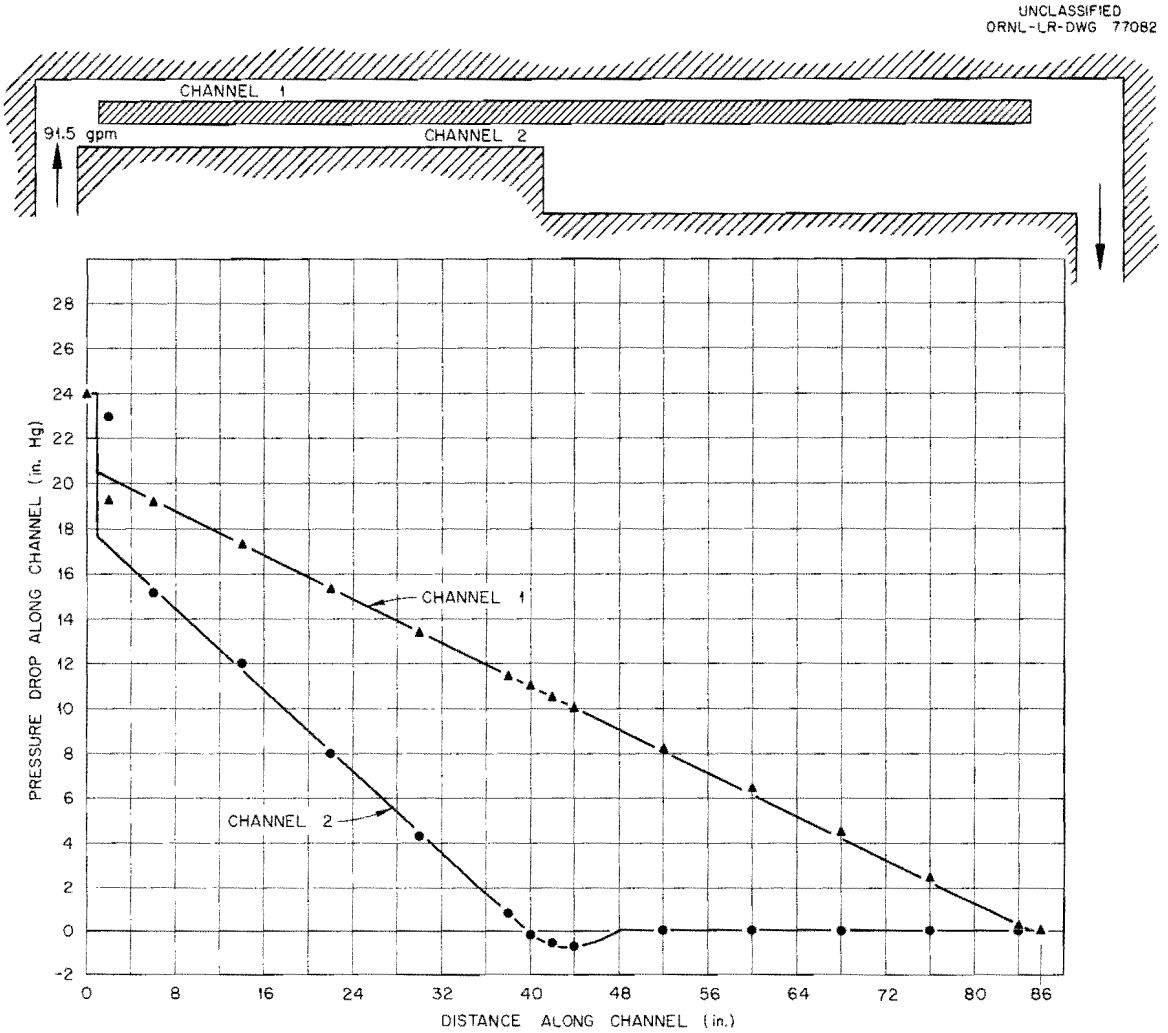


Fig. 47. Pressure Drop for Parallel Channels with No Holes.

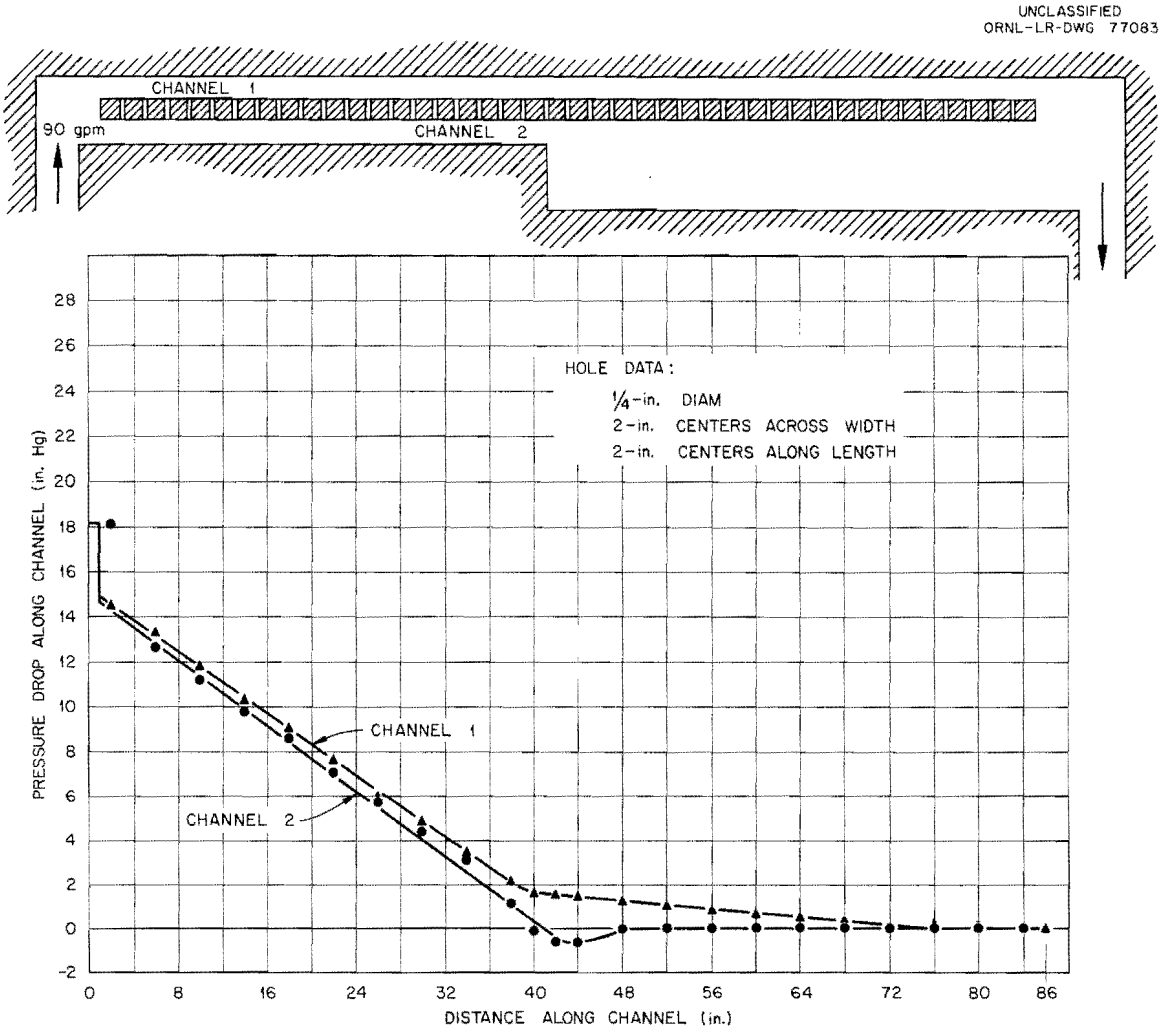


Fig. 48. Pressure Drop for Parallel Channels with 1.227% of Plate Area Occupied by Holes.

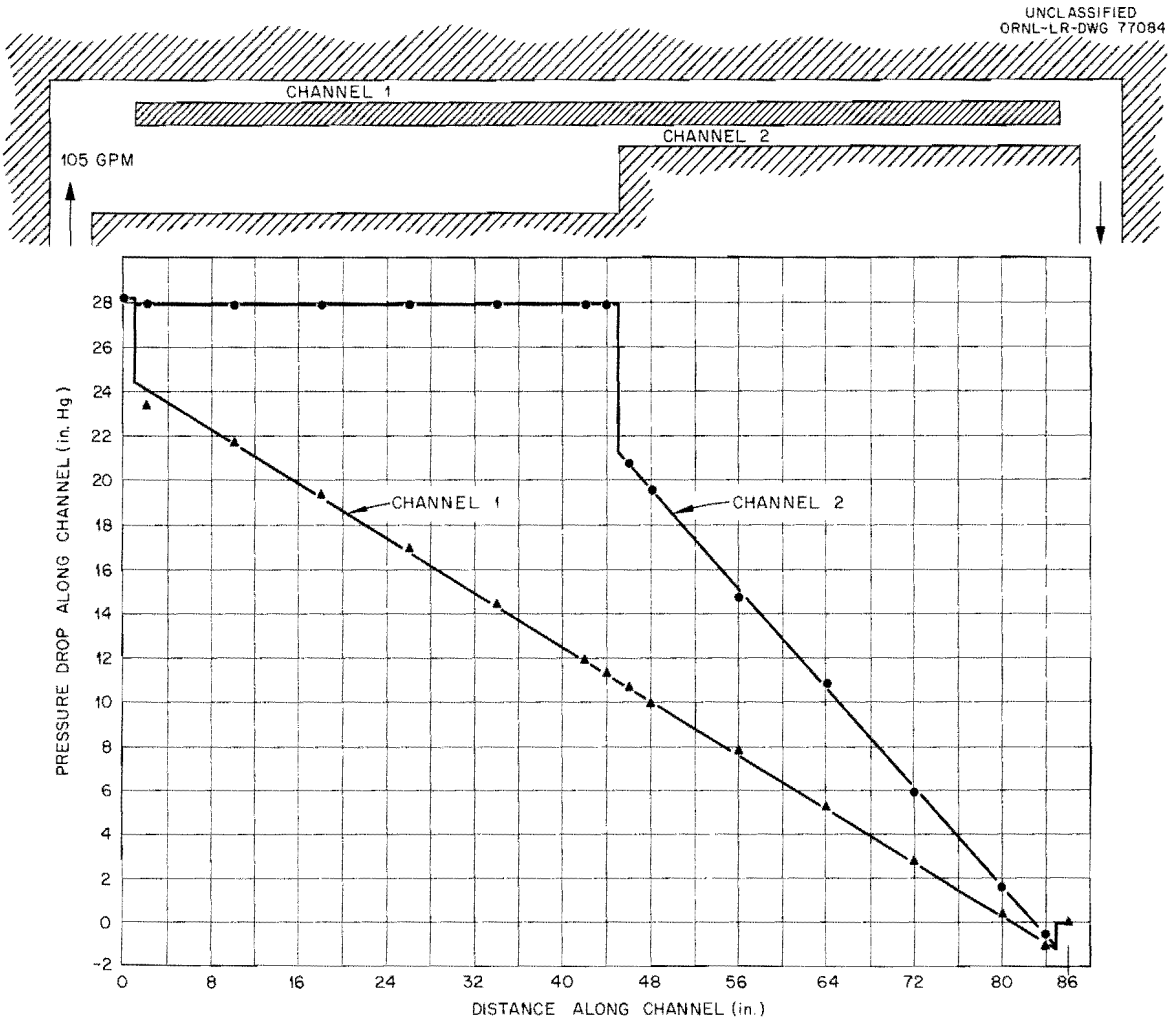


Fig. 49. Pressure Drop for Parallel Channels with No Holes.

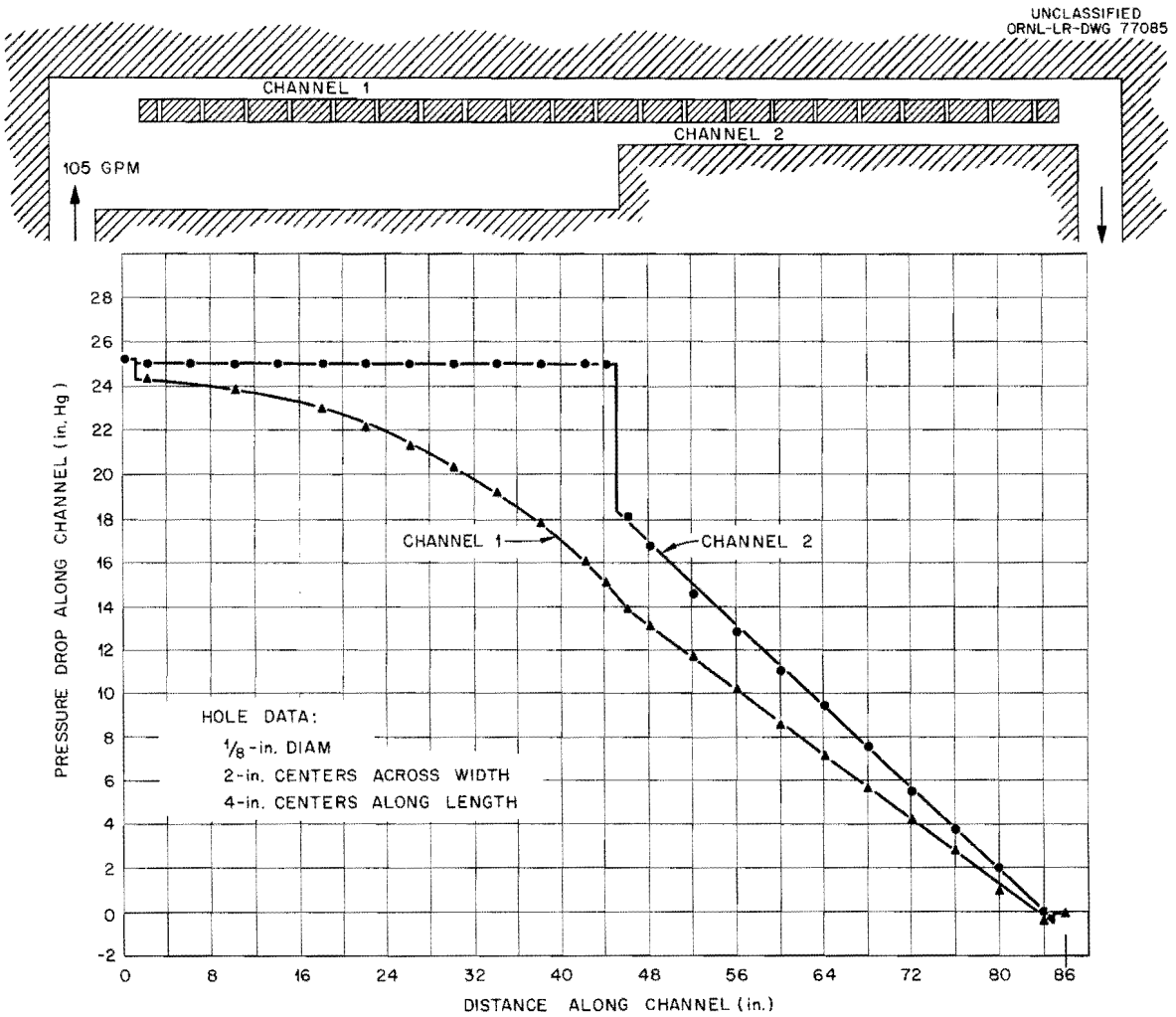


Fig. 50. Pressure Drop for Parallel Channels with 0.154% of Plate Area Occupied by Holes.

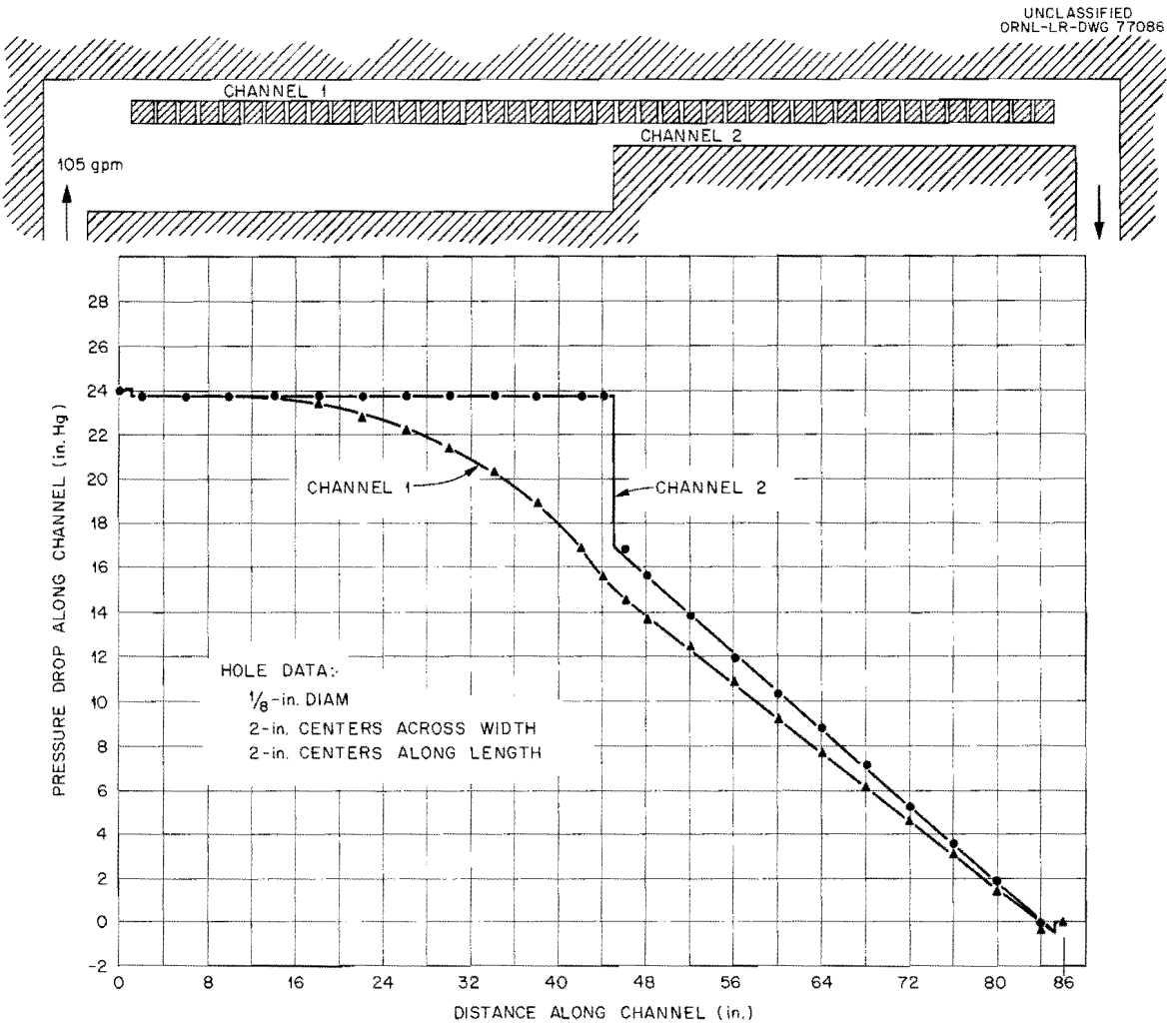


Fig. 51. Pressure Drop for Parallel Channels with 0.307% of Plate Area Occupied by Holes.

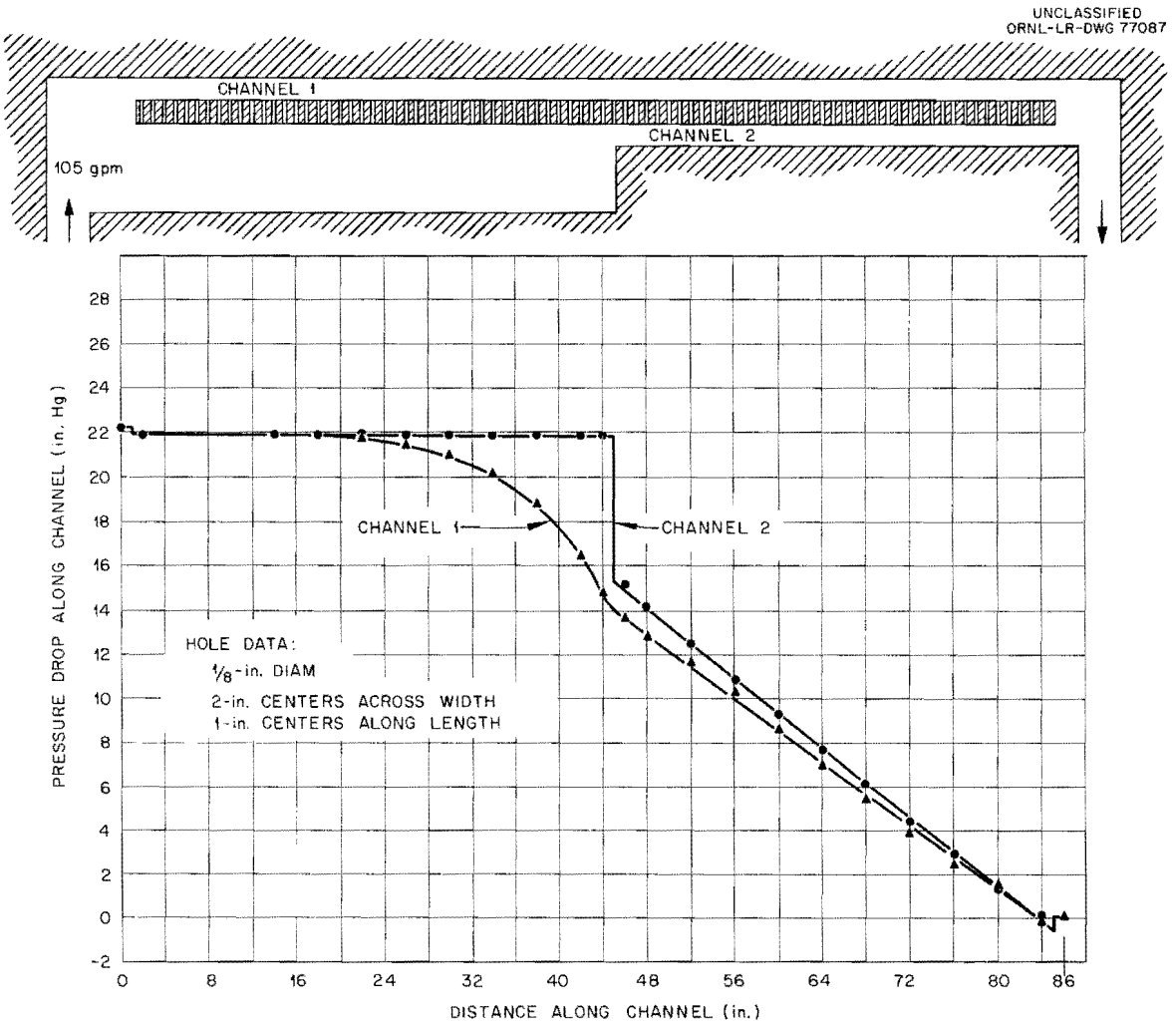


Fig. 52. Pressure Drop for Parallel Channels with 0.614% of Plate Area Occupied by Holes.

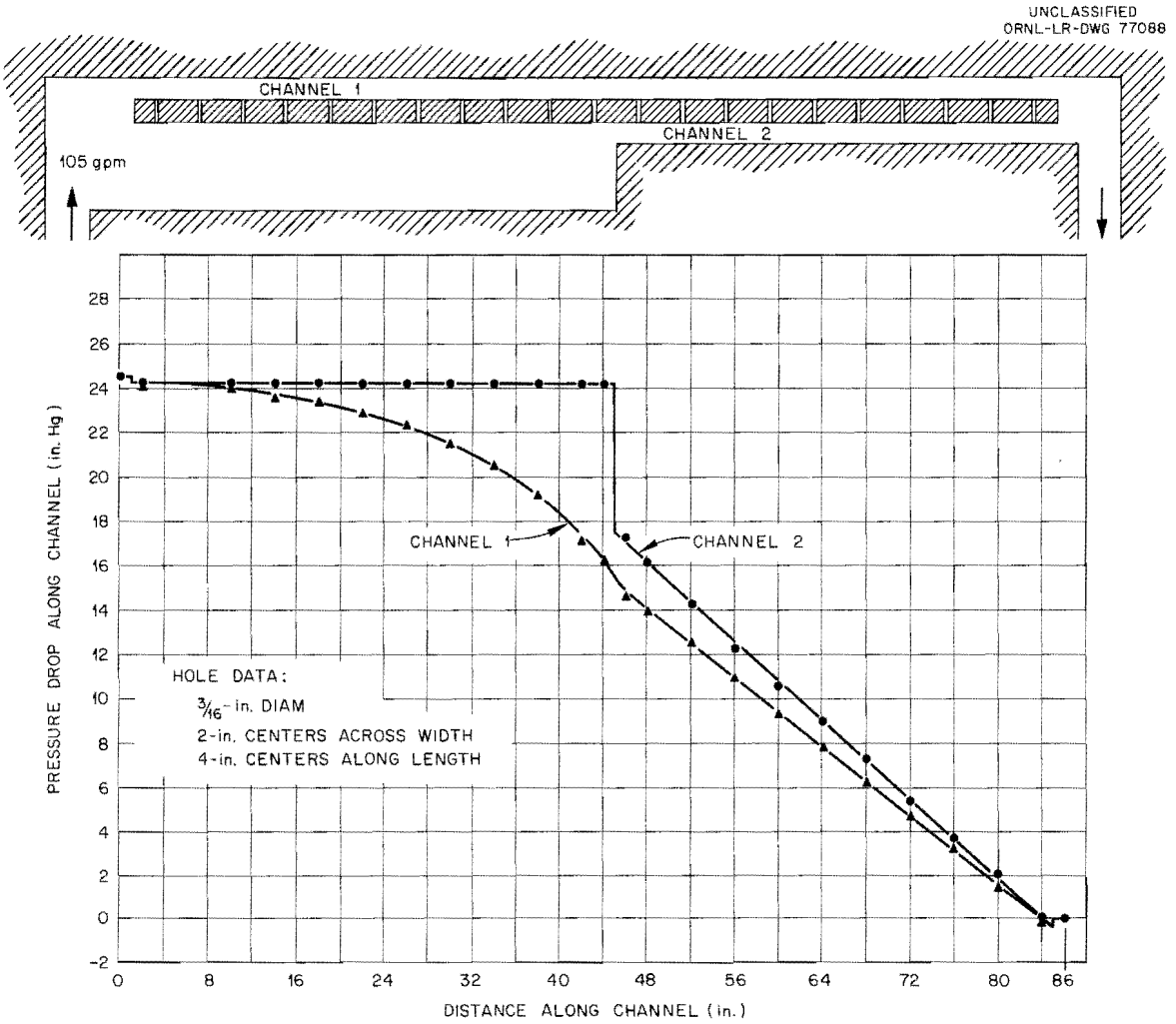


Fig. 53. Pressure Drop for Parallel Channels with 0.345% of Plate Area Occupied by Holes.

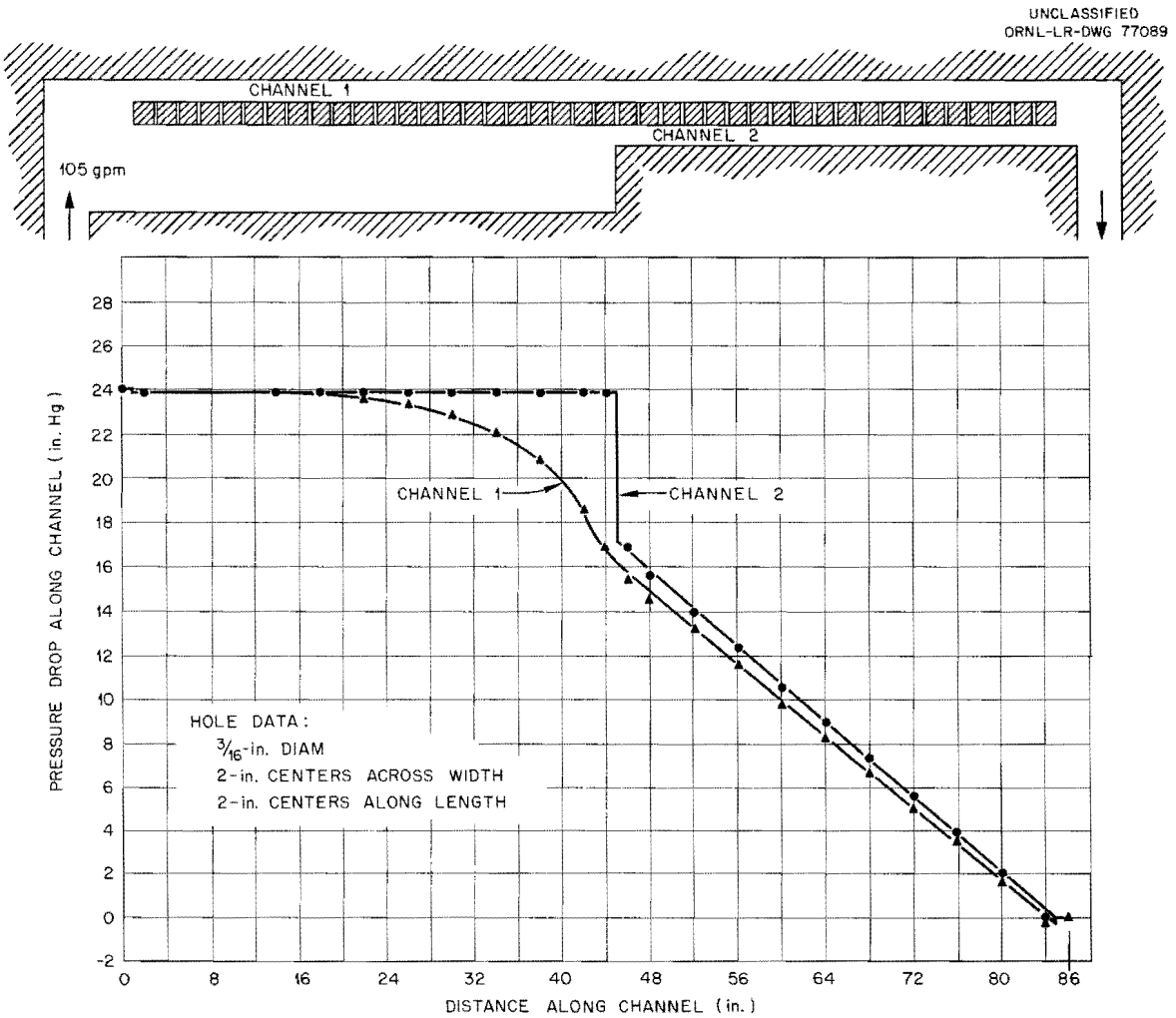


Fig. 54. Pressure Drop for Parallel Channels with 0.690% of Plate Area Occupied by Holes.

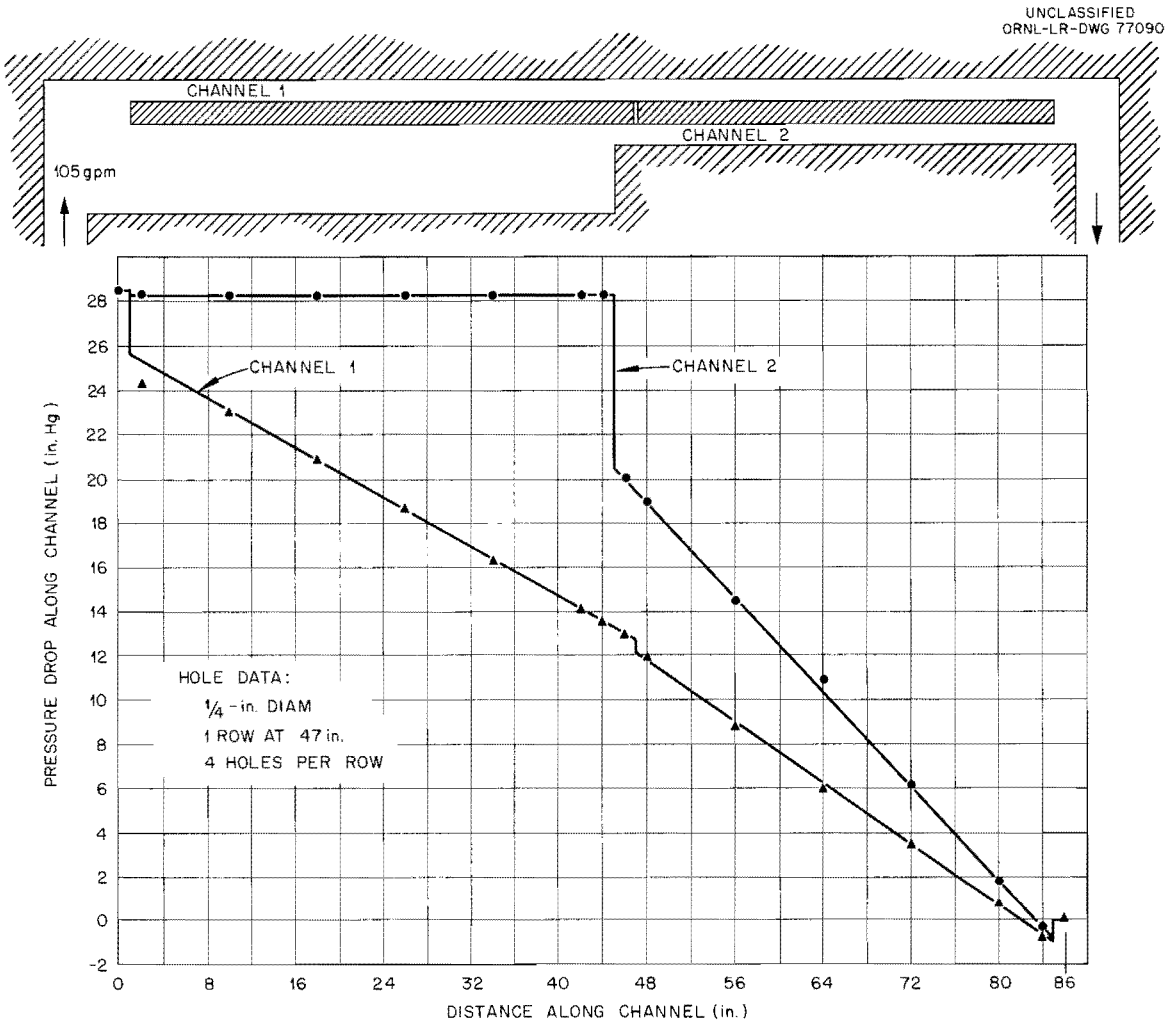


Fig. 55. Pressure Drop for Parallel Channels with Four Connecting Holes.

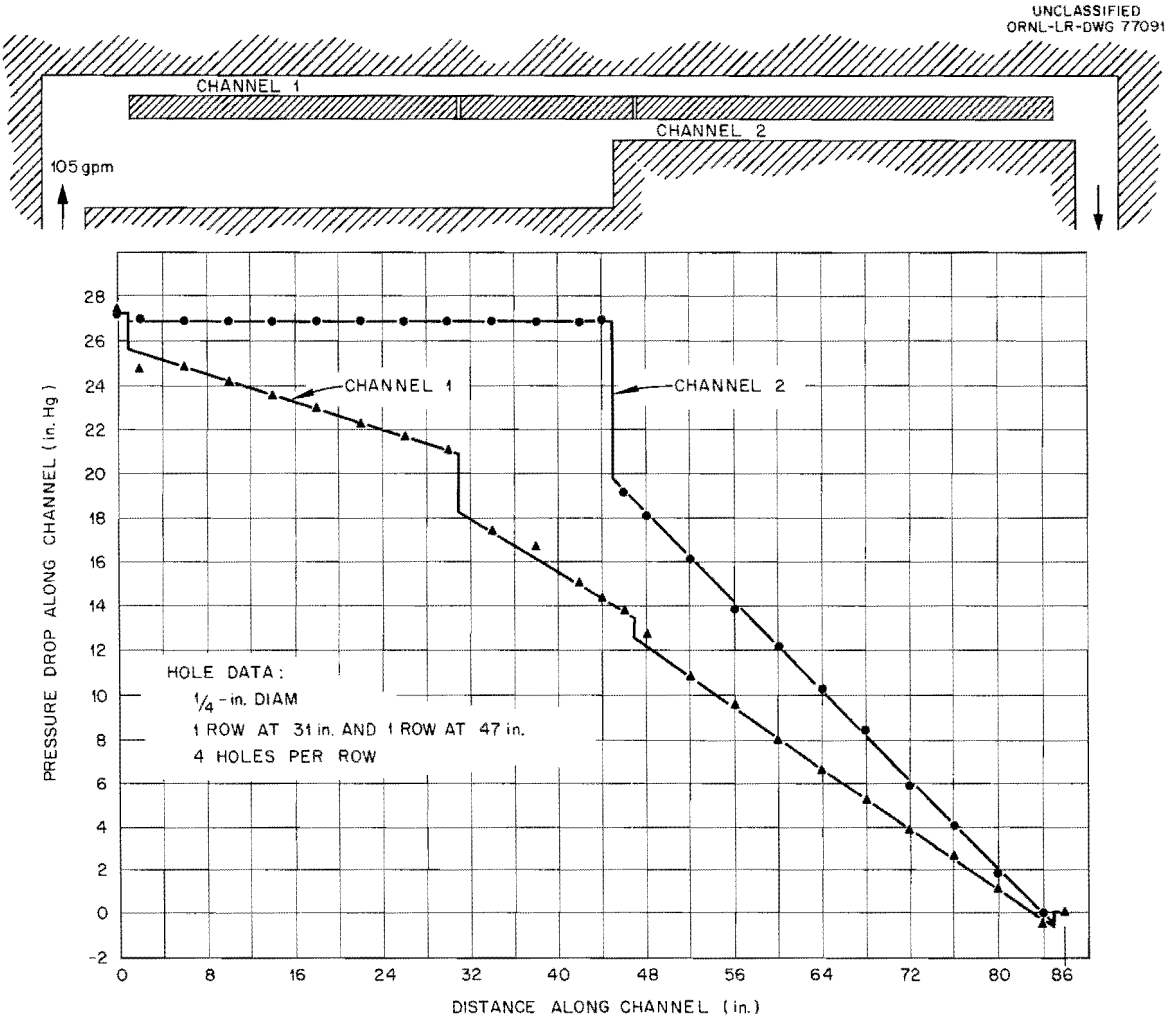


Fig. 56. Pressure Drop for Parallel Channels with Eight Connecting Holes.

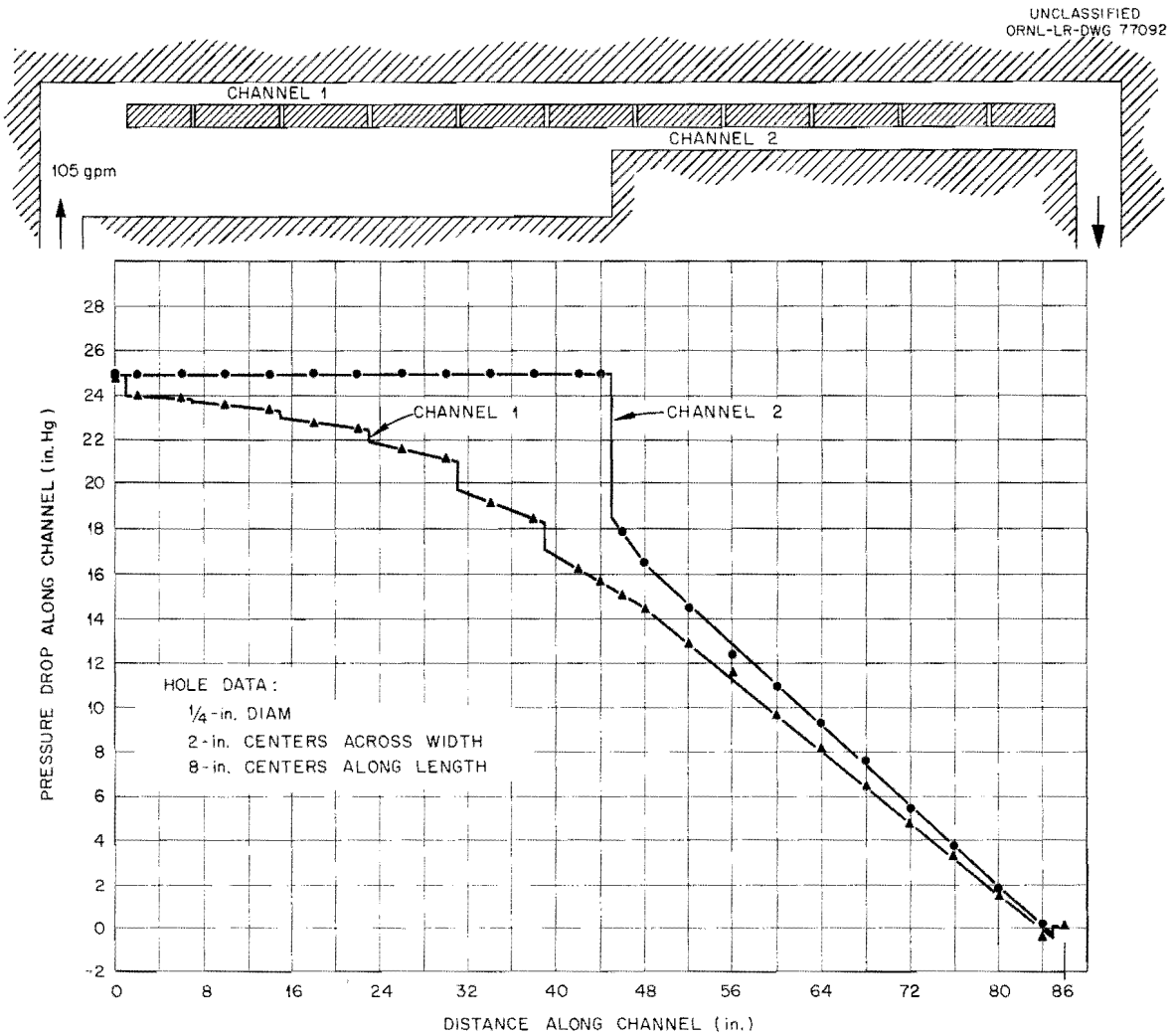


Fig. 57. Pressure Drop for Parallel Channels with 0.307% of Plate Area Occupied by Holes.

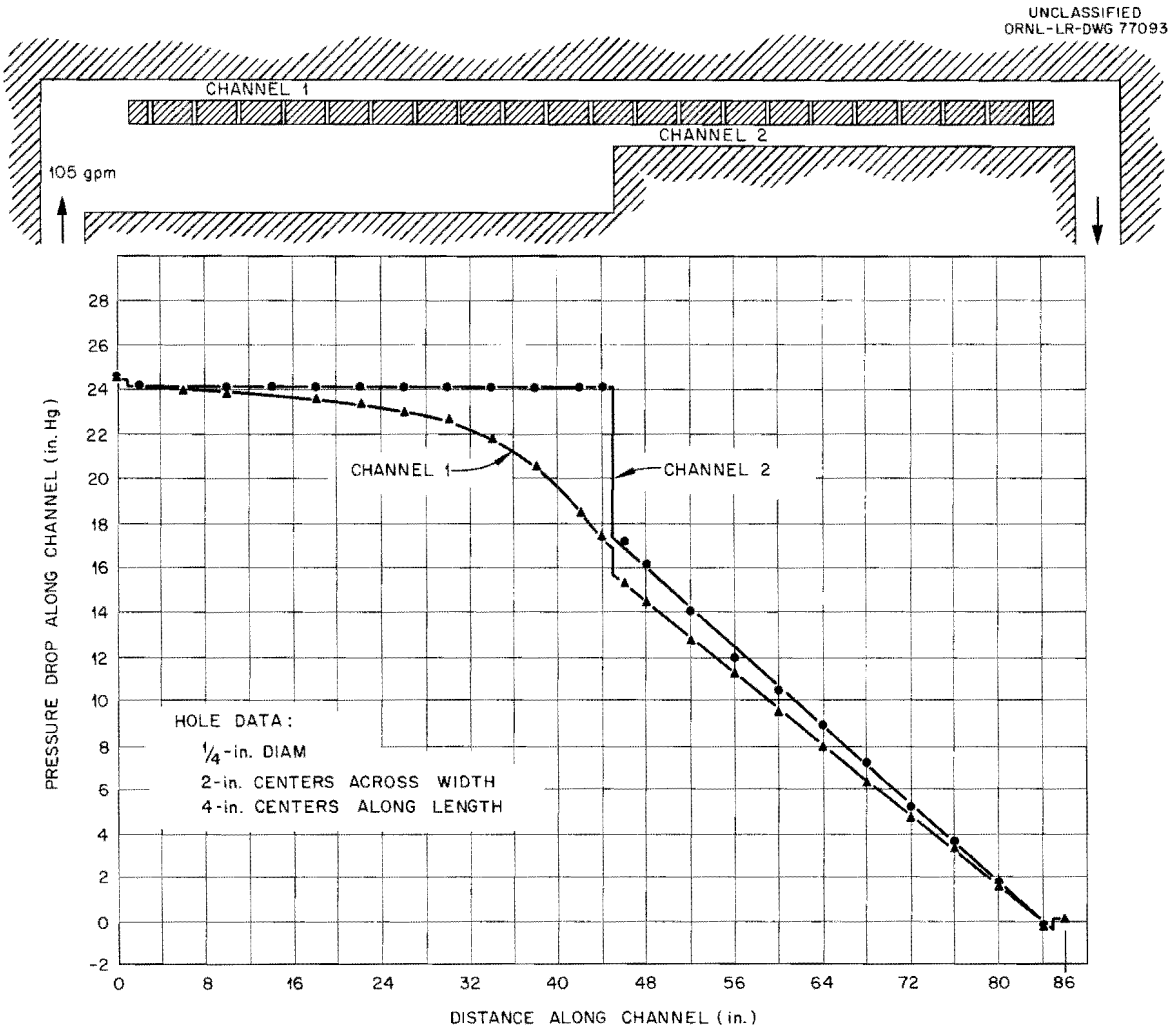


Fig. 58. Pressure Drop for Parallel Channels with 0.614% of Plate Area Occupied by Holes.

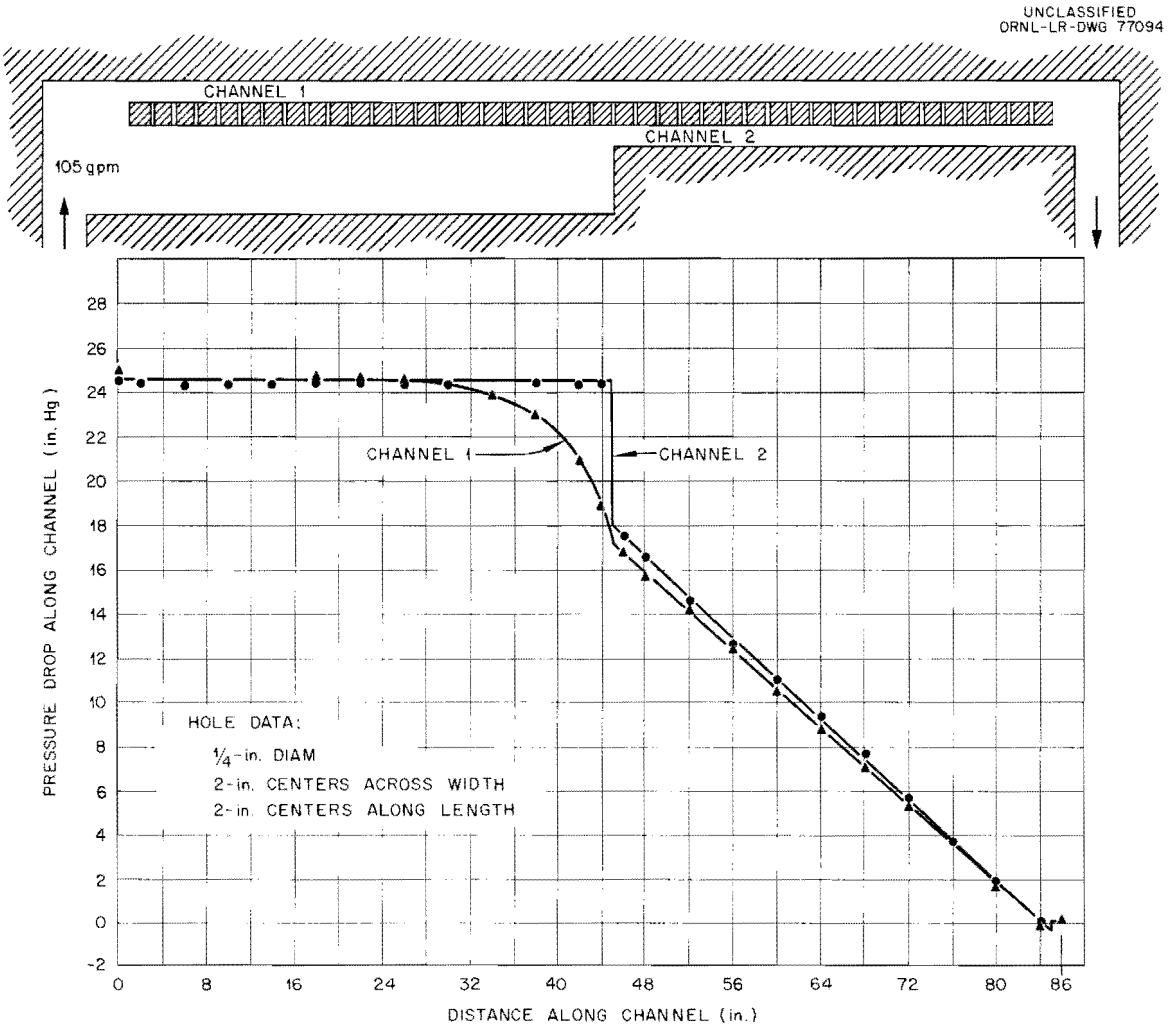


Fig. 59. Pressure Drop for Parallel Channels with 1.227% of Plate Area Occupied by Holes.

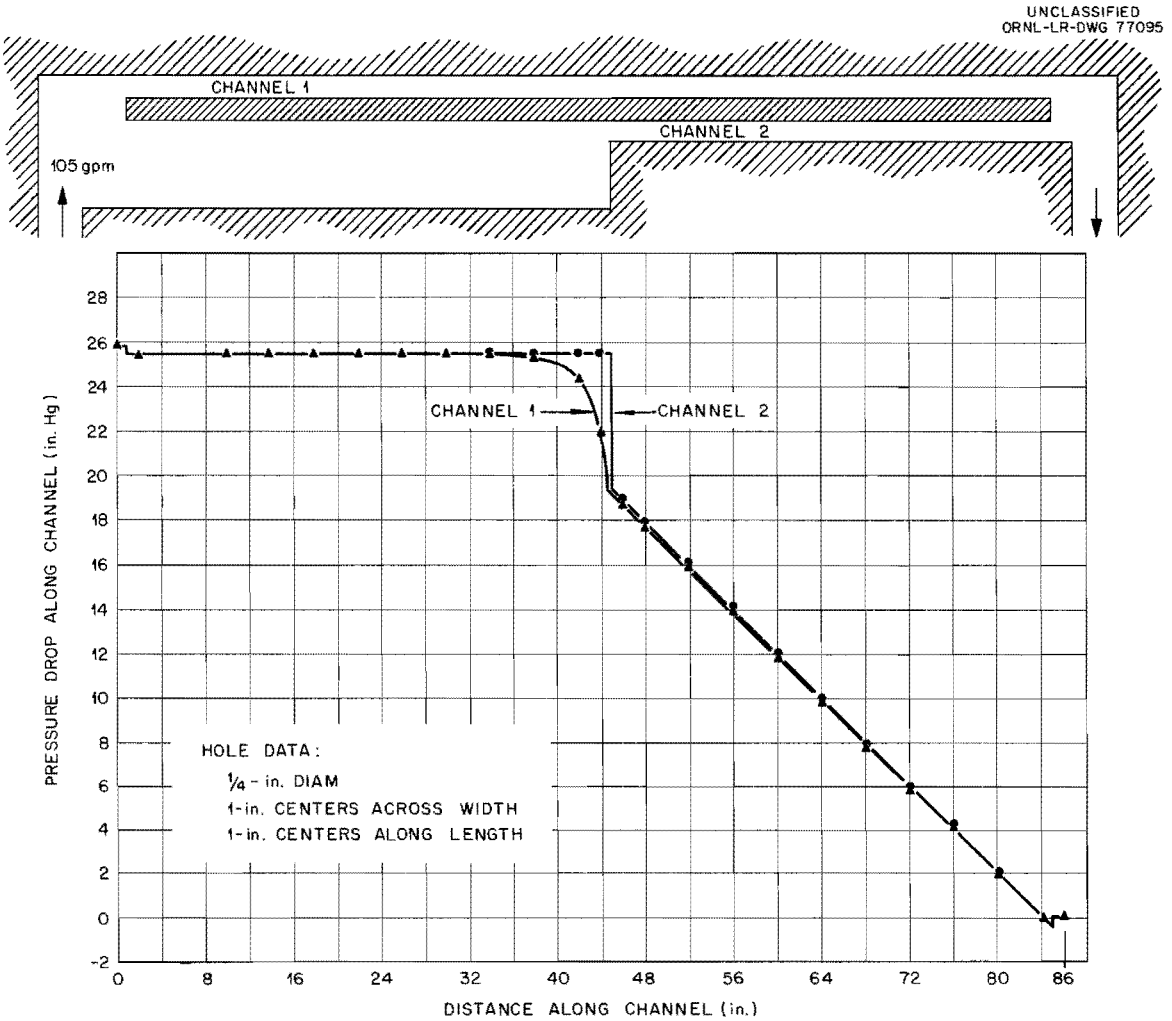


Fig. 60. Pressure Drop for Parallel Channels with 4.908% of Plate Area Occupied by Holes.

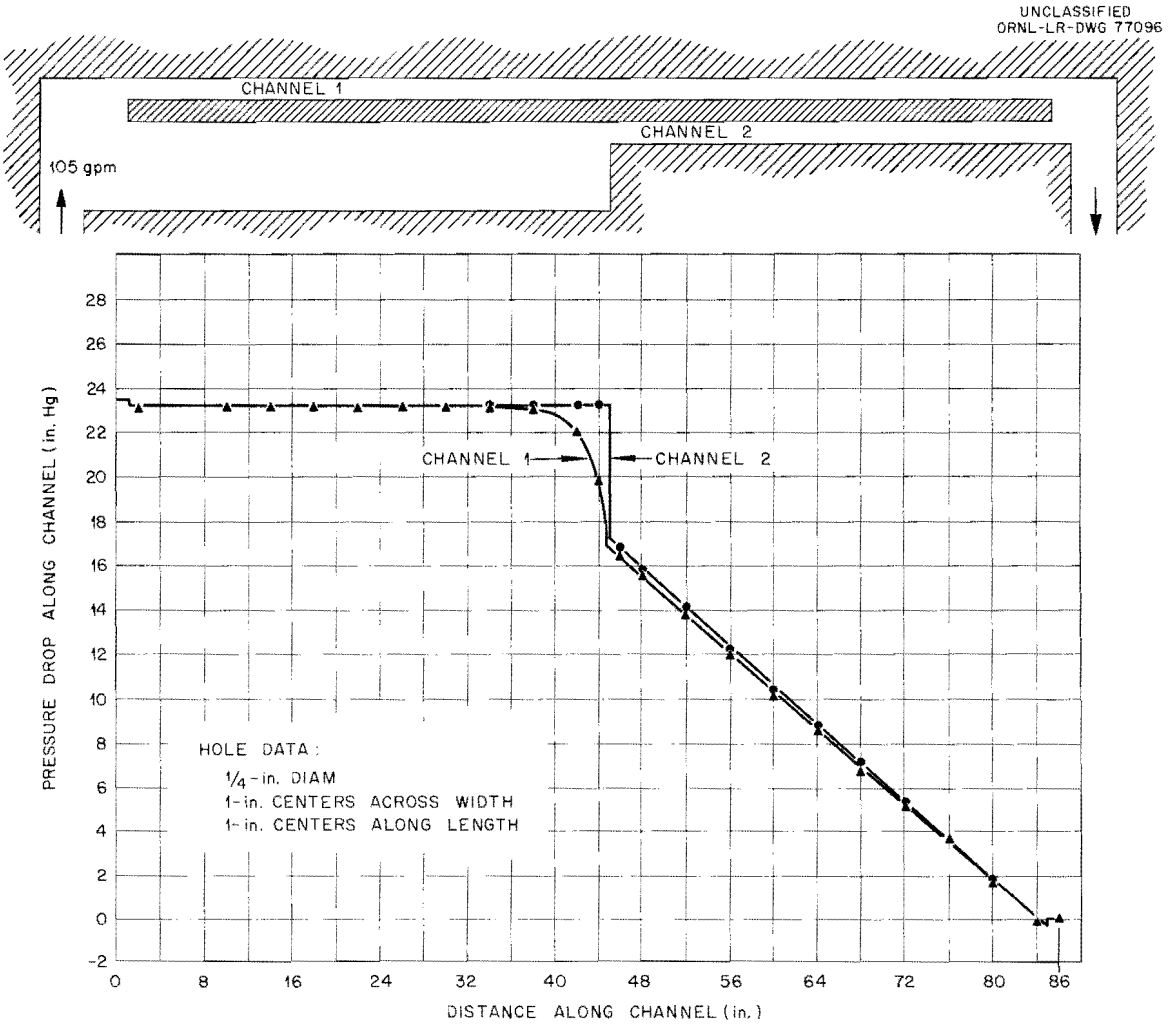


Fig. 61. Pressure Drop for Parallel Channels with 2.454% of Plate Area Occupied by Holes.

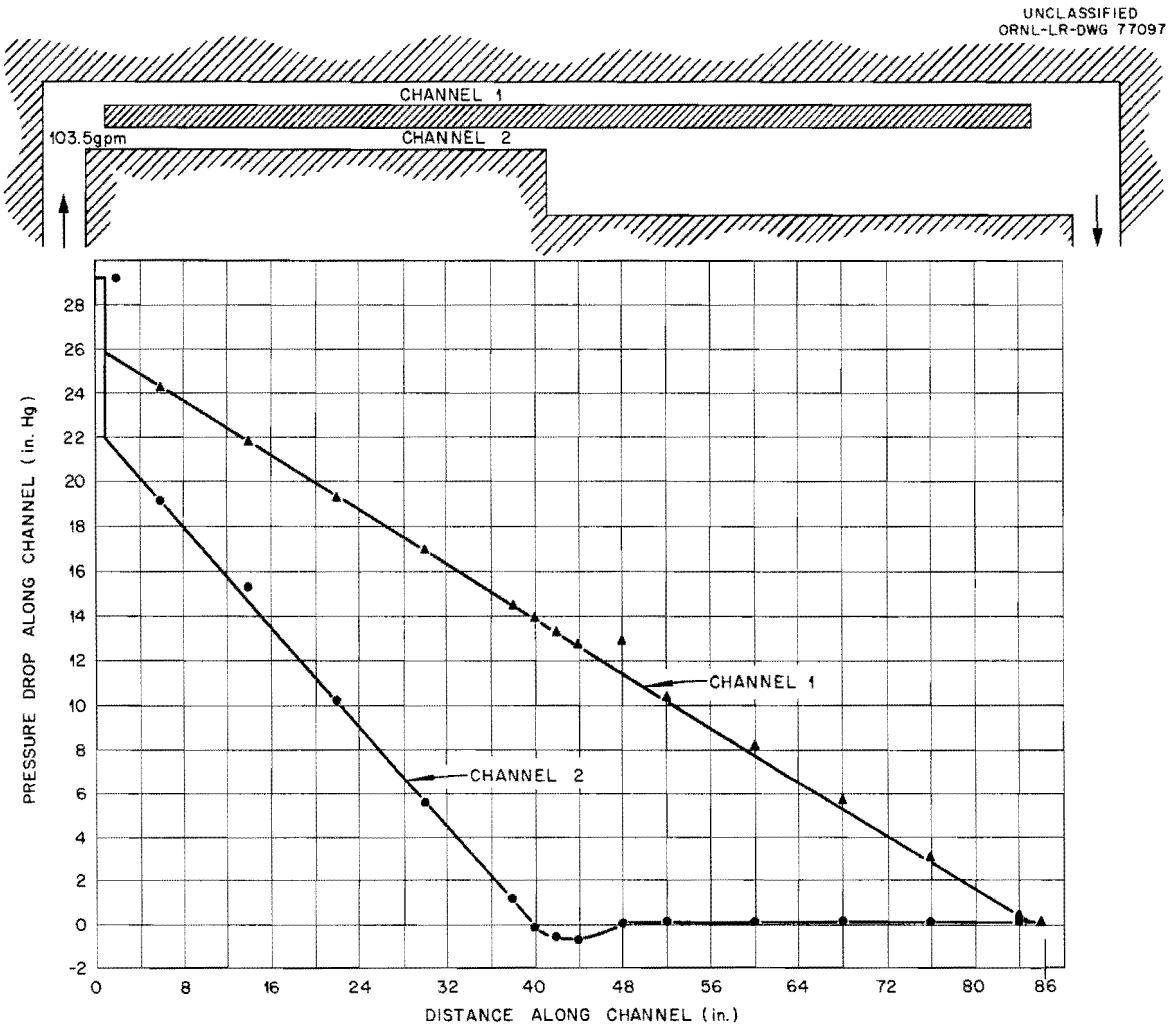


Fig. 62. Pressure Drop for Parallel Channels with No Holes.

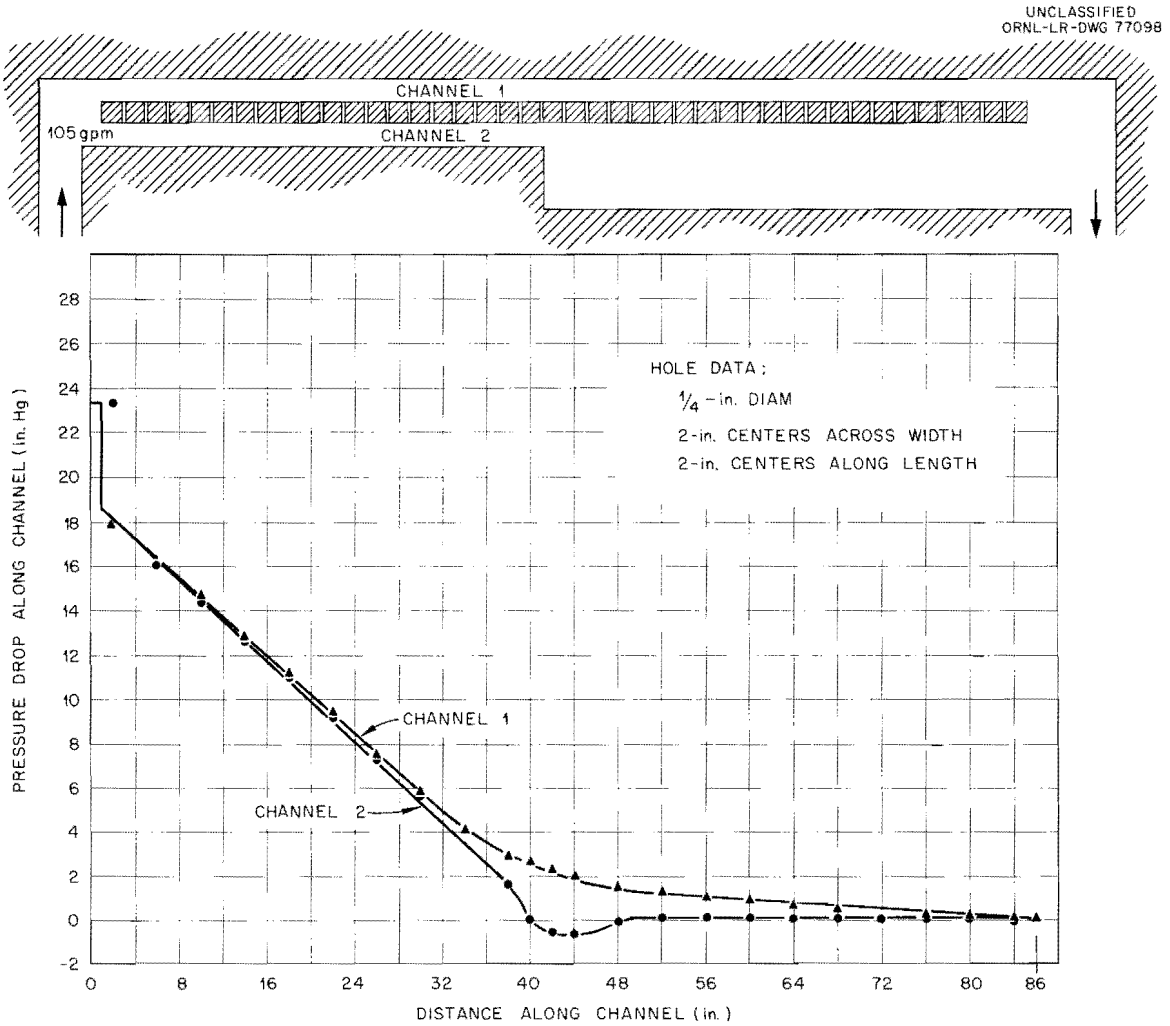


Fig. 63. Pressure Drop for Parallel Channels with 1.227% of Plate Area Occupied by Holes.

## Internal Distribution

1. G. M. Adamson
2. S. E. Beall
3. M. Bender
4. R. J. Beaver
5. A. M. Billings
6. F. T. Binford
7. A. L. Boch
8. R. B. Briggs
9. T. G. Chapman
10. R. D. Cheverton
11. H. C. Claiborne
12. T. E. Cole
13. J. A. Cox
14. J. E. Cunningham
15. G. J. Dixon
16. A. P. Fraas
17. W. R. Gambill
18. J. C. Griess
19. S. H. Hanauer
20. J. W. Hill
21. R. M. Hill
22. N. Hilvety
23. R. E. Hoskins
24. L. B. Holland
25. J. E. Jones
26. W. H. Kelley
27. J. A. Lane
28. C. F. Leitten, Jr.
29. R. N. Lyon
30. H. G. MacPherson
31. W. D. Manly
32. R. V. McCord
33. J. R. McGuffey
34. H. A. McLain
35. J. R. McWherter
36. A. J. Miller
37. L. C. Oakes
38. A. M. Perry
39. M. W. Rosenthal
40. T. H. Row
41. H. W. Savage
42. A. W. Savolainen
43. R. E. Schappel
44. I. Spiewak
45. M. J. Skinner
46. P. N. Stevens
47. R. S. Stone
48. J. A. Swartout
49. J. W. Tackett
50. D. B. Trauger
51. A. M. Weinberg
52. T. A. Welton
53. J. H. Westsik

54-55. Central Research Library (CRL)
56-58. Y-12 Document Reference Section (DRS)
59-61. Laboratory Records Department (LRD)
62. Laboratory Records Department — Record Copy (LRD-RC)

## External Distribution

63-77. Division of Technical Information Extension (DTIE)
78. Research and Development Division, ORO
79-80. Reactor Division, ORO